

# Electro-magnetic wave emission

from the Sun

Part - II



C. Kathiravan

Sun & Solar system Group

Indian Institute of Astrophysics  
Bangalore

[kathir@iiap.res.in](mailto:kathir@iiap.res.in)

# Talk PLAN

- 1** **Discovery & Nature of solar radio emission**
- 2** **Quiet Sun, Slowly Varying Component, & the Transients**  
(Observational view point & Very little theory)
- 3** **Radio → Sun – Earth connection**

# Nature of Solar Radio emission

---

**Can the entire  
radio band be used  
for observations??**

---

**Radio band : ~300 GHz – ~3 kHz**

# Sun & Earth

Obs. in  $\approx 7 - 40$  MHz band is difficult because of RFI

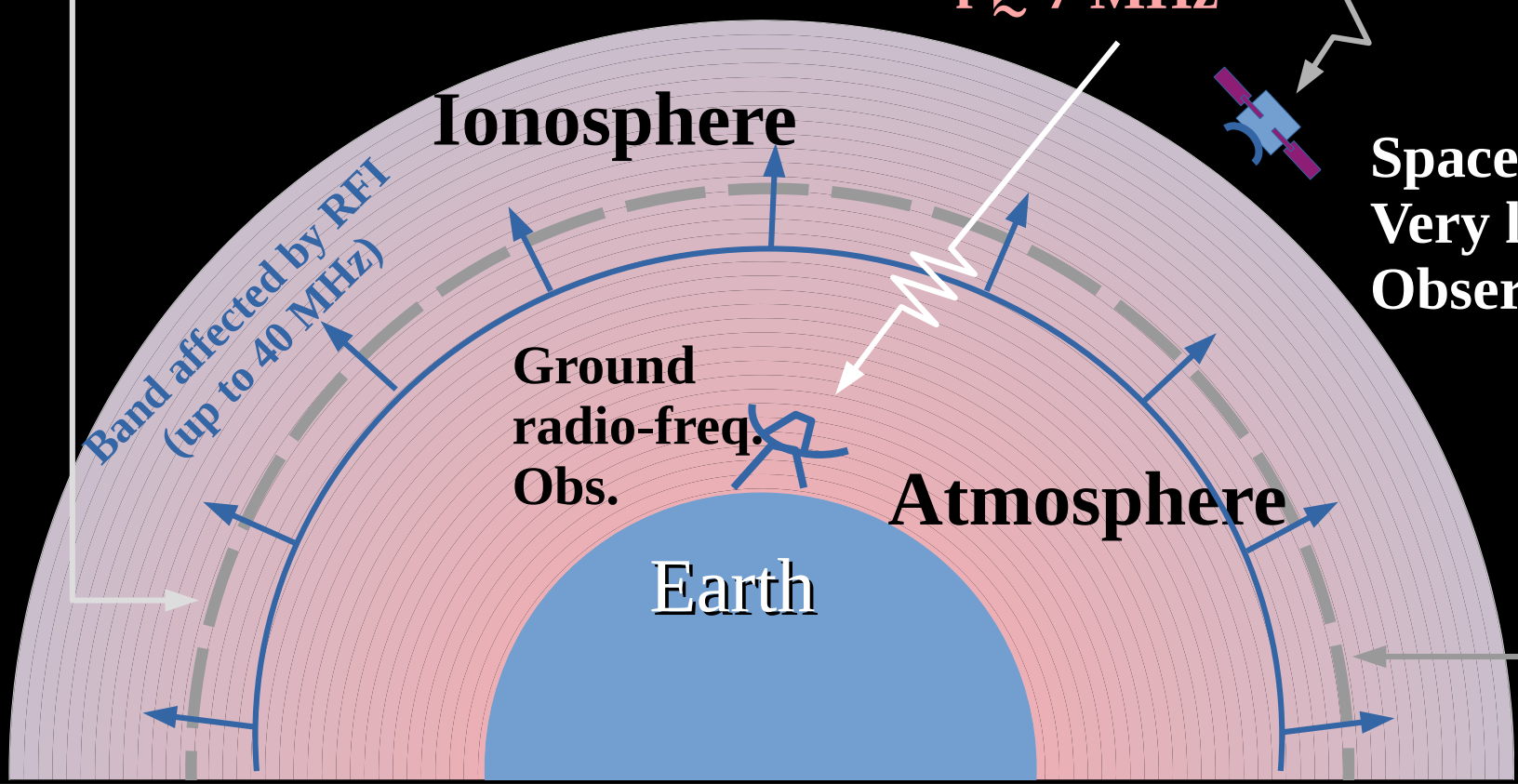
Crucial to establish connectivity between Coronal & IP events



$f \lesssim 7$  MHz  
 $\lambda \gtrsim 43$  m

$f \gtrsim 7$  MHz

Space based Very low-freq. Observations



---

**Has the Sun been  
observed over the  
entire radio band ??**

---

**Yes, Of course ...**

---

**Can you show  
some examples ??**

---

# Solar Radio Emission

- ① Quiet Sun Component (QSC)  
(Thermal)
- ② Slowly Varying Component (SVC)  
(Thermal & Non-thermal)
- ③ Transient Component (TC)  
(Thermal & Non-thermal)

---

**How these different  
Components were  
found & classified ??**

---

The Radio Quiet Sun

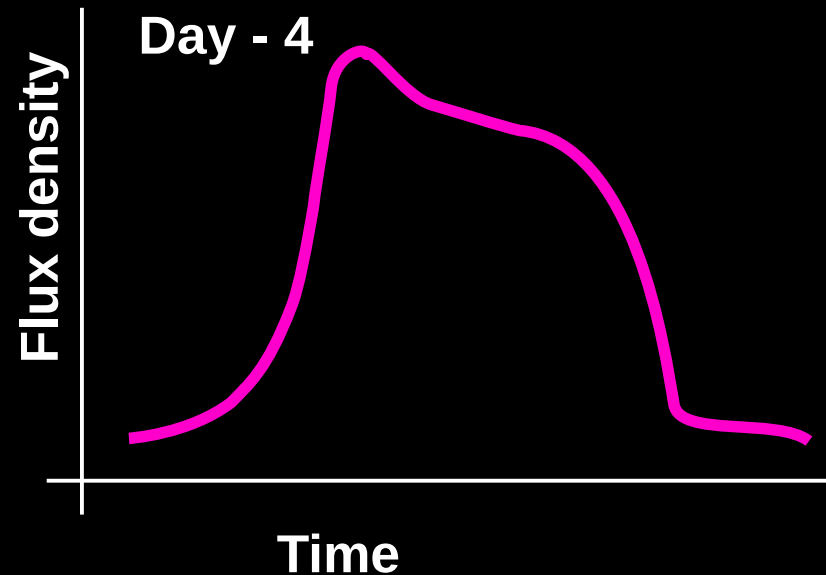
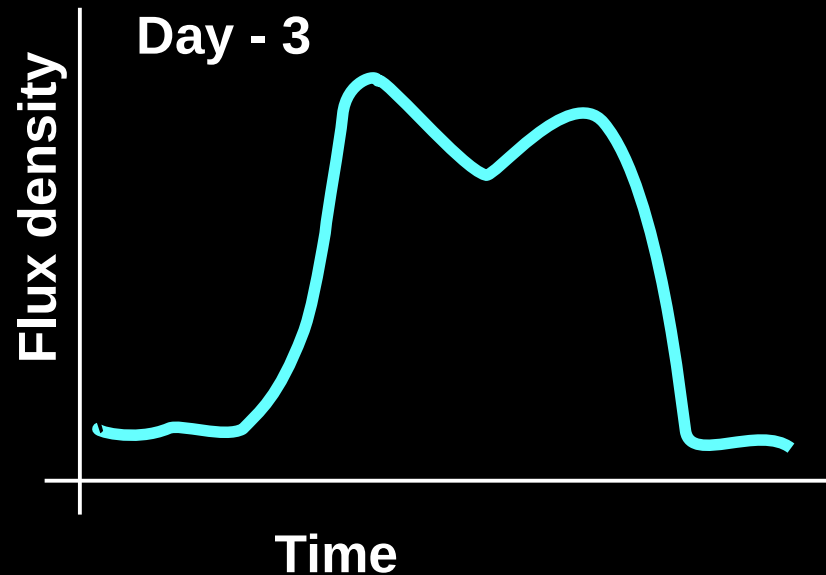
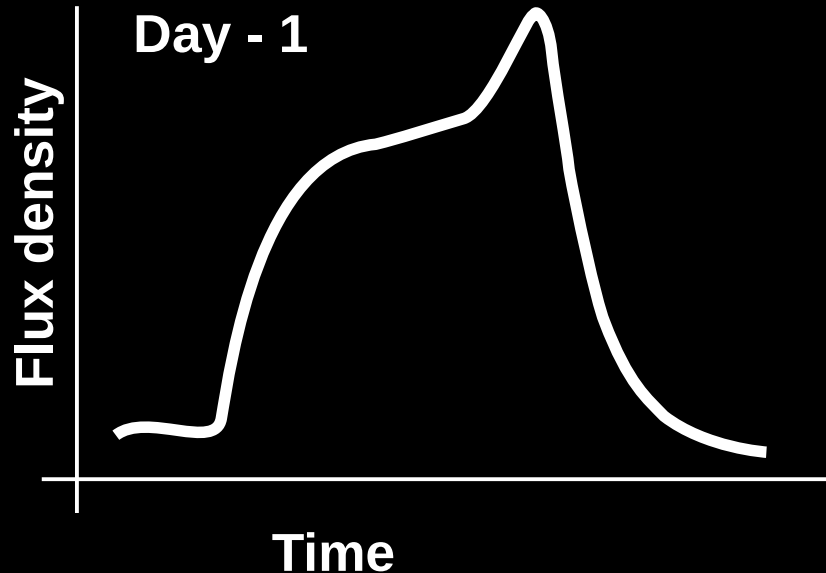
The Radio Quiet Sun

1

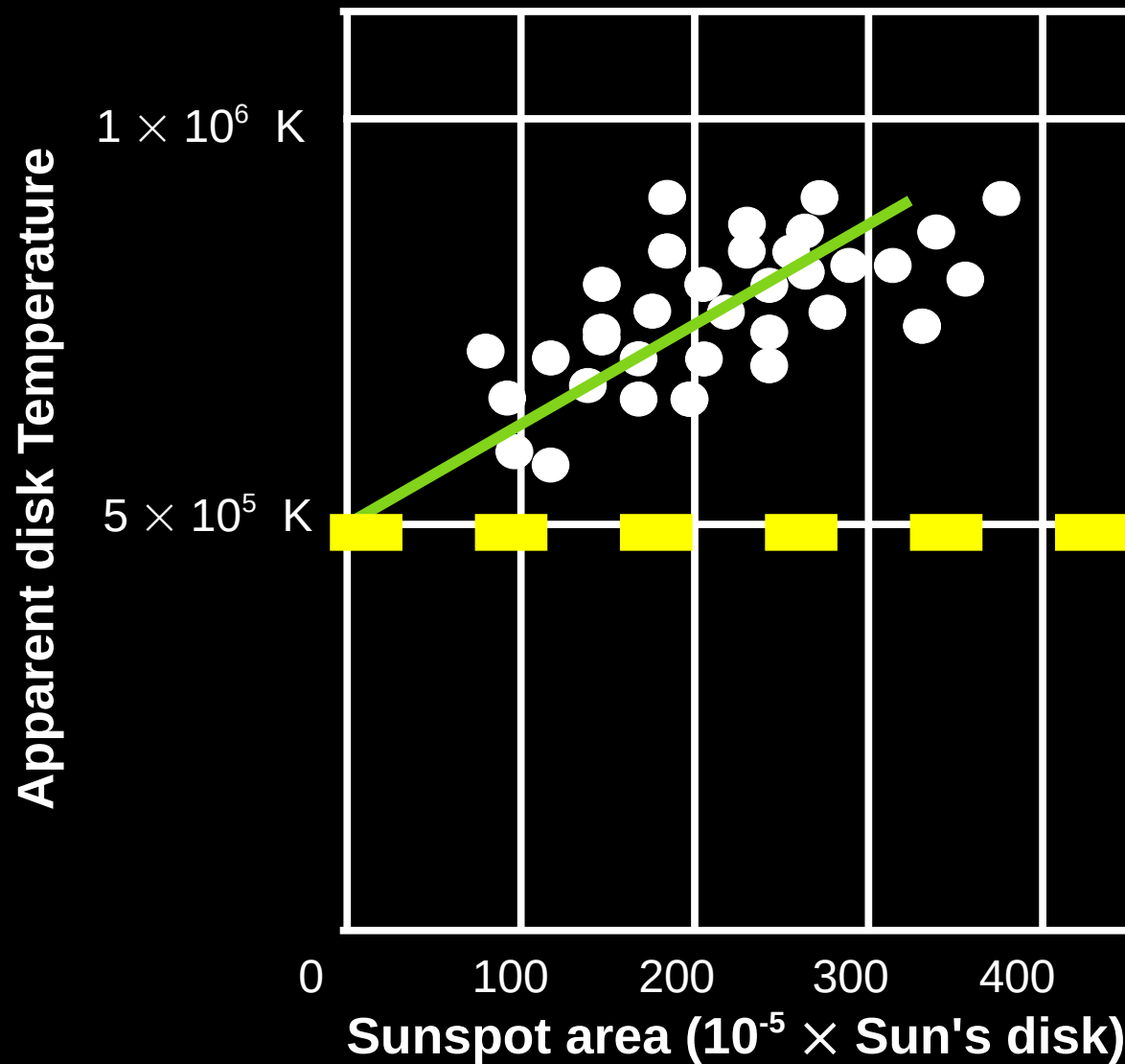
**The Radio Quiet Sun**

The Radio Quiet Sun

**1D scan of the Sun : Flux density @ a specific frequency**



# 1D Scan of the Sun $T_b$ (1.5 m / 200 MHz) Vs Sunspot area



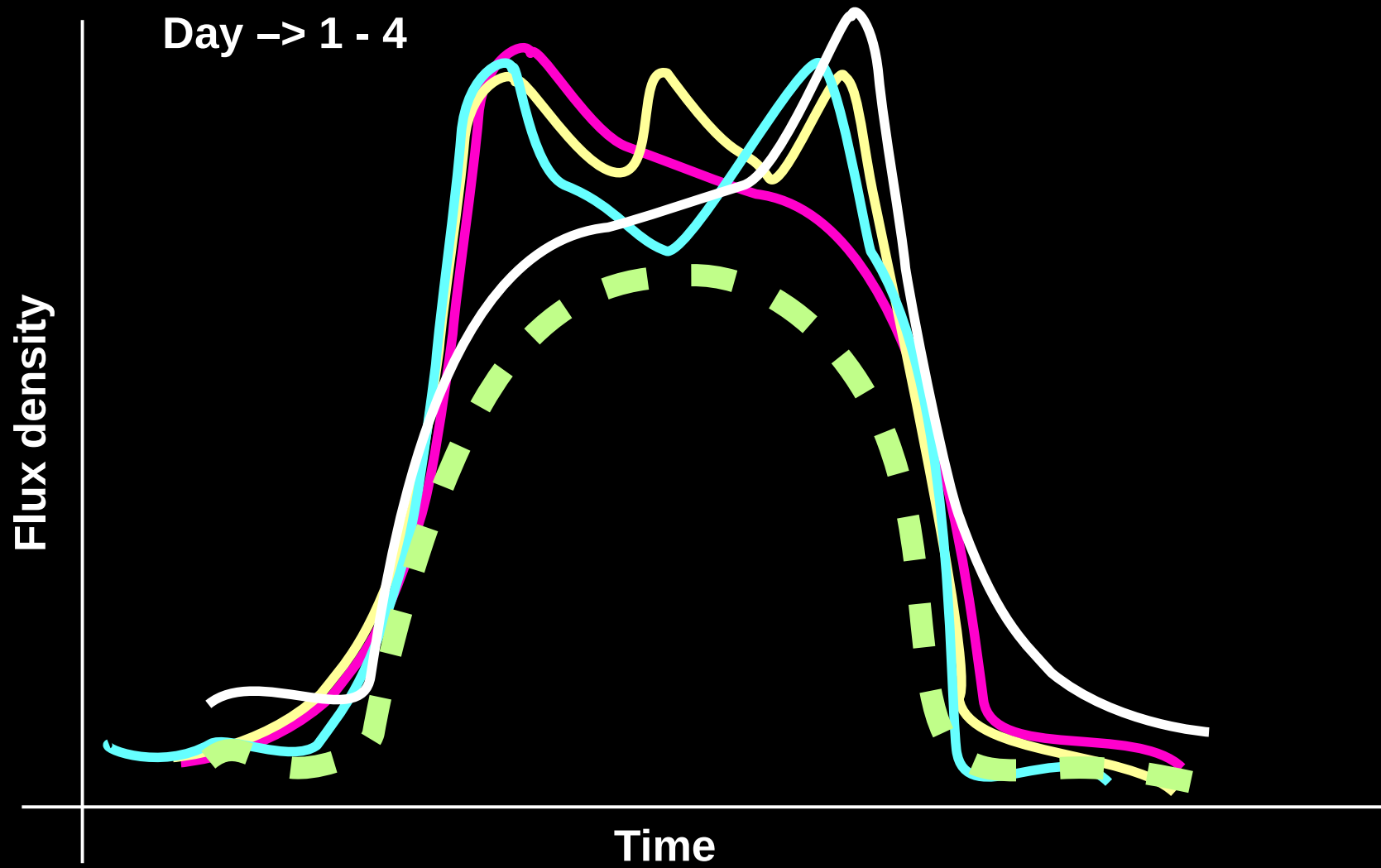
**Pawsey et al., Au. J. Sci. Res.-A, 2, 198 (1949)**

## 1D Scan of the Sun $T_b$ (1.5 m / 200 MHz) Vs Sunspot area

1. There is a base level below which the radio intensity (or brightness temperature) never falls.
2. This was obtained by extrapolating the fit to zero sunspot area.
3. Radio astronomers attributed this minimum level to the background corona which is called the quiet Sun brightness temperature as it is independent of solar activity.

Pawsey et al., Au. J. Sci. Res.-A, 2, 198 (1949)

# 1D Scan of the Sun : Flux density (Superposition)



Boischot, A., Ann d' Astrophys., 21, 273 (1958)

## 1D Scan of the Sun : Flux density (Superposition)

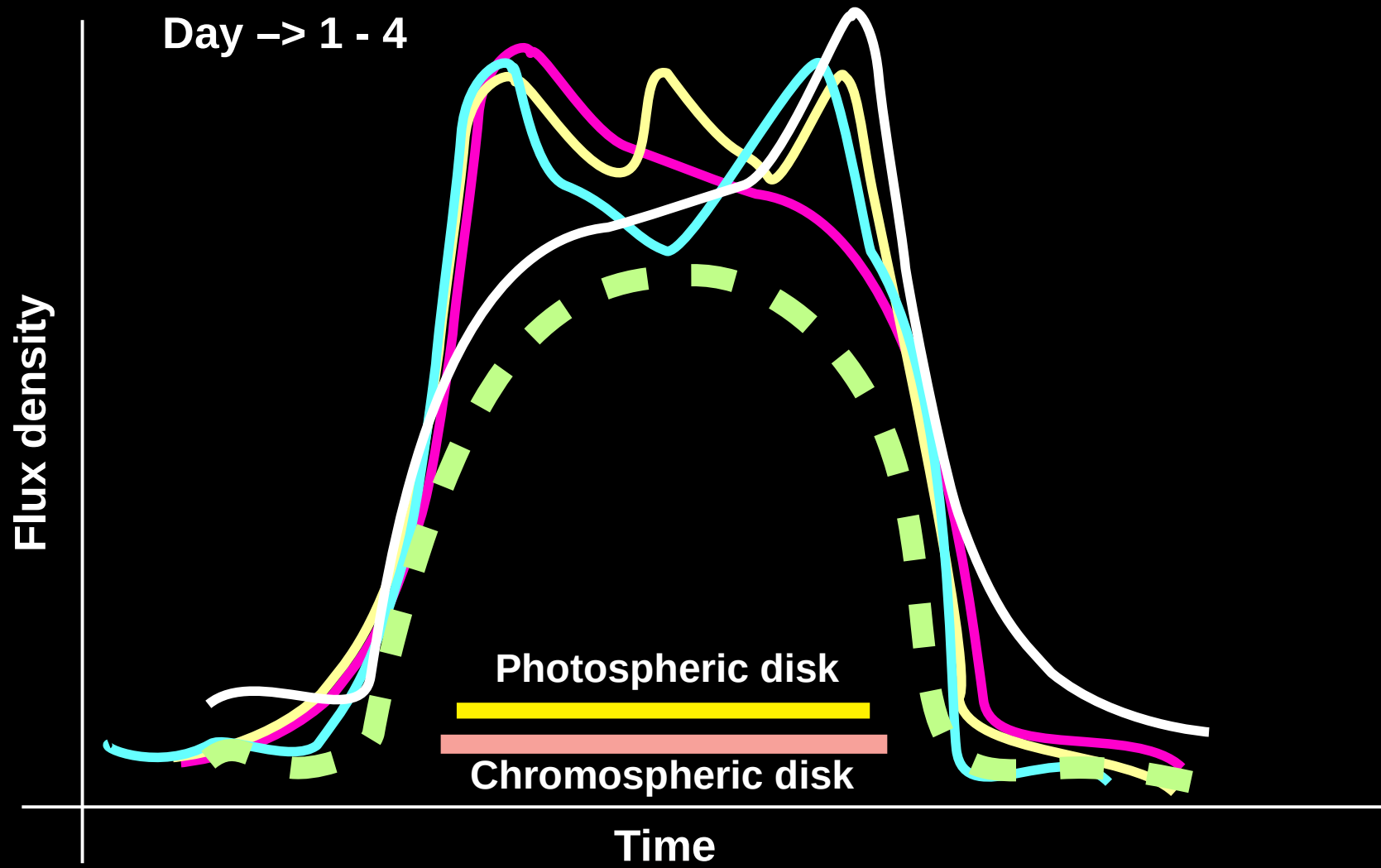
Day → 1 - 4

If we superpose the flux density distribution, there is an inner envelope and the enhanced emissions are seen above that. This is known as the quiet Sun or background flux density distribution.

Time

**Boischot, A., Ann d' Astrophys., 21, 273 (1958)**

# 1D Scan of the Sun : Flux density (Superposition)



Boischot, A., *Ann d' Astrophys.*, 21, 273 (1958)

## 1D Scan of the Sun : Flux density (Superposition)

Day  $\rightarrow$  1 - 4

The size of the radio quiet Sun is more than the size of the Photosphere or Chromosphere which implies that the radio radiation comes above the Photosphere and the Chromosphere.

Photospheric disk

Chromospheric disk

Time

Boischot, A., *Ann d' Astrophys.*, 21, 273 (1958)

# Quiet Sun Flux density spectrum : Blackbody

$$S = \left( \frac{2 k_B T_b}{\lambda^2} \right) \Omega_s$$

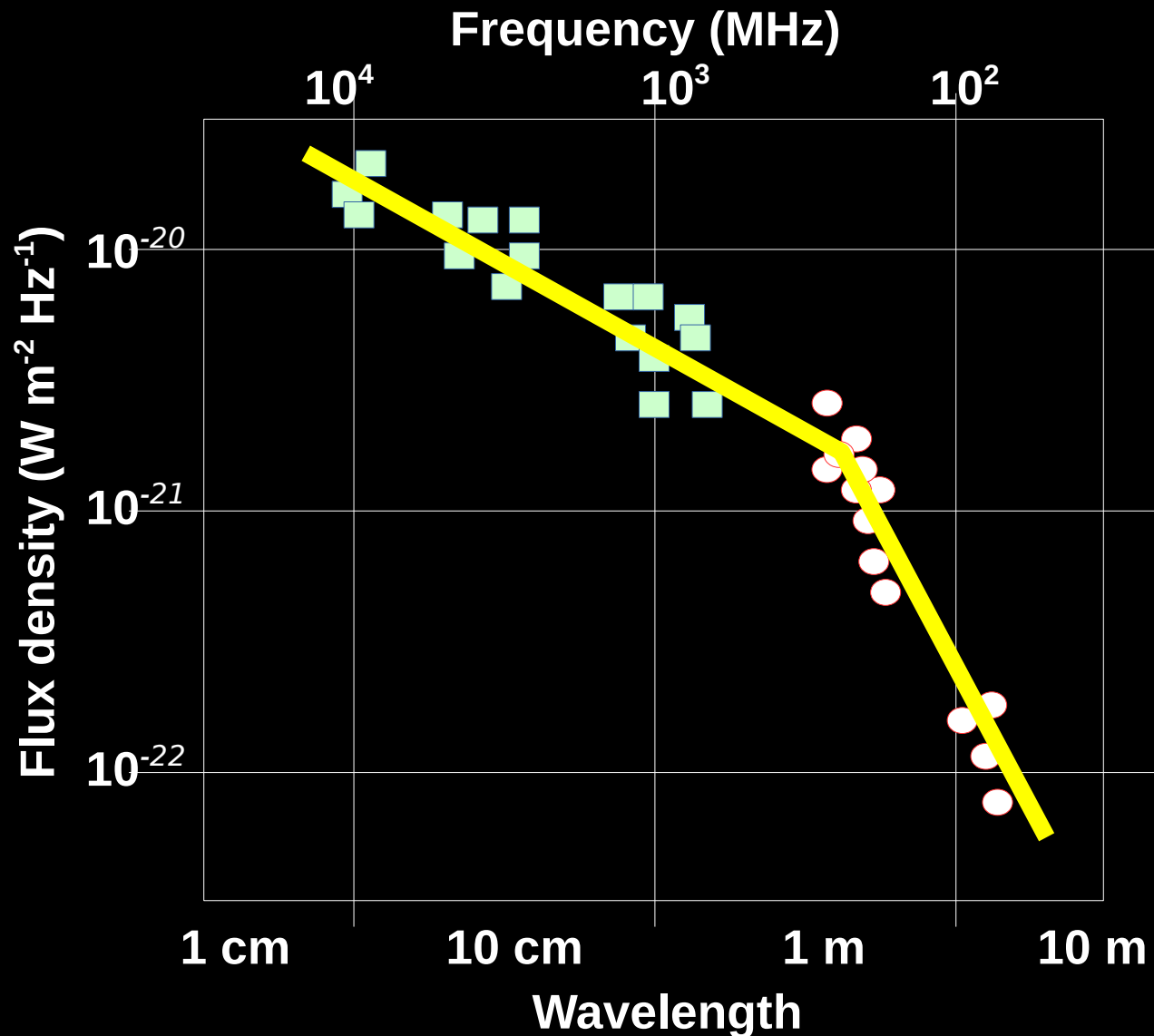
$S \rightarrow$  flux density of the source

$k_B \rightarrow$  Boltzmann constant

$T_b \rightarrow$  Brightness temperature

$\lambda \rightarrow$  Wavelength

$\Omega_s \rightarrow$  Source solid angle

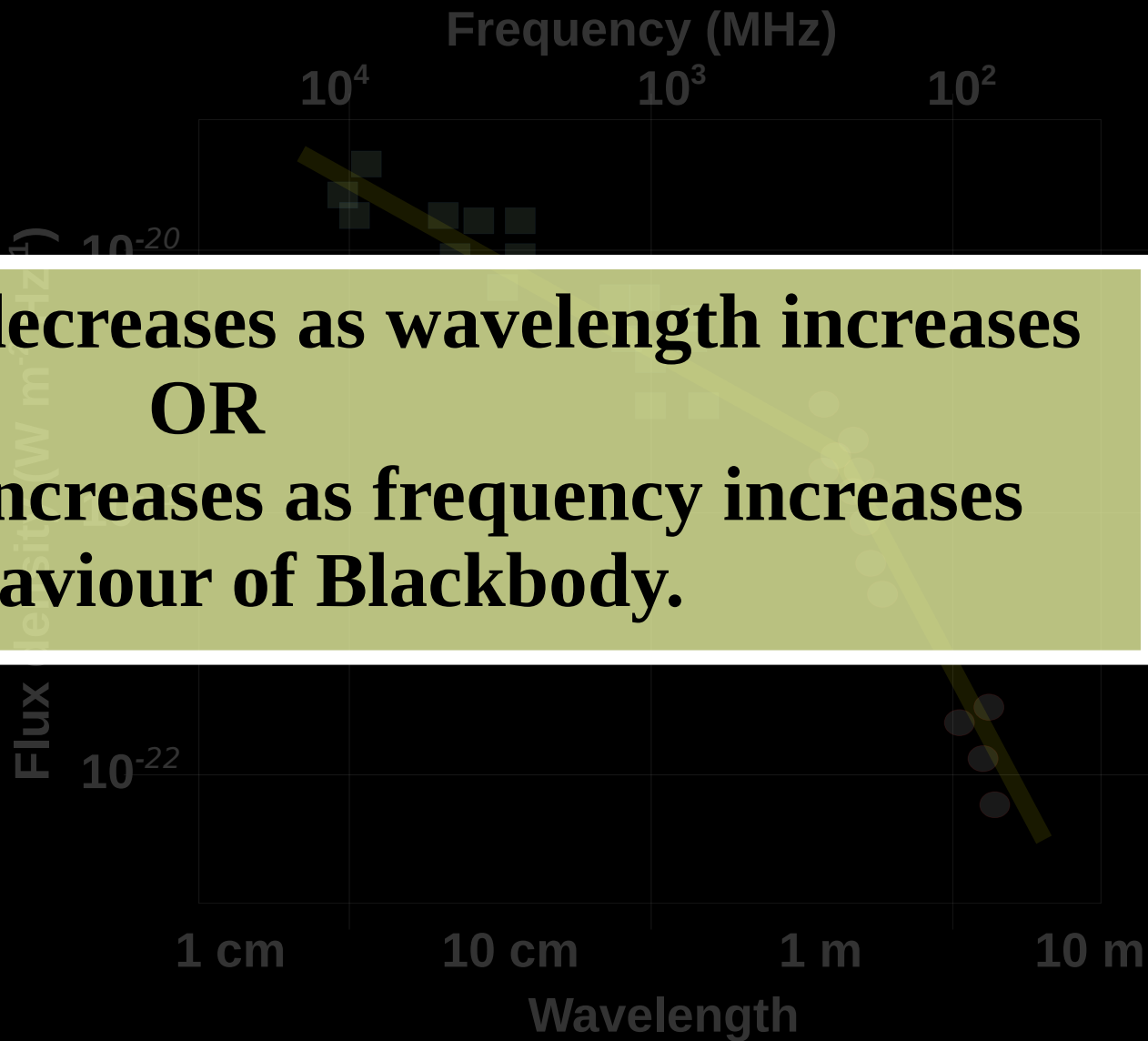


Smerd, S. F., *Annals of IGY*, 34 (1964)

# Quiet Sun Flux density spectrum : Blackbody

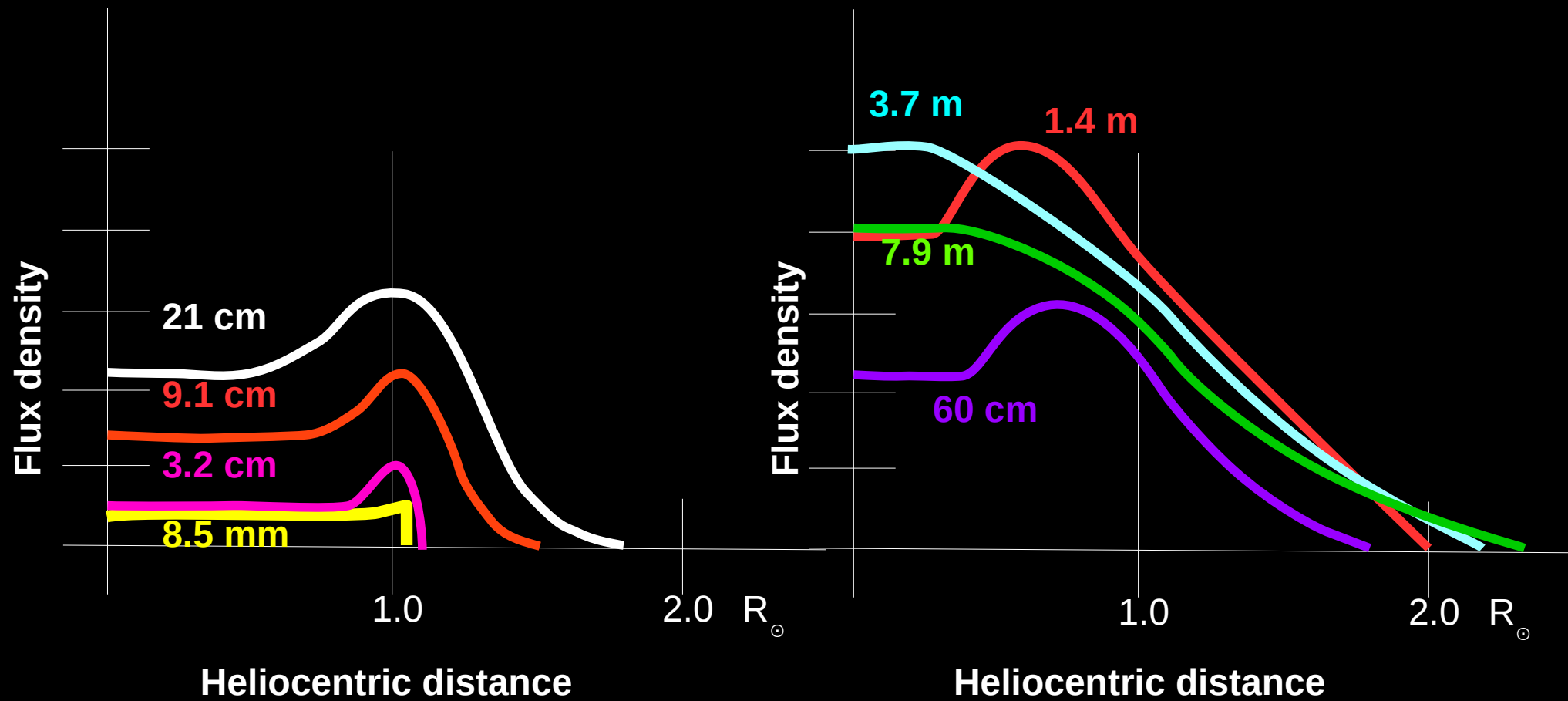
The quiet Sun flux decreases as wavelength increases  
 OR  
 The quiet Sun flux increases as frequency increases  
 – A behaviour of Blackbody.

$T_b \rightarrow$  Brightness temperature  
 $\lambda \rightarrow$  Wavelength  
 $\Omega_s \rightarrow$  Source solid angle



Smerd, S. F., Annals of IGY, 34 (1964)

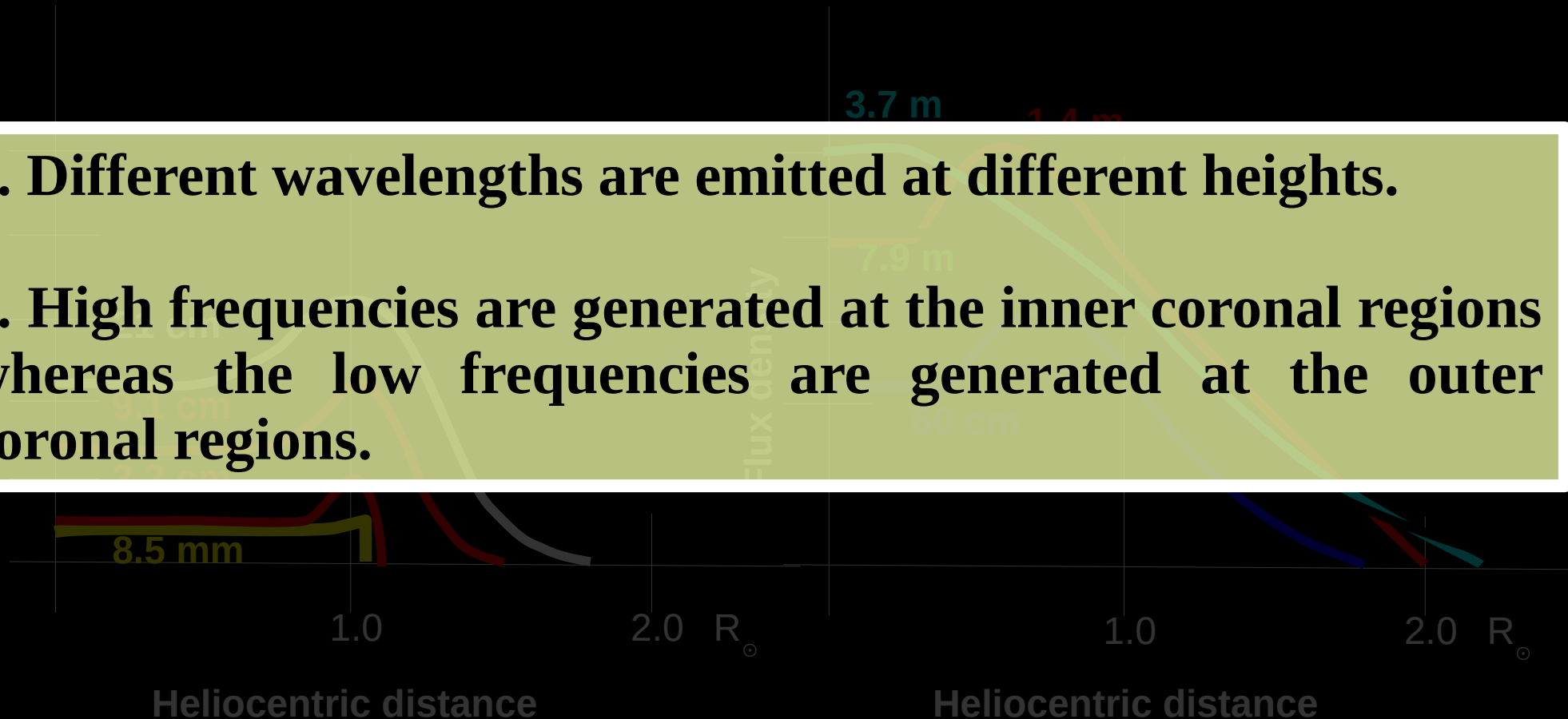
# Quiet Sun flux profiles at different $\lambda$ s (mm – deca-m)



Smerd, S. F., Au. J. Sci. Res.-A, 3, 34 (1950)

## Quiet Sun flux profiles at different $\lambda$ s (mm – deca-m)

1. Different wavelengths are emitted at different heights.
2. High frequencies are generated at the inner coronal regions whereas the low frequencies are generated at the outer coronal regions.



Smerd, S. F., *Au. J. Sci. Res.-A*, 3, 34 (1950)

# Quiet Sun Brightness Temperature ( $T_b$ )

$$S = \left( \frac{2 k_B T_b}{\lambda^2} \right) \Omega_s$$

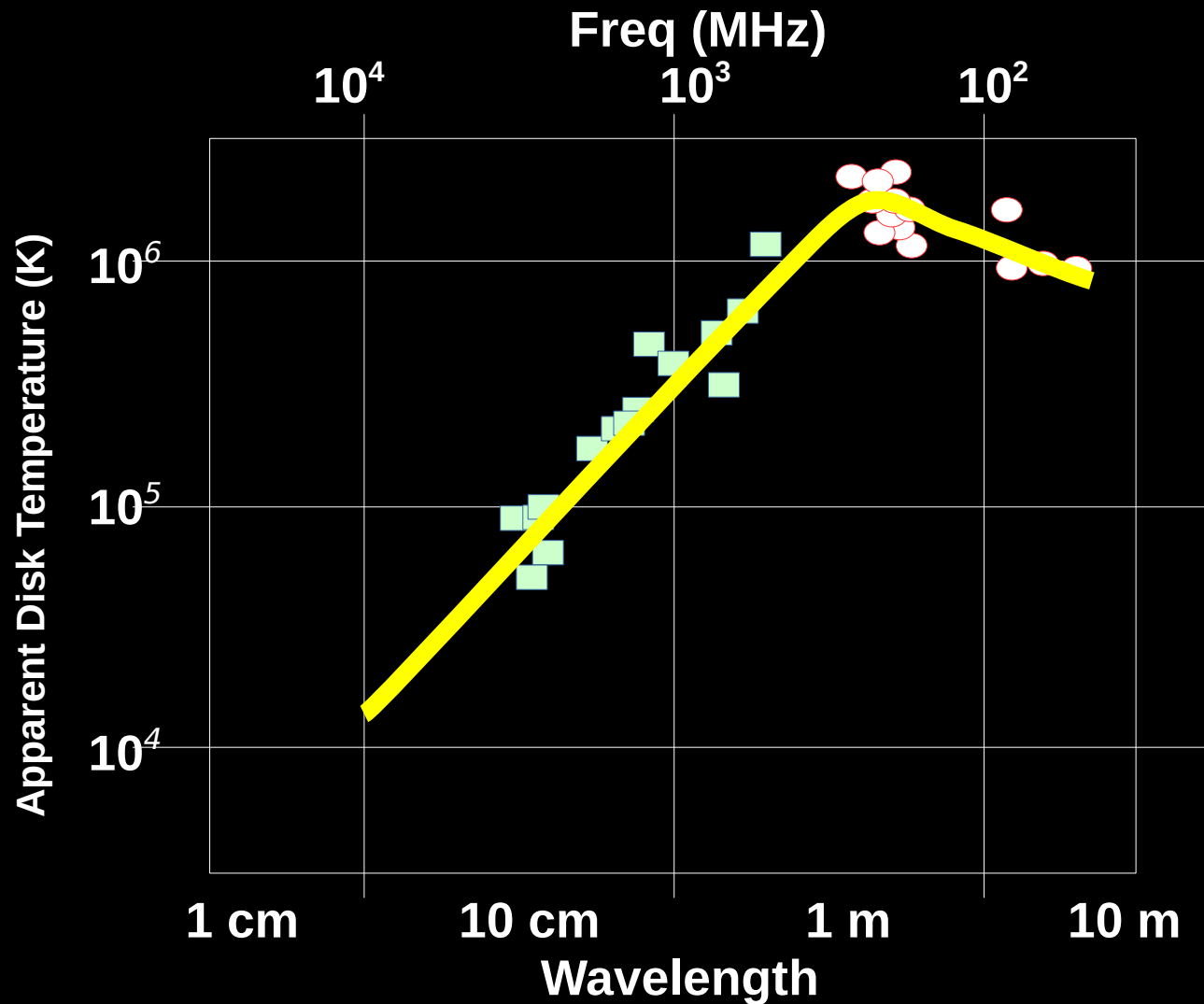
$S \rightarrow$  flux density of the source

$k_B \rightarrow$  Boltzmann constant

$T_b \rightarrow$  Brightness temperature

$\lambda \rightarrow$  Wavelength

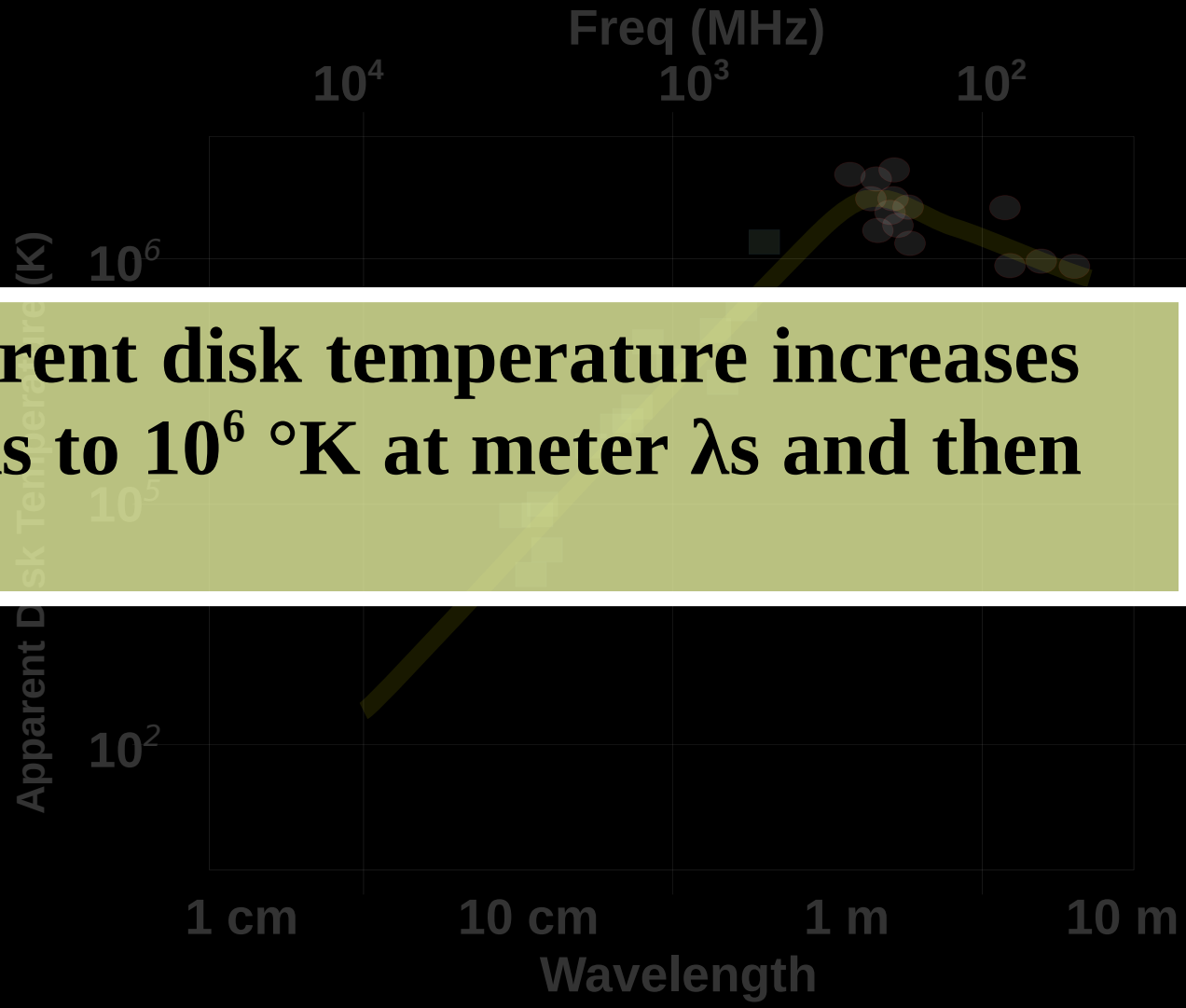
$\Omega_s \rightarrow$  Source solid angle



Smerd, S. F., *Annals of IGY*, 34 (1964)

# Quiet Sun Brightness Temperature ( $T_b$ )

$$S = \left( \frac{2 k_B T_b}{c} \right) \Omega_s$$

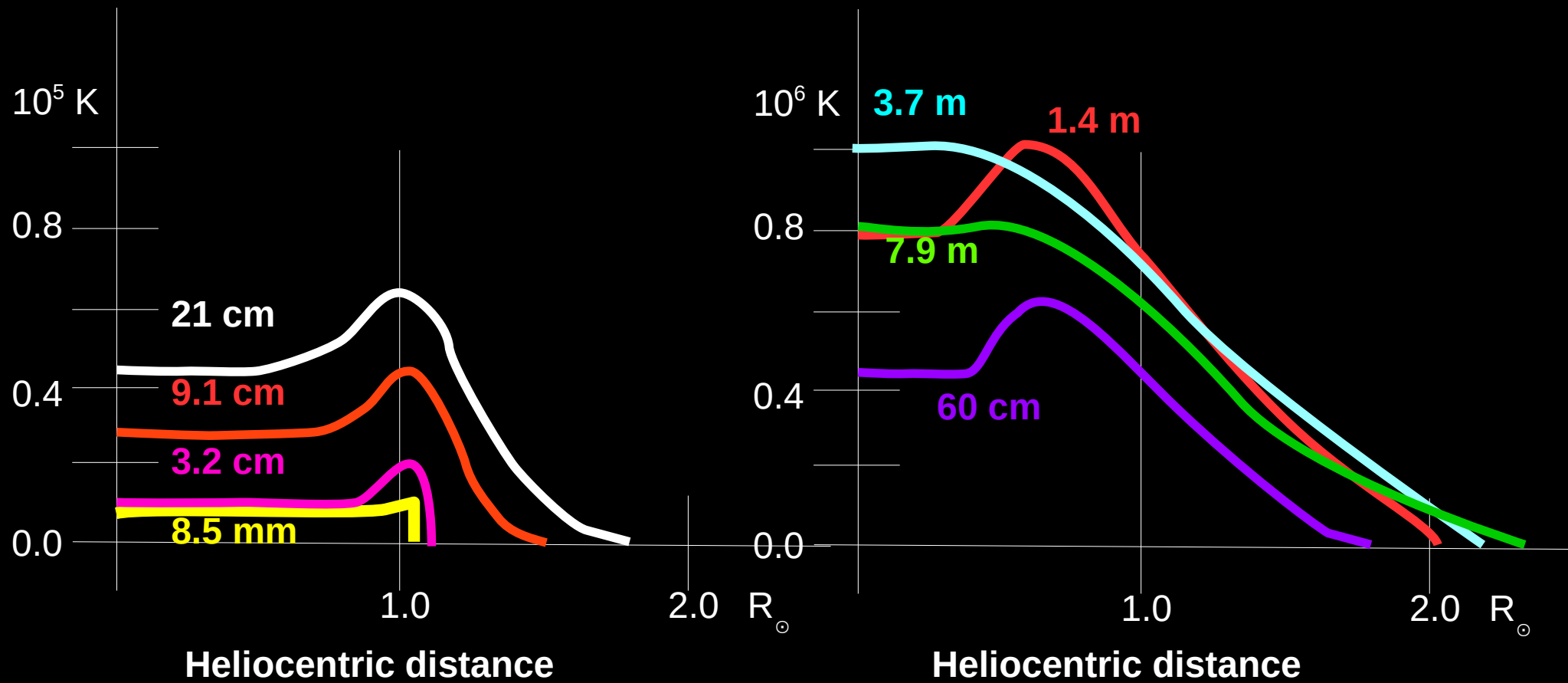


**The quiet Sun apparent disk temperature increases from 10<sup>4</sup> °K at cm λs to 10<sup>6</sup> °K at meter λs and then starts decreasing.**

- $k_B$  → Boltzmann constant
- $T_b$  → Brightness temperature
- $\lambda$  → Wavelength
- $\Omega_s$  → Source solid angle

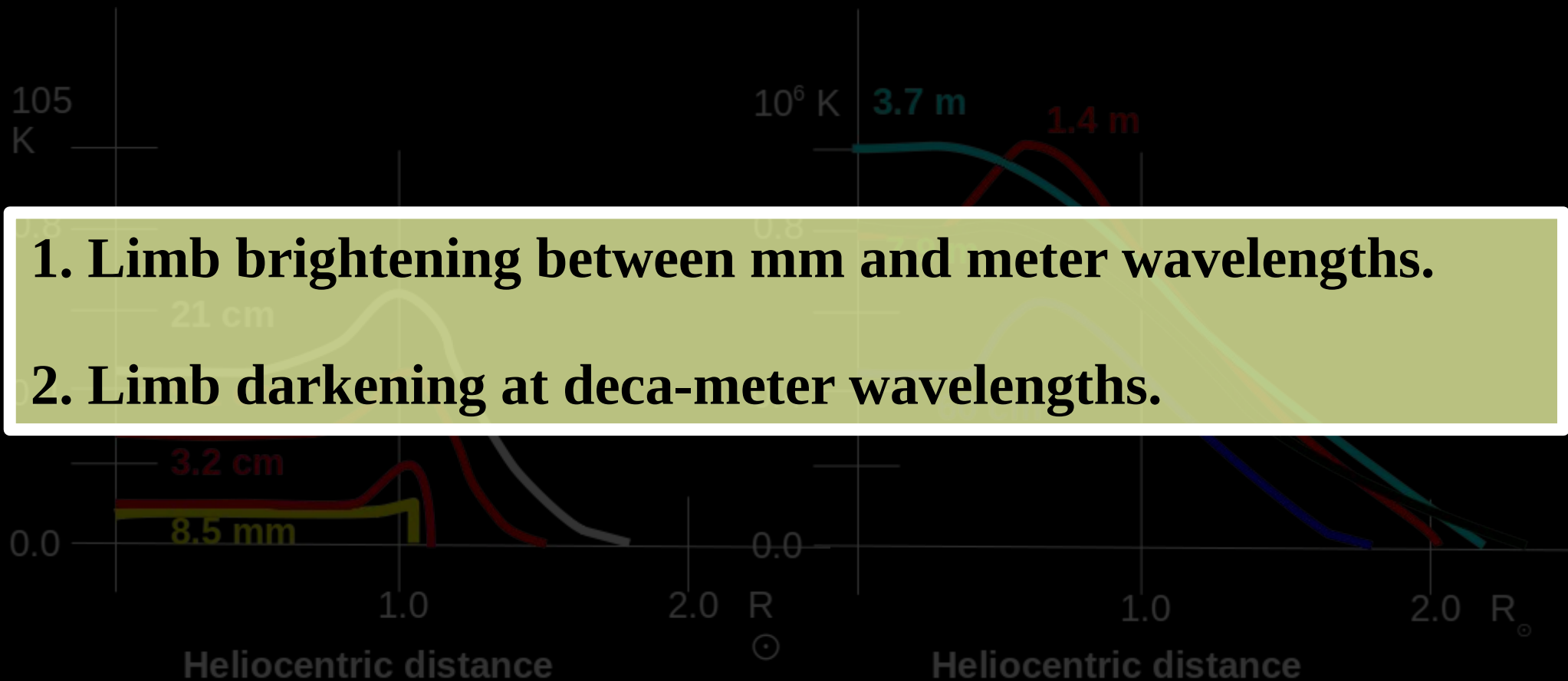
**Smerd, S. F., Annals of IGY, 34 (1964)**

# Quiet Sun Brightness Temperature at different $\lambda$ s (mm - deca-m)



Smerd, S. F., *Au. J. Sci. Res.-A*, 3, 34 (1950)

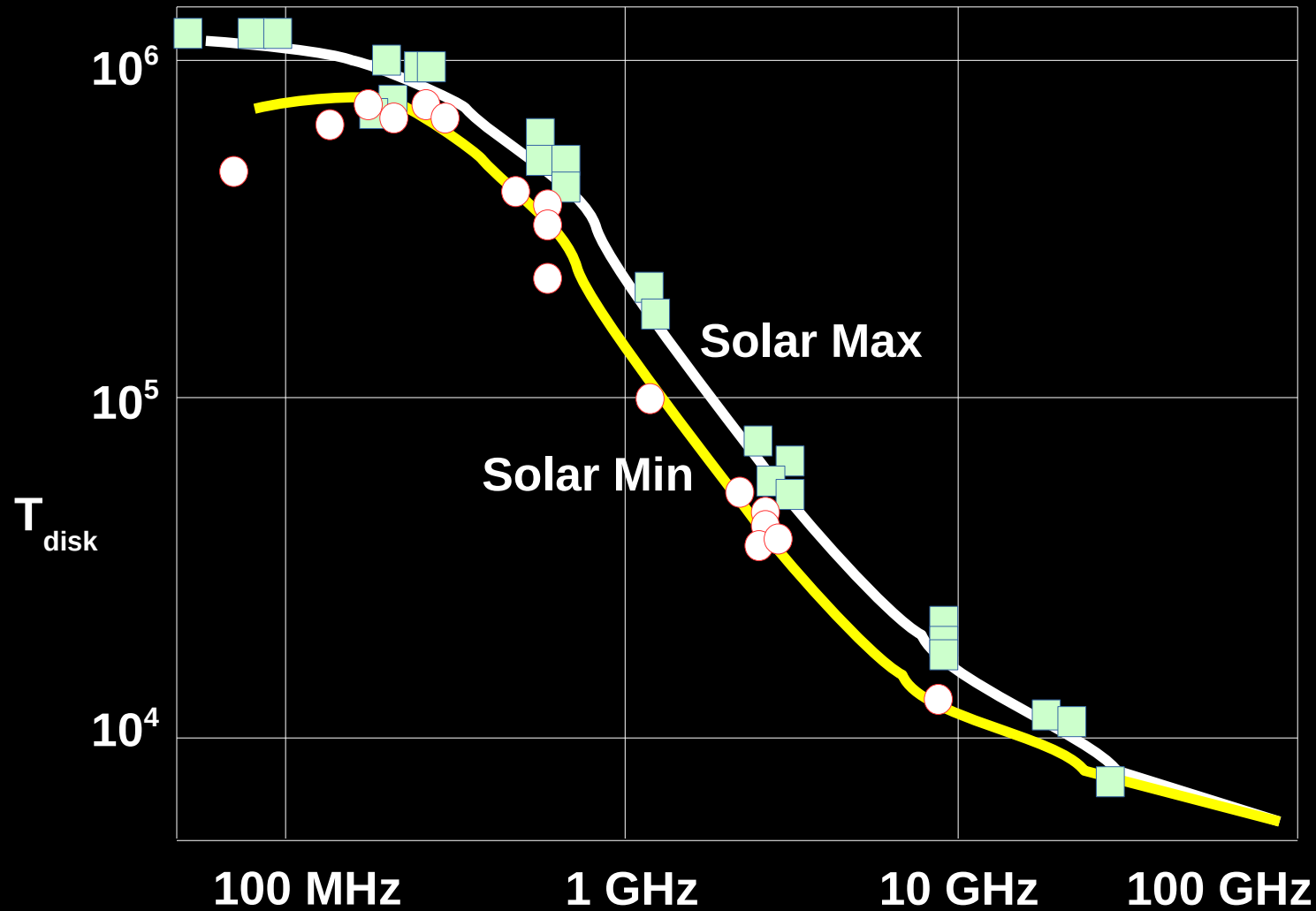
# Quiet Sun Brightness Temperature at different $\lambda$ s (mm - deca-m)



1. Limb brightening between mm and meter wavelengths.
2. Limb darkening at deca-meter wavelengths.

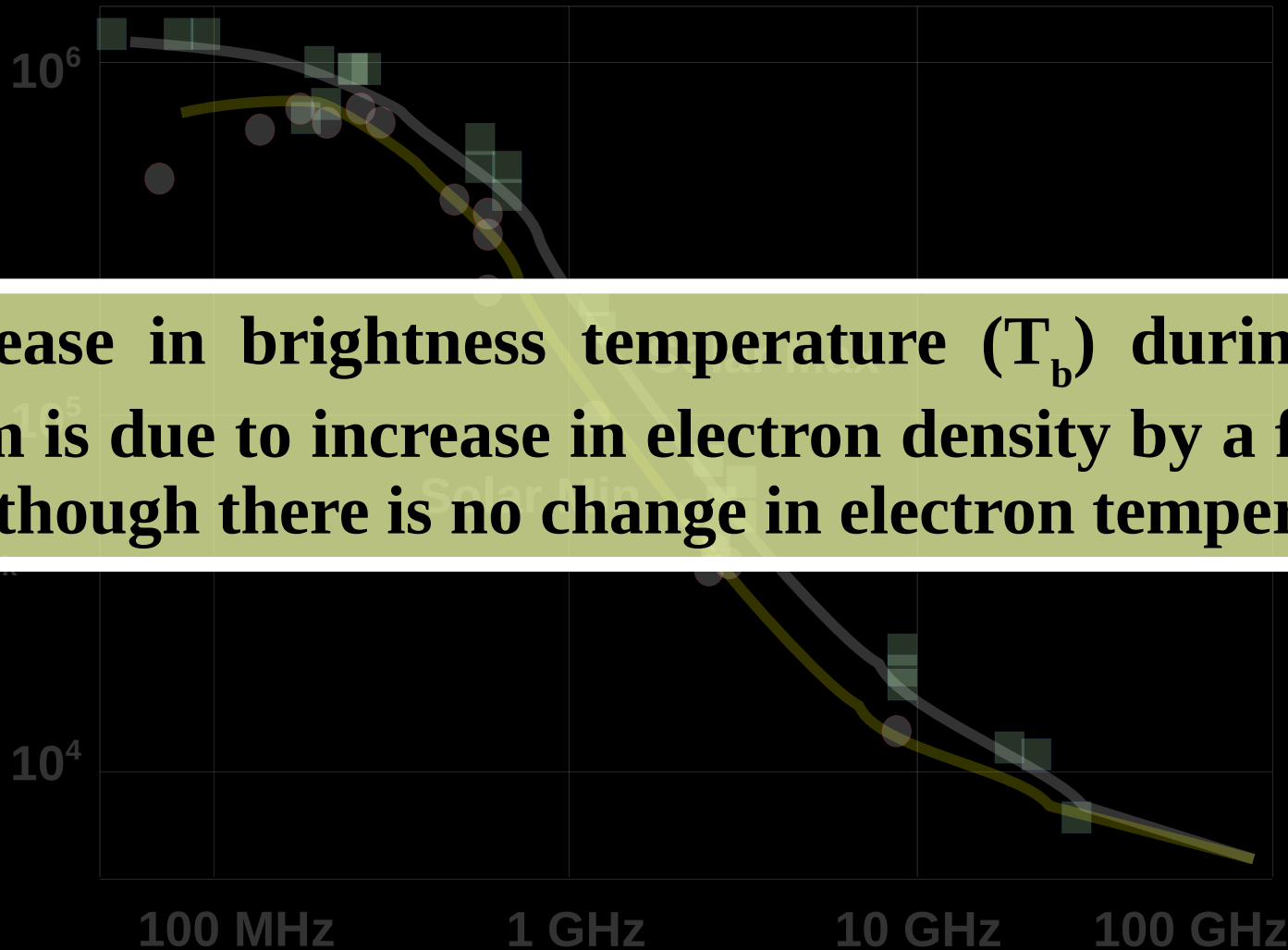
Smerd, S. F., *Au. J. Sci. Res.-A*, 3, 34 (1950)

# Quiet Sun Brightness Temperature (Solar Cycle IGY)



Allen, C. W., IAUS, 4 (1957)

## Quiet Sun Brightness Temperature (Solar Cycle IGY)

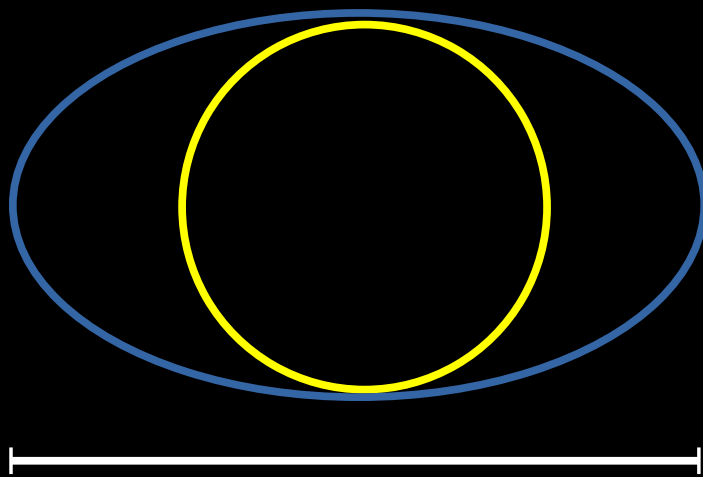


The increase in brightness temperature ( $T_b$ ) during solar maximum is due to increase in electron density by a factor  $\approx 1.5-2.0$  although there is no change in electron temperature.

Allen, C. W., IAUS, 4 (1957)

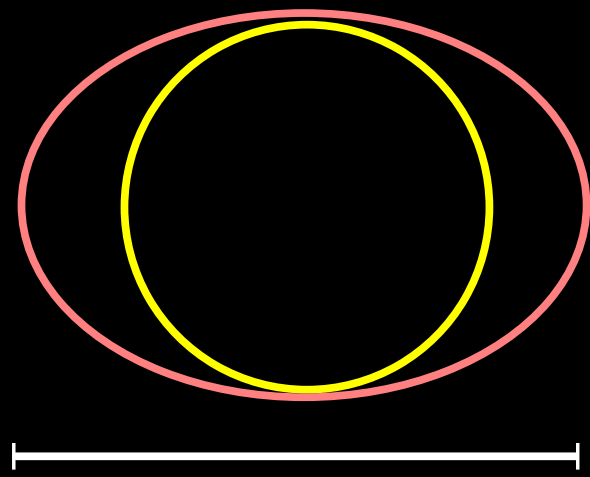
# Quiet Sun dimension vs Solar Cycle

Solar Maximum



$52' \pm 4'$

Solar Minimum



$42' \pm 3'$

Avignon et al., Compt. Rend., 255, 2859 (1961)

## Quiet Sun dimension vs Solar Cycle

1. During solar maximum the equatorial diameter of the radio Sun is maximum and reaches a minimum during solar minimum at any observing frequency (ex: 169 MHz / 1.77 meter) and the polar diameter does not change much.

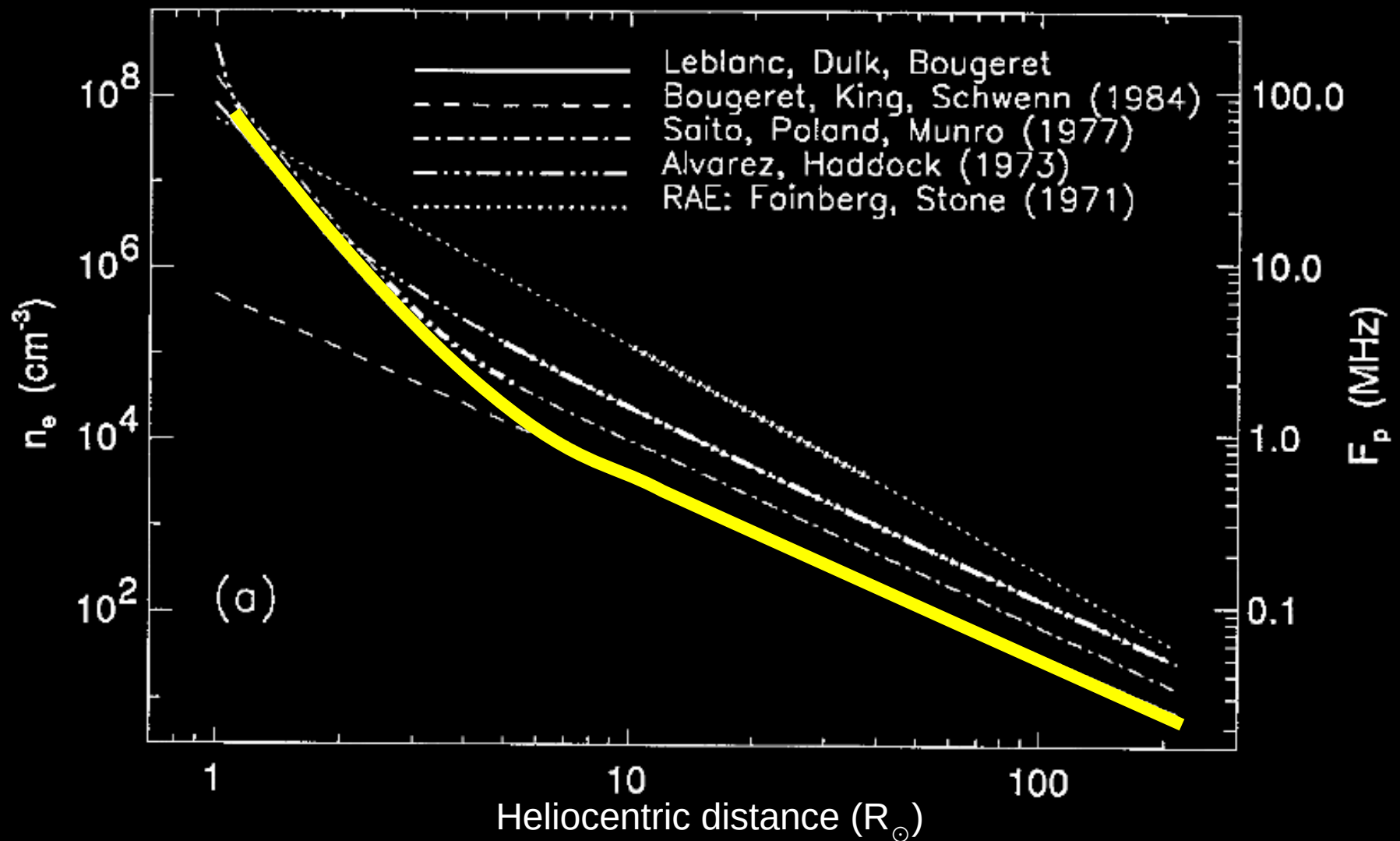
2. This is not the case with optical observations – during maximum it is spherical.

Avignon et al., Compt. Rend., 255, 2859 (1961)

## Coronal electron density models

1. By measuring the diameter of the Quiet Sun at different radio frequencies (from radio observations with frequencies greater than 15 MHz) and using the corresponding electron densities, the background coronal electron density models can be generated.
2. One should carefully remove the contribution from other structures to minimize the errors.
3. The active Sun data are used to determine density estimates with frequencies less than 15 MHz.

# Coronal electron density model (from Corona to 1 AU)



Leblanc et al., Sol. Phy., 183, 165 (1998)

## Coronal electron density model (from Corona to 1 AU)



$$N_e = 3.3 \times 10^5 r^{-2} + 4.1 \times 10^6 r^{-4} + 8.0 \times 10^7 r^{-6} \text{ cm}^{-3}$$

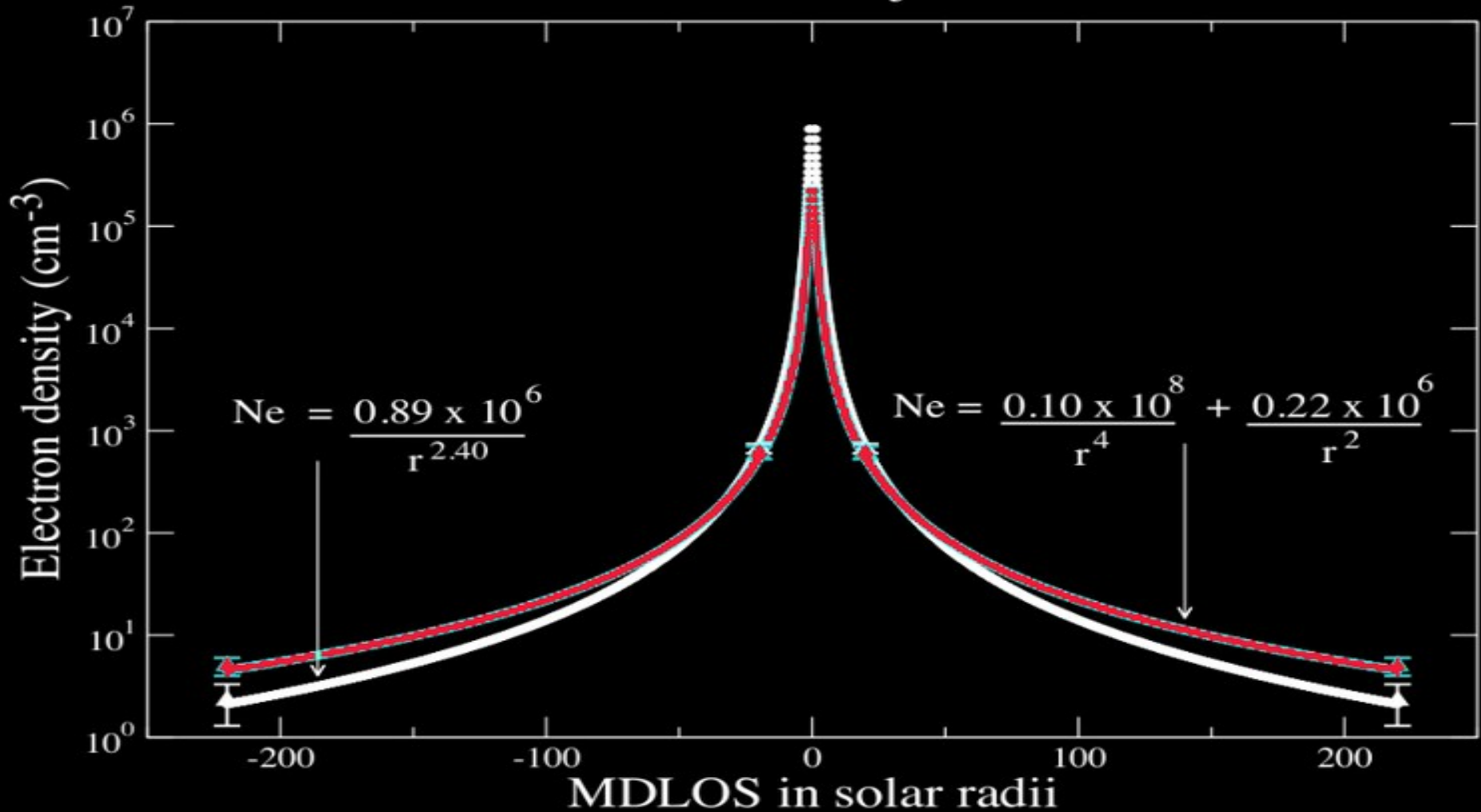
$N_e \rightarrow$  Electron number density

$r \rightarrow$  heliocentric distance (in Units of  $R_\odot$ )

Leblanc et al., Sol. Phy., 183, 165 (1998)

# Coronal electron density model (from Corona to 1 AU)

MEX 2008 conjunction



Verma et al., A&A, 550, A124 (2013)

## Coronal electron density model (from Corona to 1 AU)

MEX 2008 conjunction

This method measures the travel-time delay of radio signals between the spacecraft and the Earth station to determine the electron number density.

$$\Delta \tau = \frac{1}{2cn_{critic}(f)} \int_E^S N_e(L) dl$$

$\Delta \tau \rightarrow$  Travel-time delay

$E \rightarrow$  Earth Station

$S \rightarrow$  Satellite location (in Units of  $R_\odot$ )

$c \rightarrow$  Velcocity of light

$n_{critic} \rightarrow$  Critical ELeCtron density

$f \rightarrow$  Carrier frequency

Verma et al., A&A, 550, A124 (2013)

---

**There are other models  
from radio / WL observations**

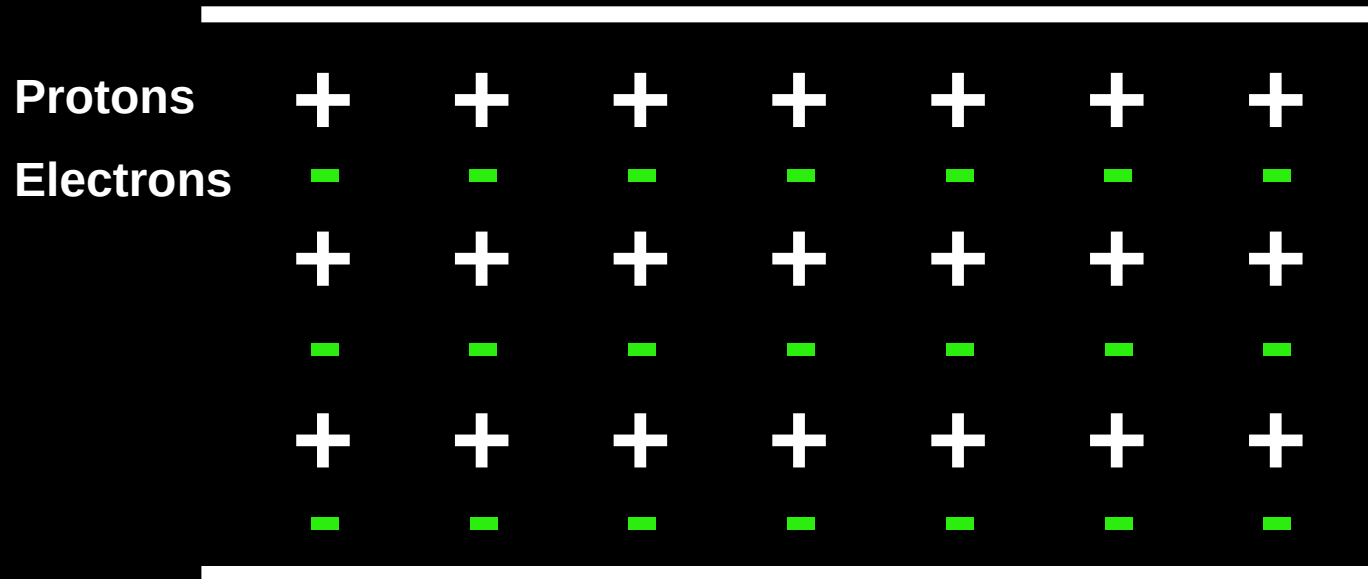
**Not discussed due to time constraint**

---

**Why Sun behaves differently  
at different frequency bands ??**

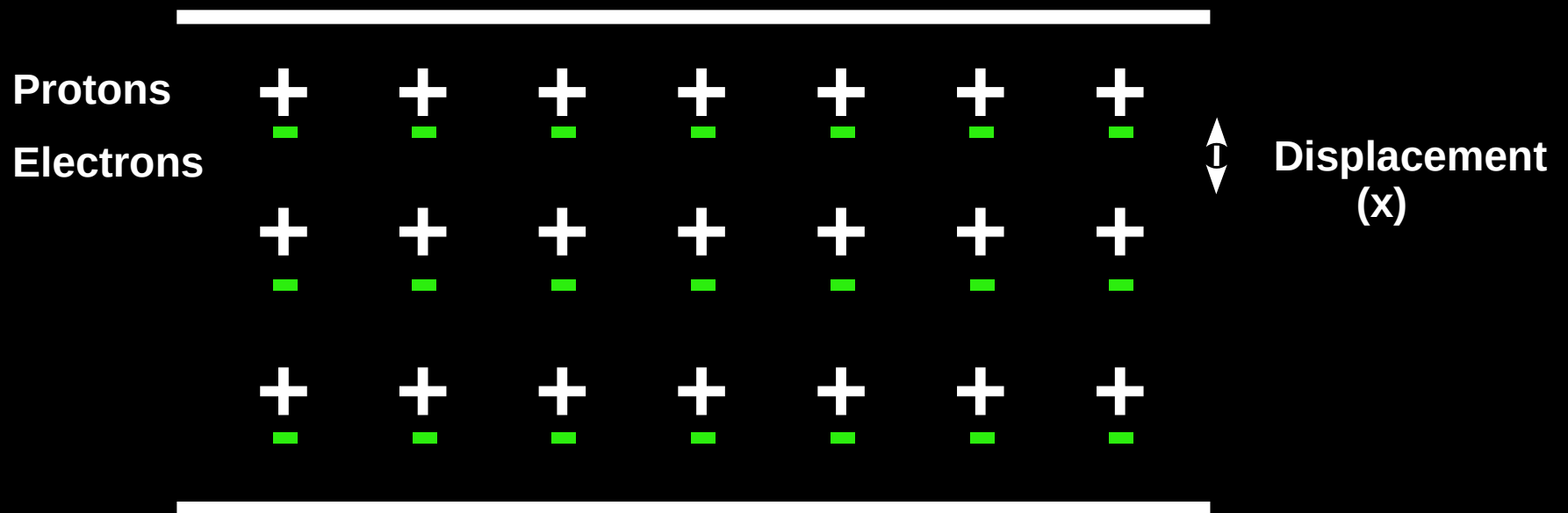
**Radio wave propagation in a plasma**

# Plasma oscillations – Plasma frequency



**Unit volume (Charge Neutrality) → Net Charge = 0**

# Plasma oscillations – Plasma frequency



$$F = ma = -eE$$

$$x \sim A \sin \omega t$$

$$\omega \rightarrow 2 \pi f_p$$

$$a = d^2x/dt^2$$

$\omega \rightarrow$  angular plasma frequency

$$f_p = (e^2 N_e / \pi m_e)^{1/2} \approx 9 N_e^{1/2}$$

## Radio wave propagation in a plasma medium

$$\mu = \sqrt{1 - \left(\frac{f_p^2}{f^2}\right)}$$

$\mu \rightarrow$  Refractive Index

$f_p \rightarrow$  plasma frequency

$f \rightarrow$  Observing frequency

$$f_p = \sqrt{\frac{N_e e^2}{\pi m_e}}$$

$N_e \rightarrow$  electron number density

$e \rightarrow$  electron charge

$m_e \rightarrow$  electron mass

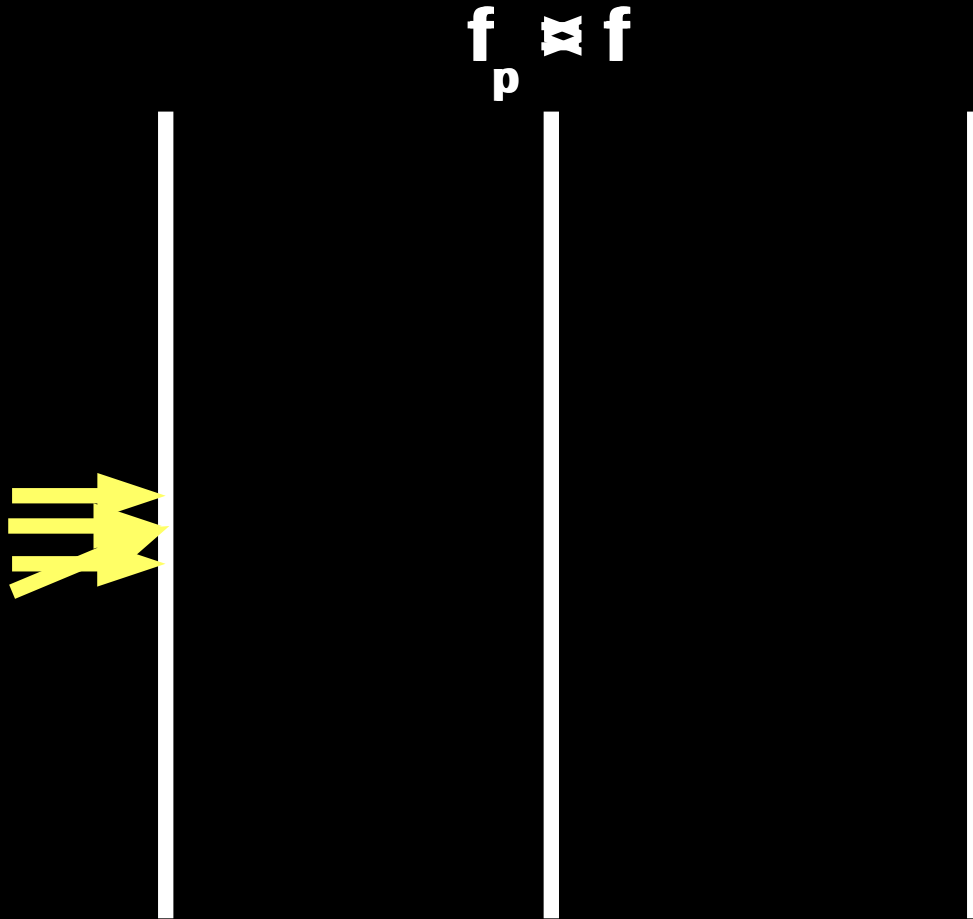
1. In a plasma medium the propagation of the radio wave is decided by the refractive index.
2. The plasma frequency to observing frequency ratio decides the nature of propagation.
3. The plasma frequency is dependent on  $N_e$

## Radio wave propagation in a plasma medium

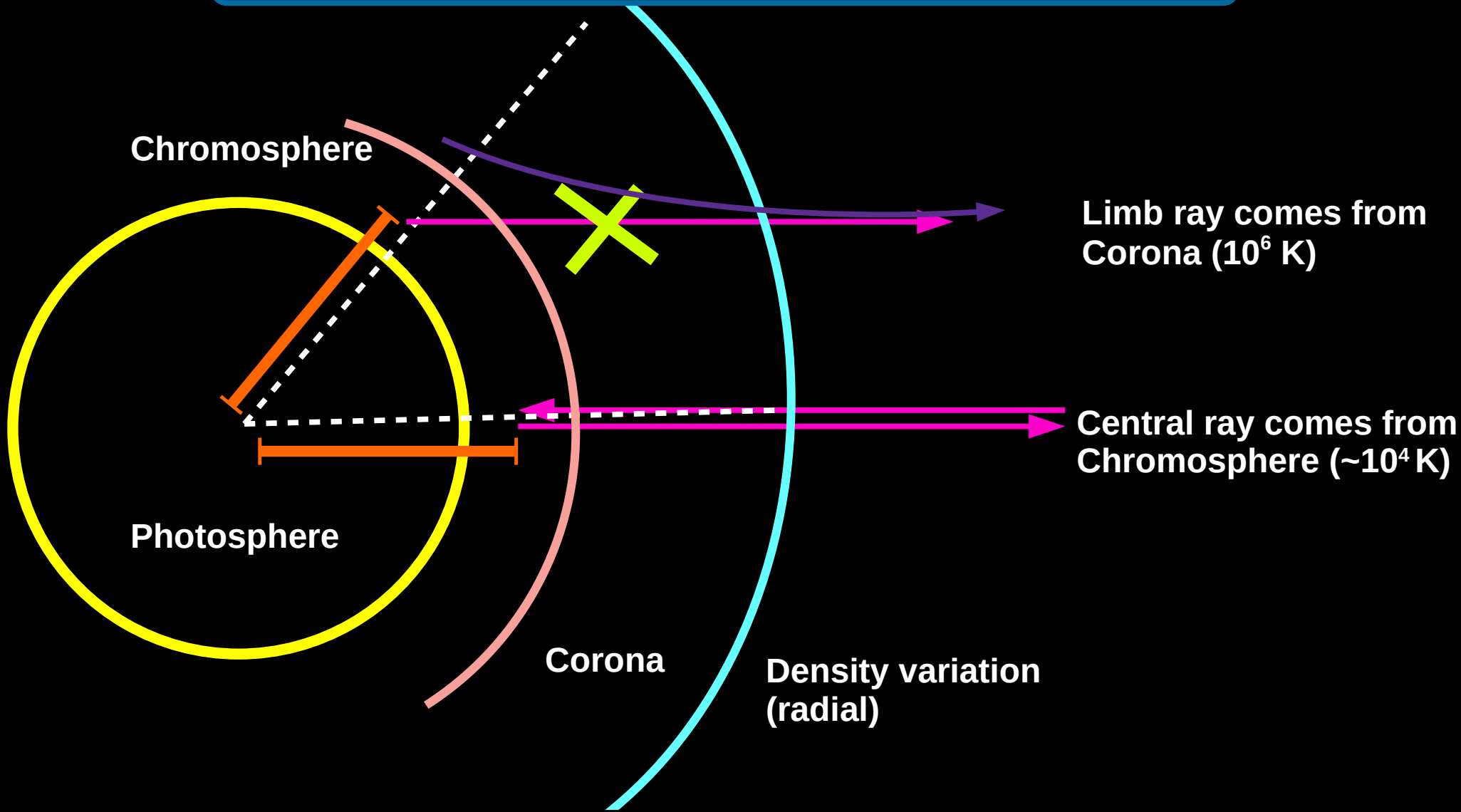
The nature of propagation is decided by  $f_p$  and  $f$ .

1.  $f_p < f \rightarrow$  Propagation (normal & Oblique)
2.  $f_p = f \rightarrow$  Absorption
3.  $f_p > f \rightarrow$  Reflection

# Radio wave propagation in a plasma medium



# Limb brightening at cm wavelengths



Jager et al., Au. J. Sci. Res.-A, 2, 322 (1949)

Aubier et al., A&A, 12, 435 (1971)

## Limb brightening at cm wavelengths

Chromosphere

The central ray at cm  $\lambda$ s reach up to the Chromosphere whereas the limb ray at cm  $\lambda$ s reach only the Corona. Hence limb brightening can be seen at cm  $\lambda$ s.

But, both central and limb rays at meter  $\lambda$ s reach up to the Corona. Hence limb darkening can only be seen at meter  $\lambda$ s.

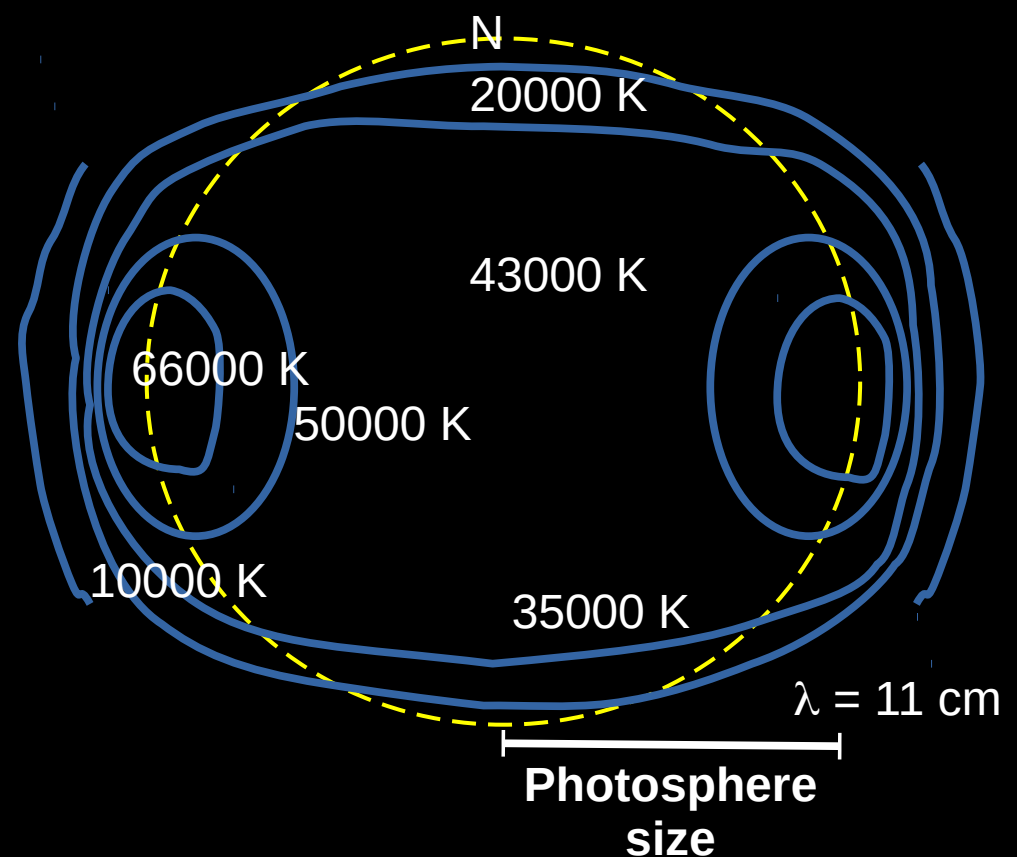
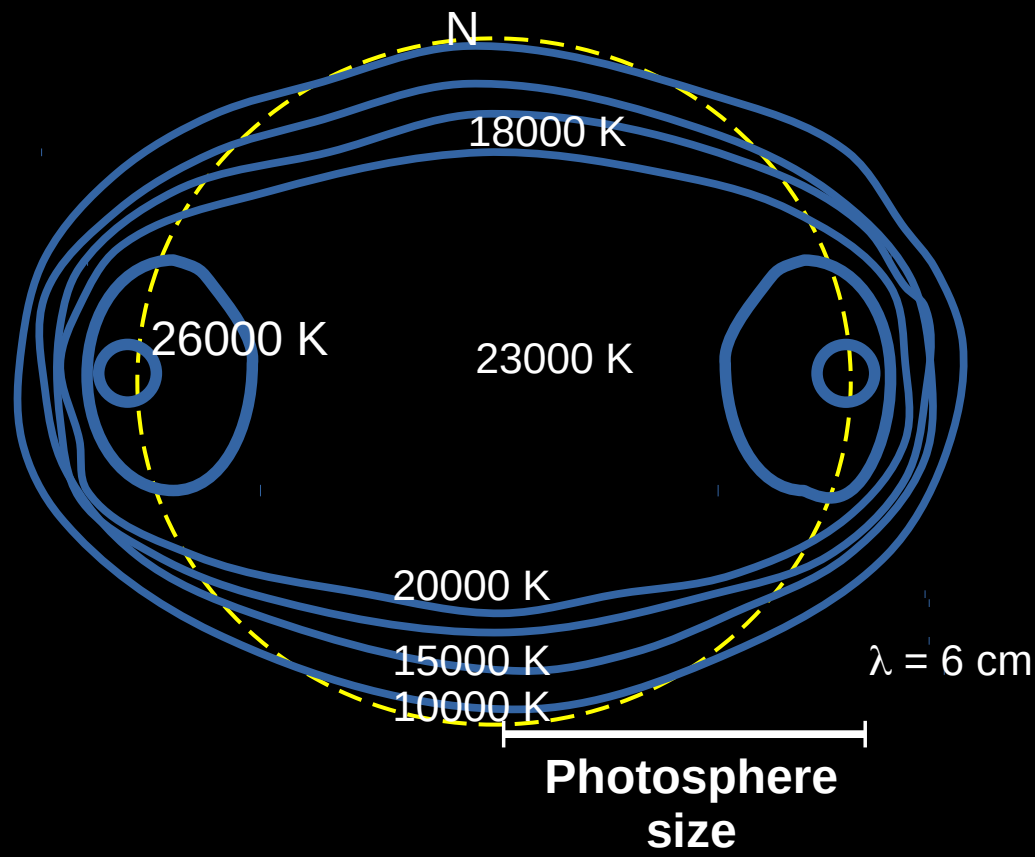
Corona

Density variation  
(radial)

Jager et al., Au. J. Sci. Res.-A, 2, 322 (1949)

Aubier et al., A&A, 12, 435 (1971)

# Limb brightening at cm wavelengths (Imaging)

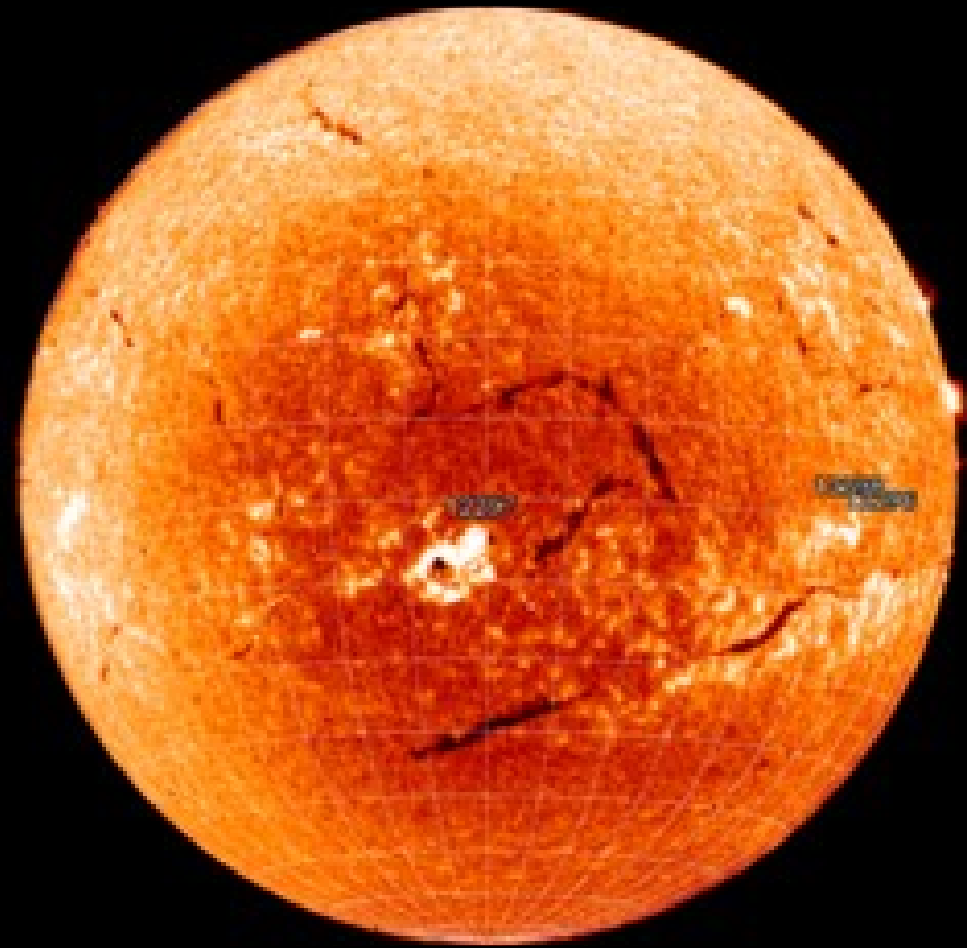
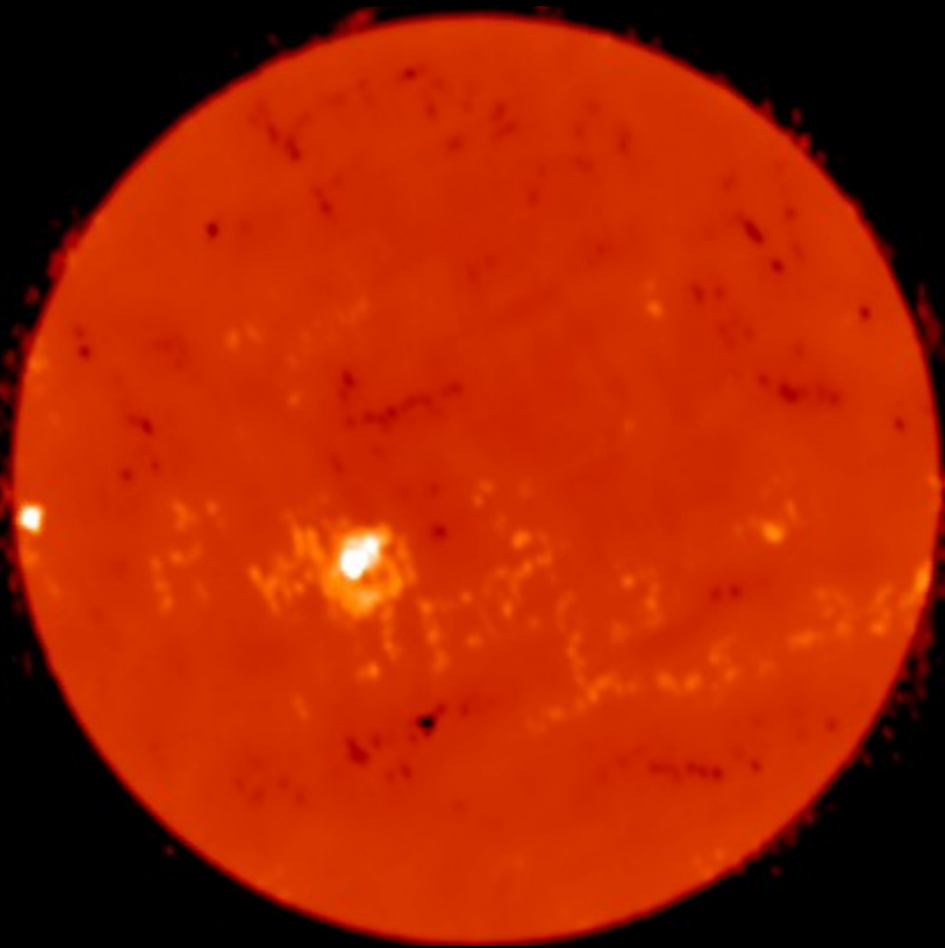


Ceballos, J. C. et al, *SoPh*, 22, 142 (1972)

**H $\alpha$  & cm- $\lambda$  radio observations**

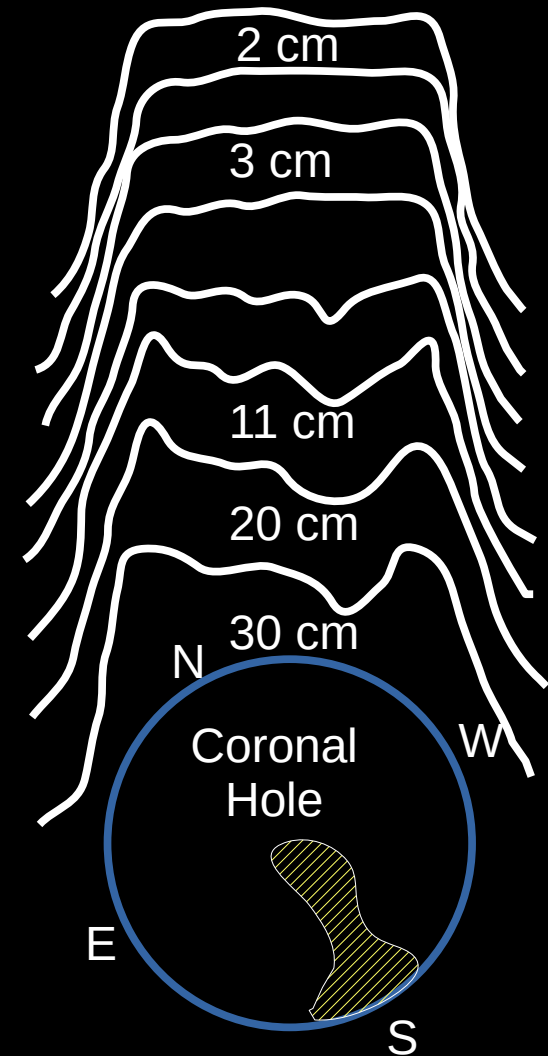
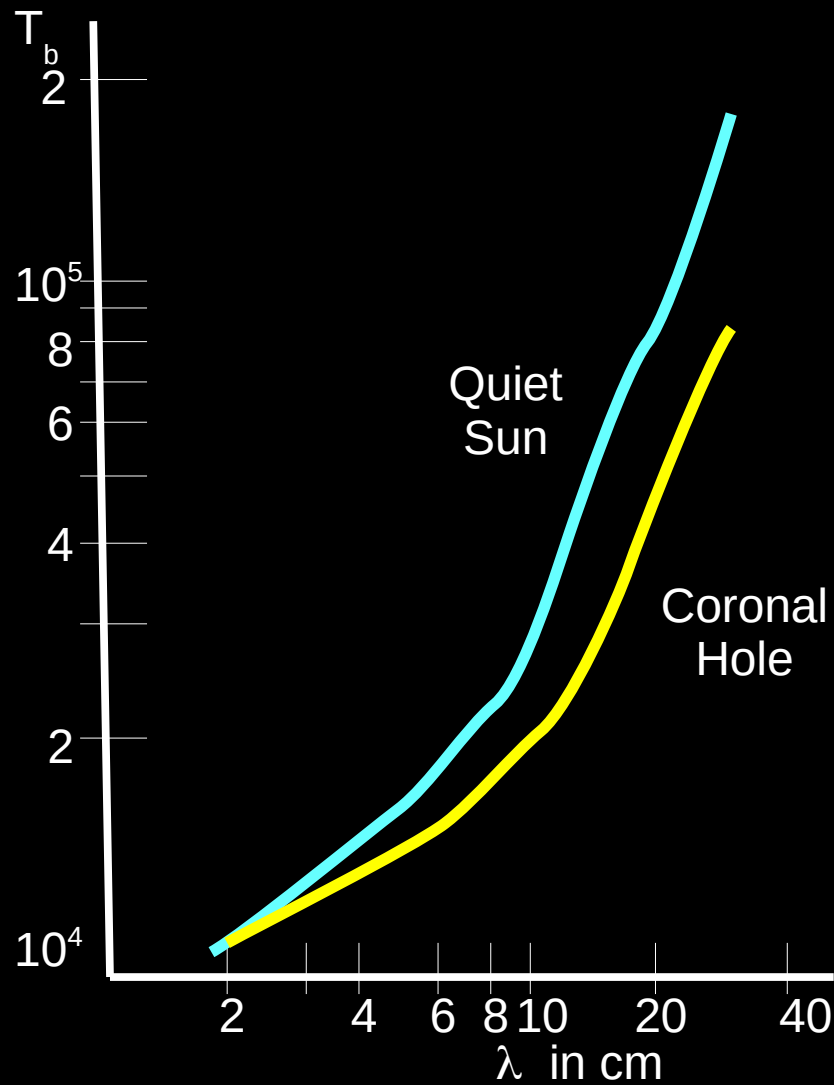
**Nobeyama Radioheliograph 17 GHz (R+L)**

**BBSO H $\alpha$**



**12/03/2015**

**2D radio observations (RATAN)**

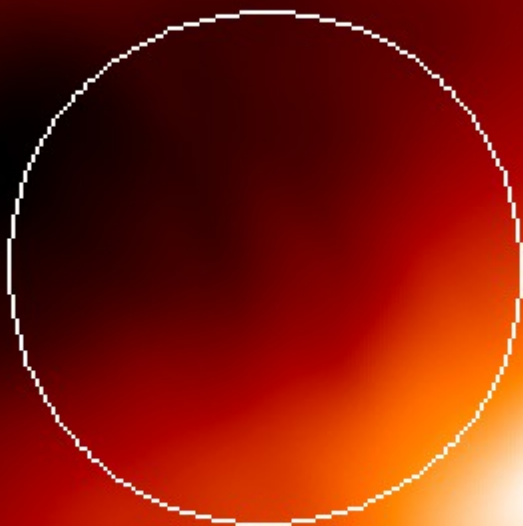


**Ceballos, J. C. et al, SoPh, 22, 142 (1972)**

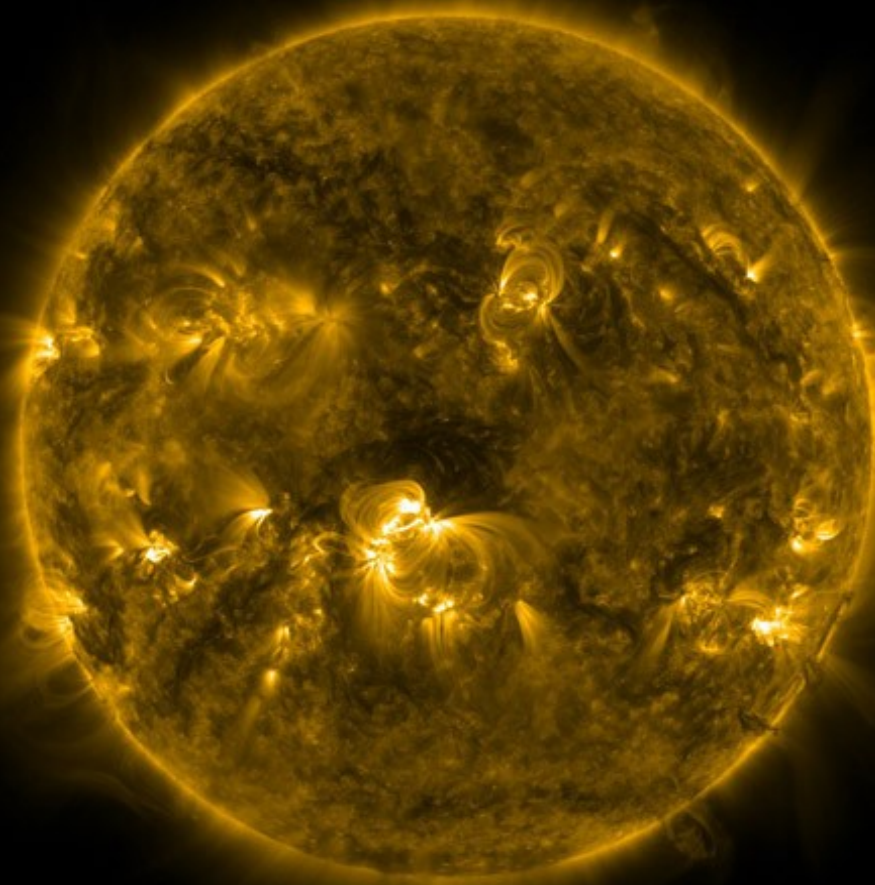
**Borovik, V. N et al. Sov. Ast. 34, 522 (1990)**

**EUV & decimeter- $\lambda$  radio observations**

NANCAY RADIOHELIOGRAPH  
327.0 Mhz



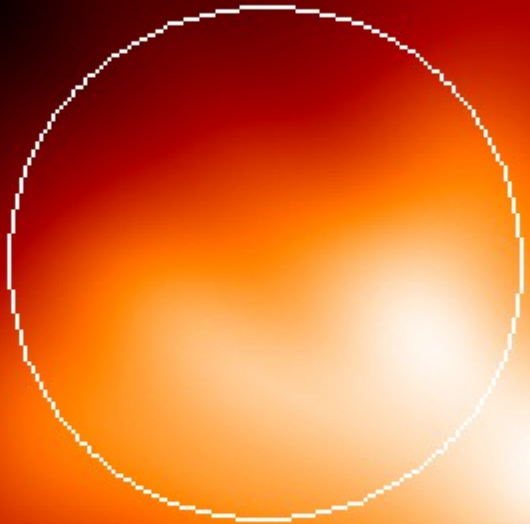
SDO AIA / 171 Å



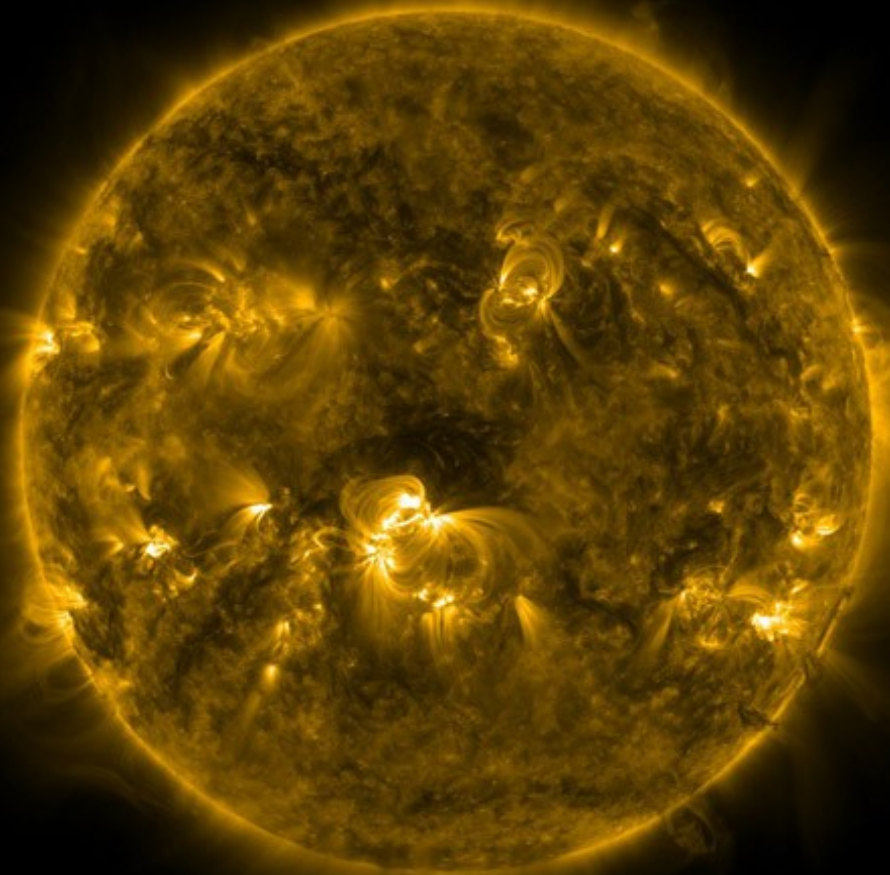
20-Jan-2015 13:43:41 UT

**EUV & meter- $\lambda$  radio observations**

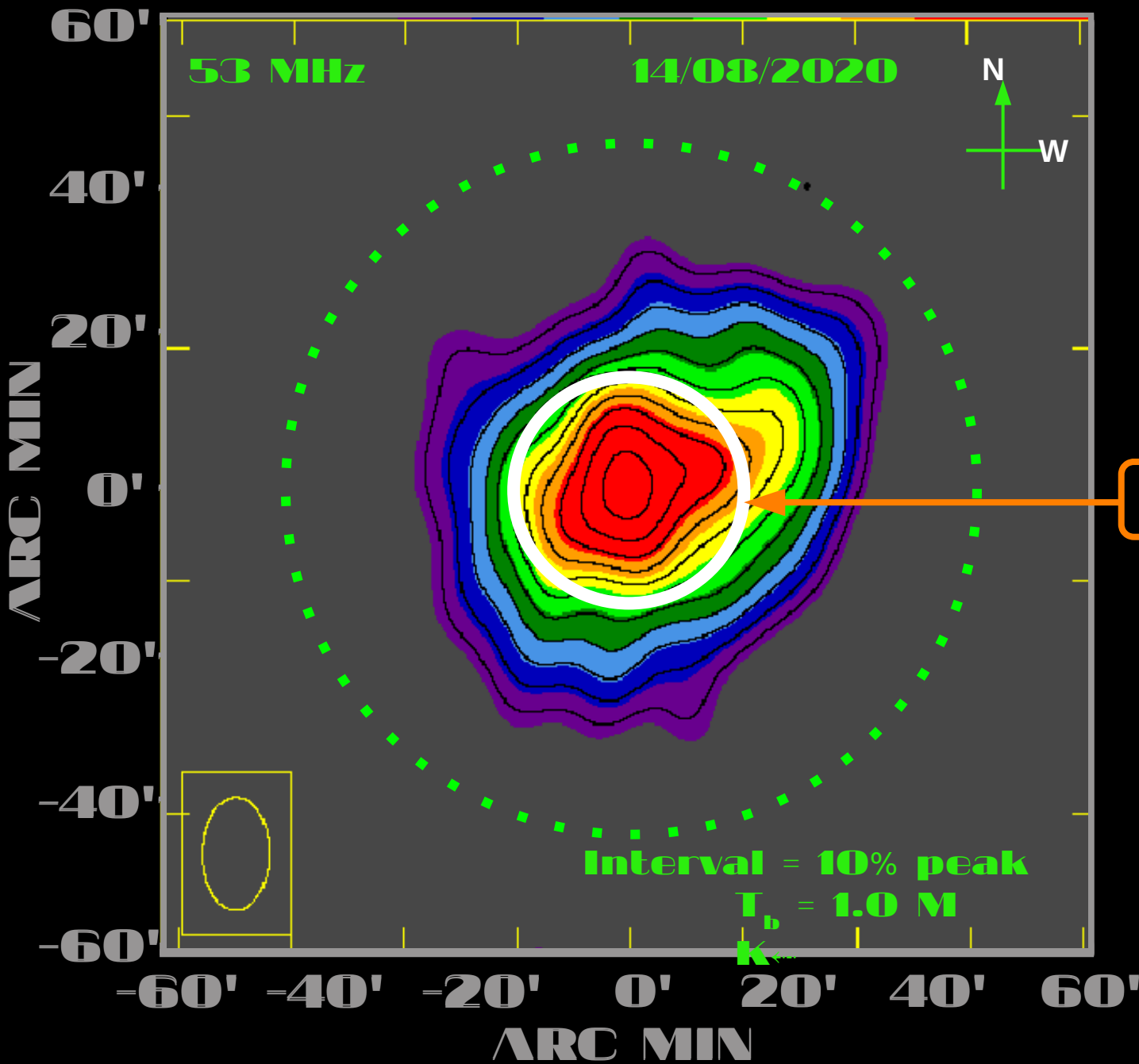
NANCAY RADIOHELIOGRAPH  
150.9 Mhz



SDO AIA / 171 Å



20-Jan-2015 13:43:41 UT



# GRAPH

Snap shots over  
Wide frequency range  
Coronal Tomography

Visible disk

Simultaneous  
53 MHz & 80 MHz

# Quiet Sun Image

**LASCO C2 & GRAPH radio observations**



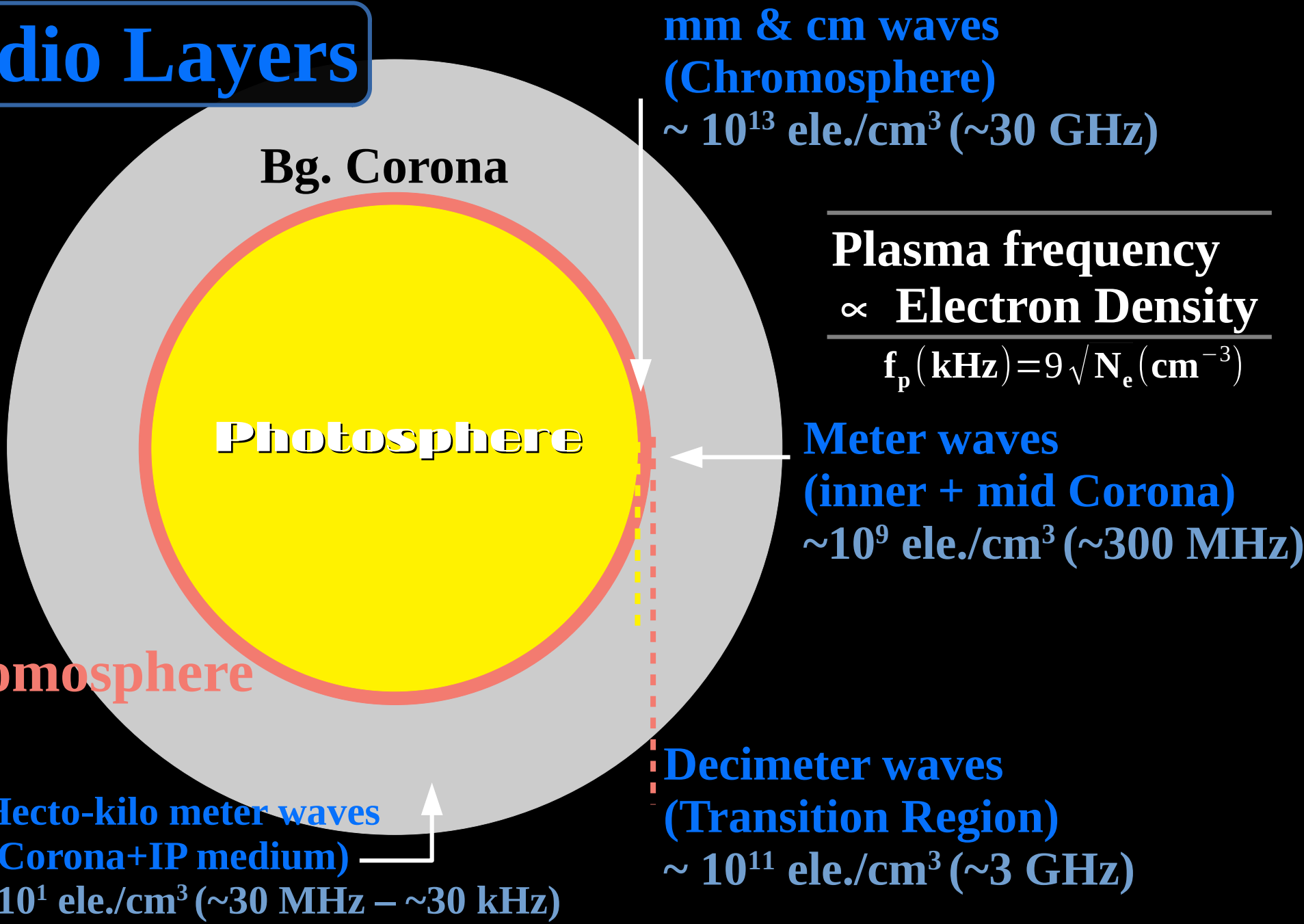
**14/08/2020**

---

**So, one can have the  
following simplified  
background coronal schematic**

**Just to remember / recollect easily**

# Radio Layers



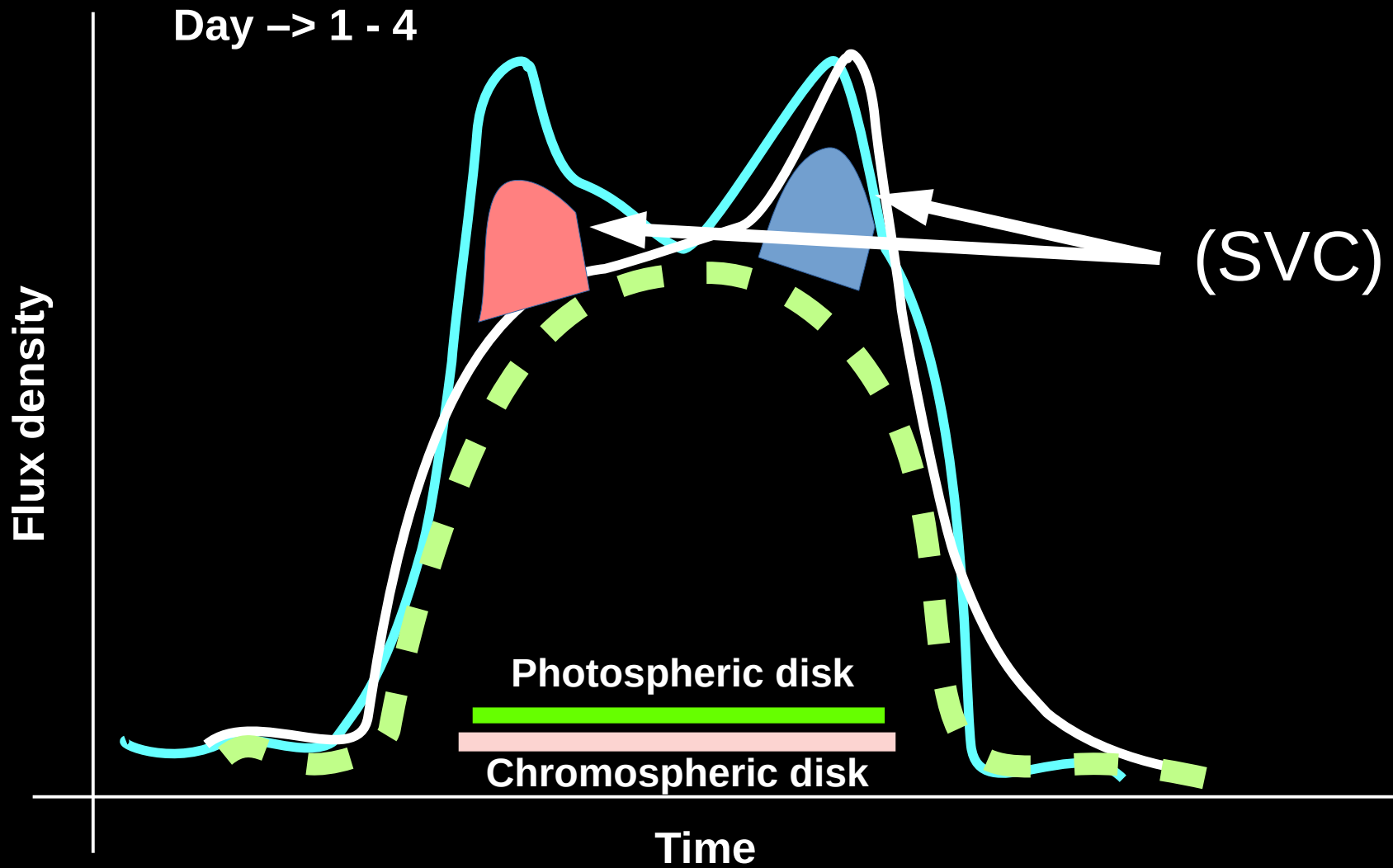
# The Slowly Varying Component

2

## The Slowly Varying Component

# The Slowly Varying Component

# Components above the Quiet Sun



Boischot, A., *Ann d' Astrophys.*, 21, 273 (1958)

## Components above the Quiet Sun

Day → 1 - 4

### Slowly Varying Component :

Sources that remain after the background is removed. These correspond to the active centers present above the photosphere.

These last for few hours to days and were found to vary slowly and hence the name SVC.

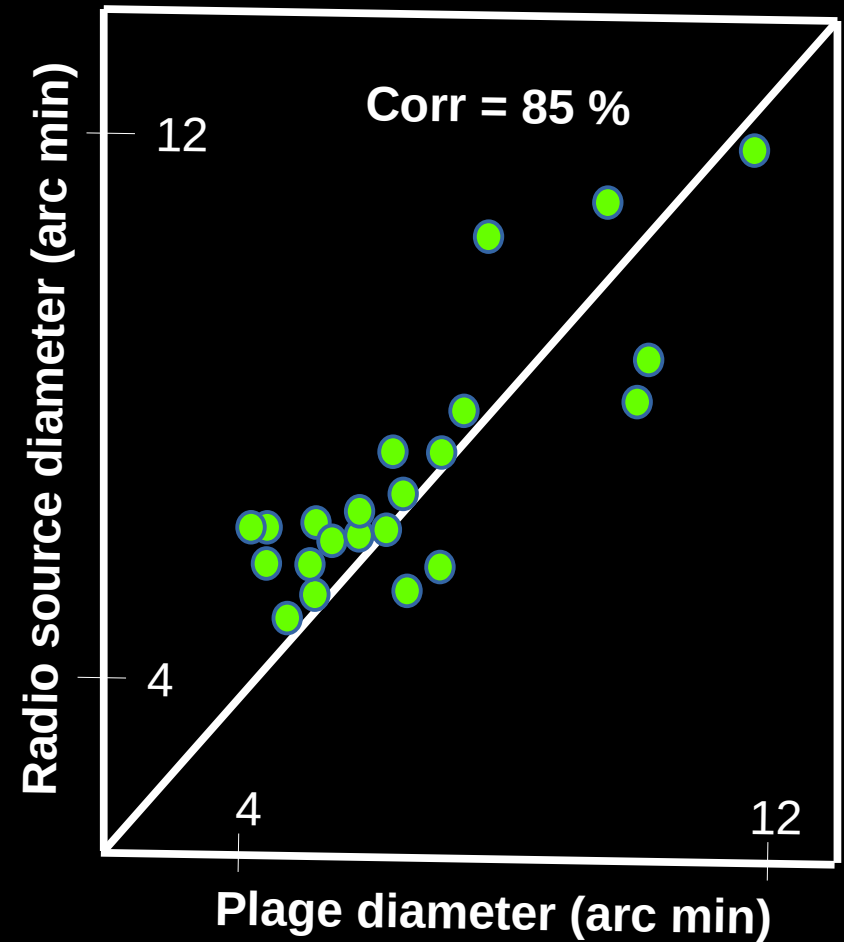
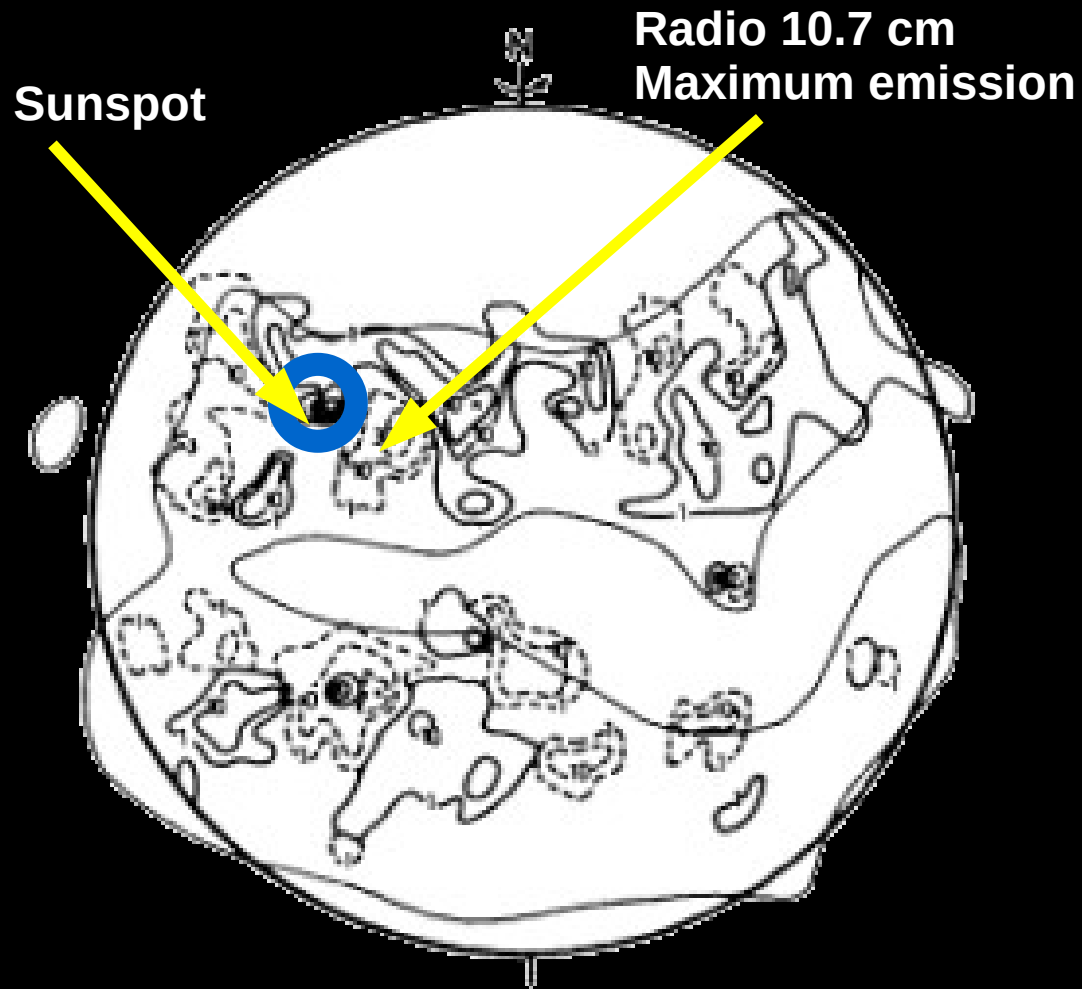
**Boischot, A., Ann d' Astrophys., 21, 273 (1958)**

---

**If the SVCs have lifetime of hours to days, then are they related to Sunspots ??**

**Since Sunspots live for a solar rotation !!**

# Slowly Varying Component (SVC)



Christiansen et al., IAU, 9, 108 (1959)

## Slowly Varying Component (SVC)

### Slowly Varying Component :

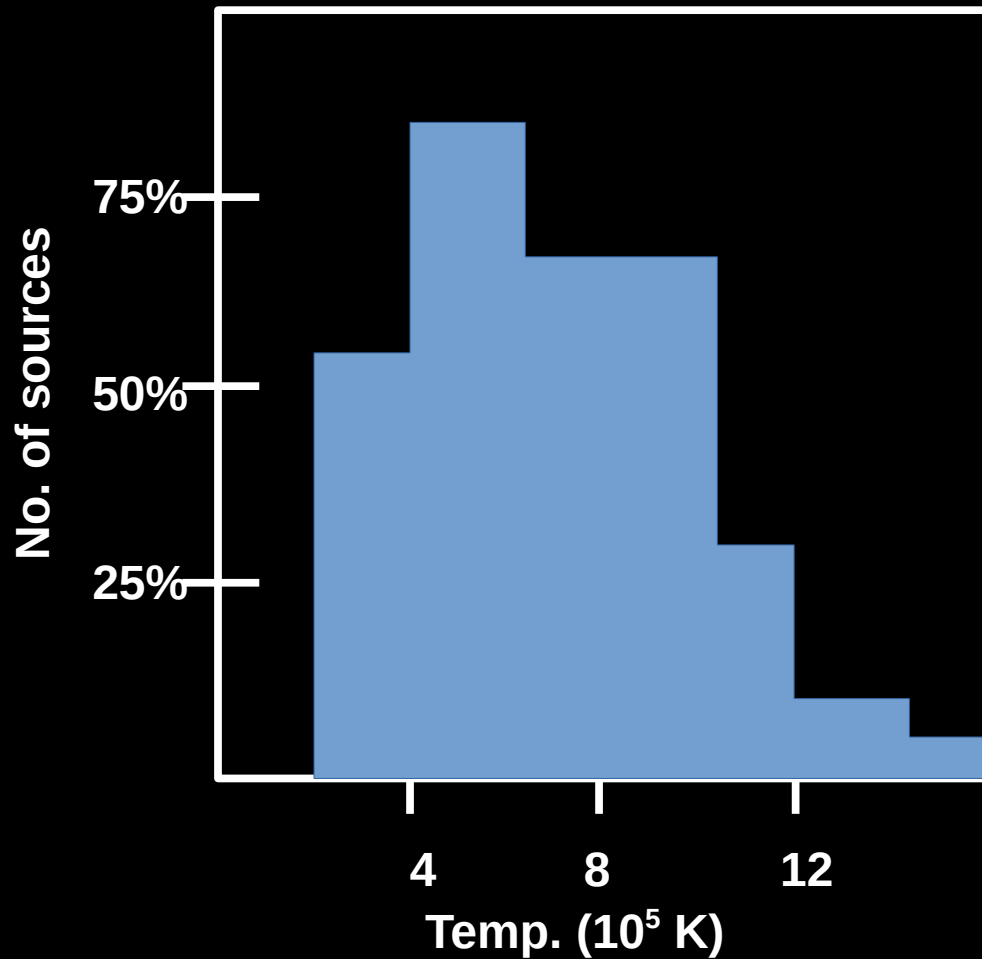
Superposition of radio contours on the magnetogram and plage image implies the radio emission is closely associated with plages around sunspots rather than the sunspots themselves.

The higher correlation coefficient between the plage and the radio source diameter is an indication of their close association.

Christiansen et al., IAU, 9, 108 (1959)

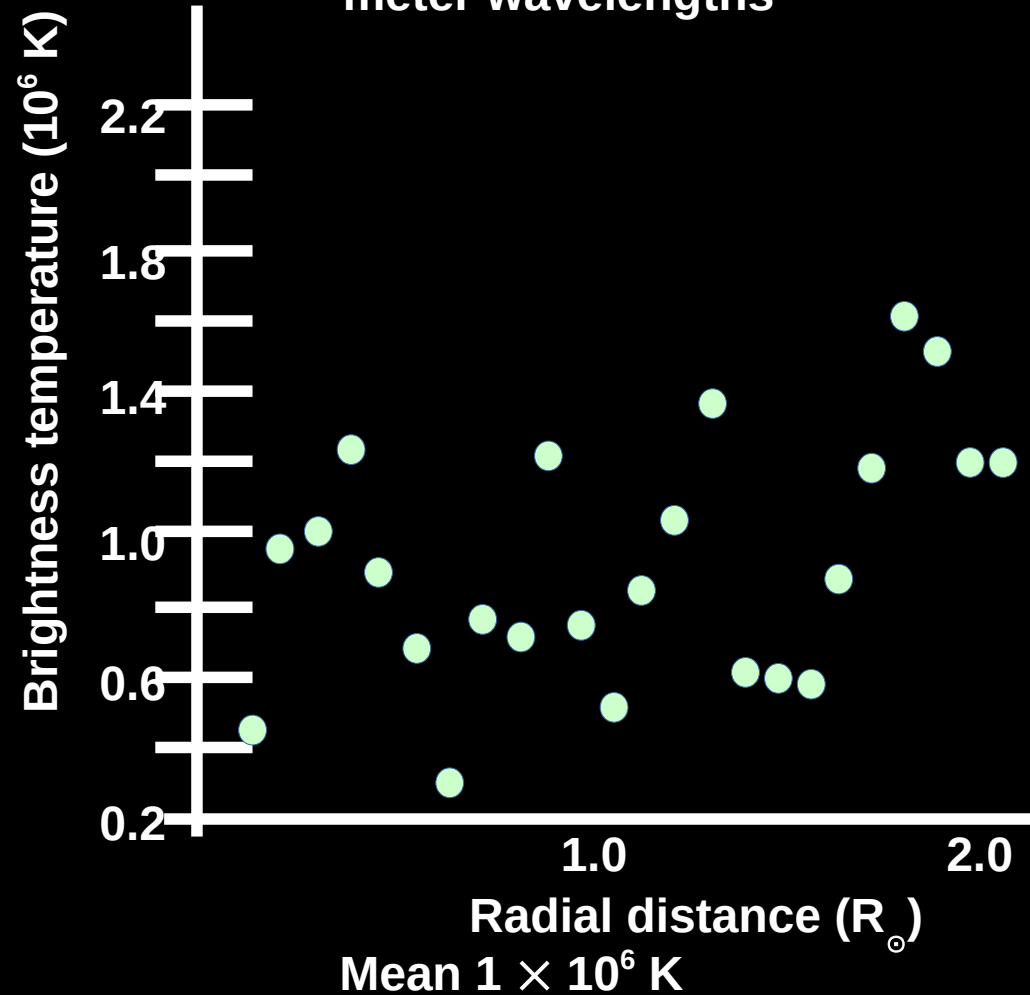
# SVC – Brightness temperature

cm wavelengths



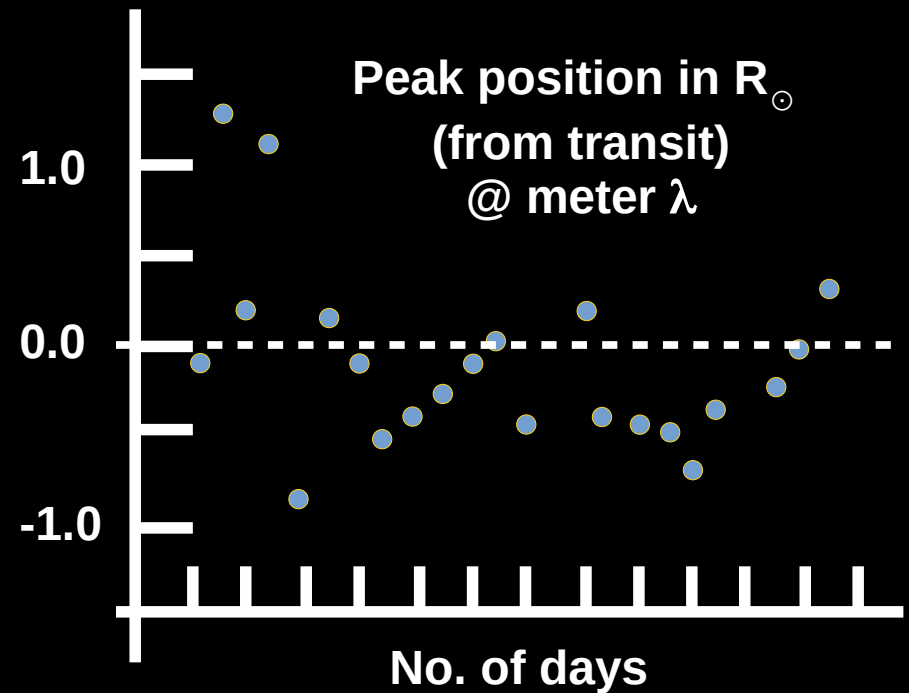
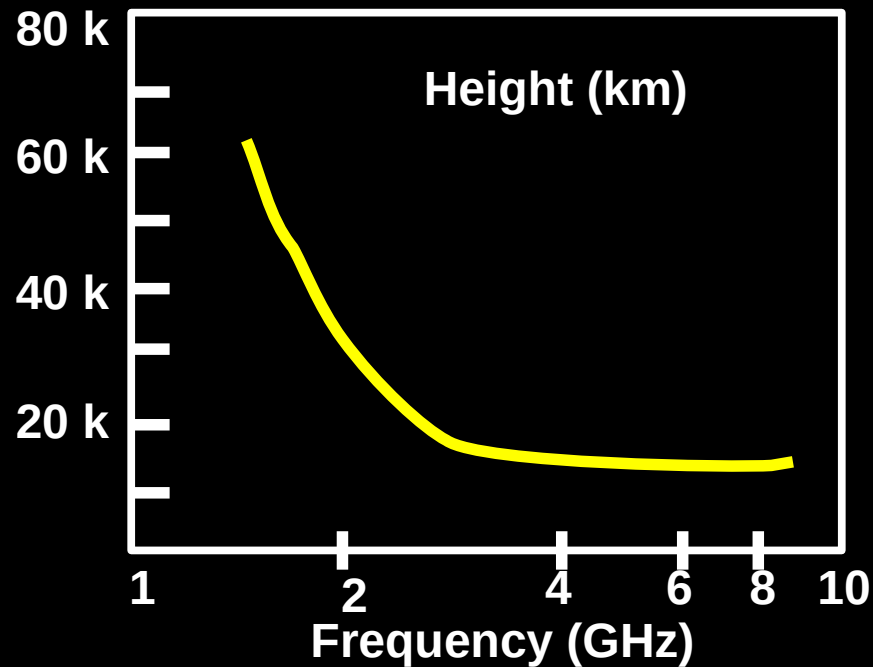
**Christiansen et al., IAU, 9, 108 (1959)**

meter wavelengths



**Sastry et al., SoPh, 73, 363 (1981)**

## SVC – Source heights

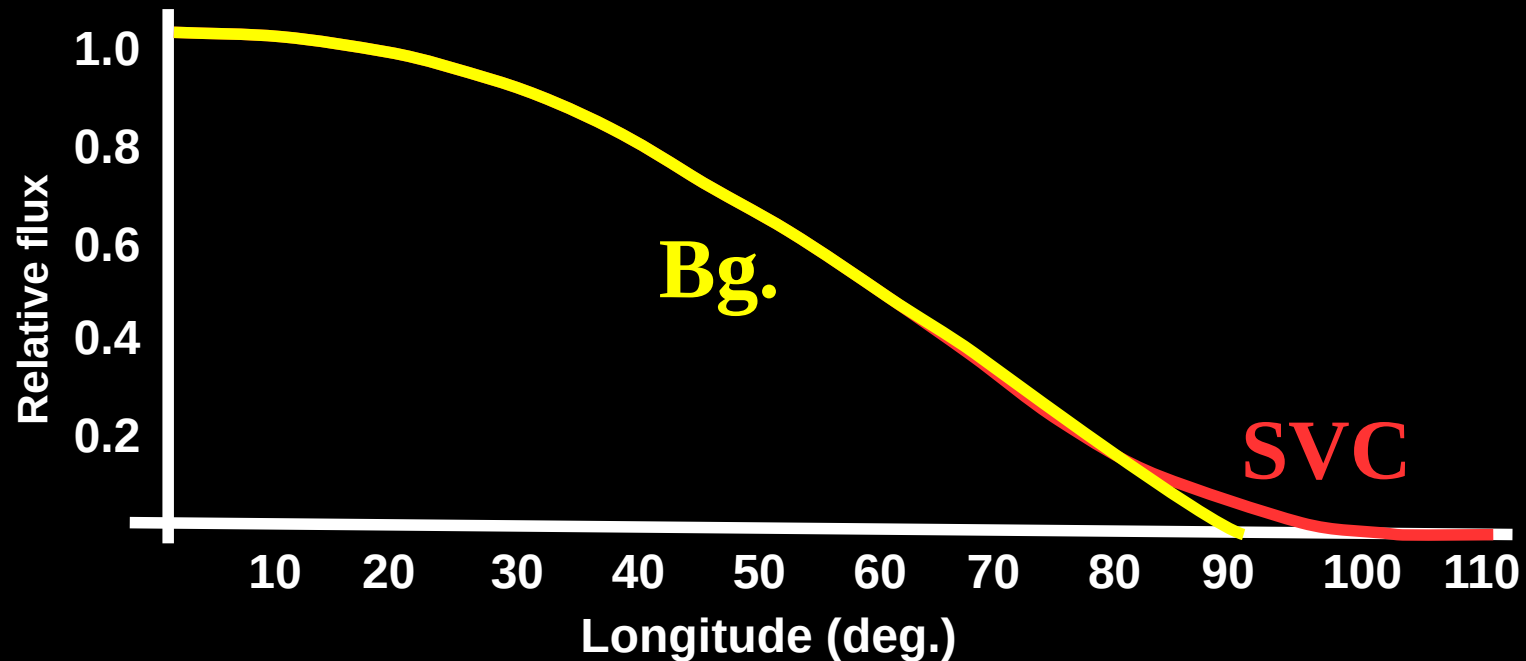


At high frequencies the source height is lesser as compared to that of low frequencies. The high frequency sources are in the chromosphere and the low frequency sources are in the corona.

Christiansen et al., IAU, 9, 108 (1959)

Sastry et al., SoPh, 73, 363 (1981)

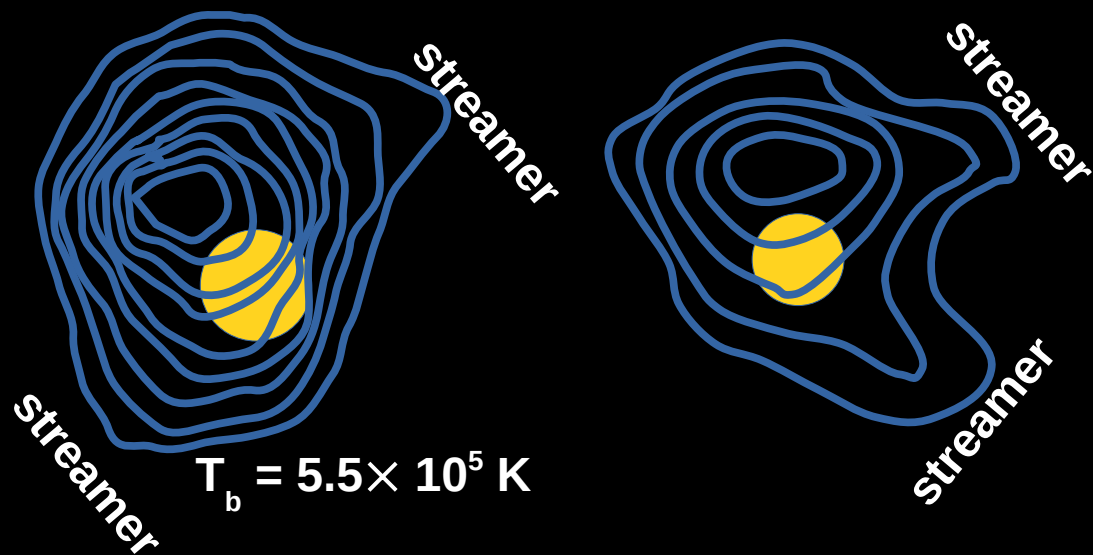
## SVC – Source Structure



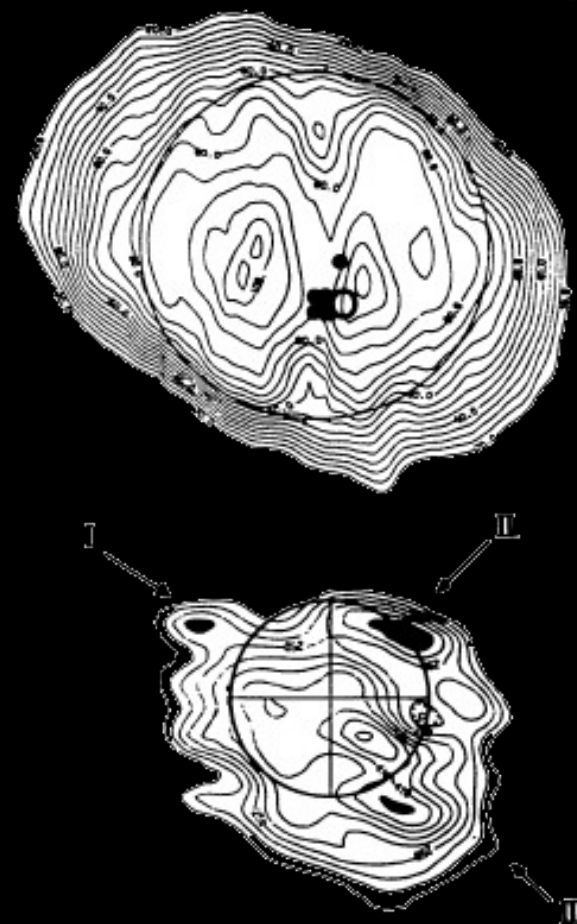
The SVC source diameter is very small (about  $10^{\circ}$ - $20^{\circ}$ ) - This implies that the source is likely a narrow current sheet located above coronal streamers.

# SVC – Imaging Observations

Decameter (34.5 MHz) observations



Meter wave (169 MHz) observations



Sastry, Ch. V. et al., SoPh, 87, 391, 1983

Lantos, P. et al. SoPh, 112, 325, 1987

## SVC – Imaging Observations

Meter wave (169 MHz) observations

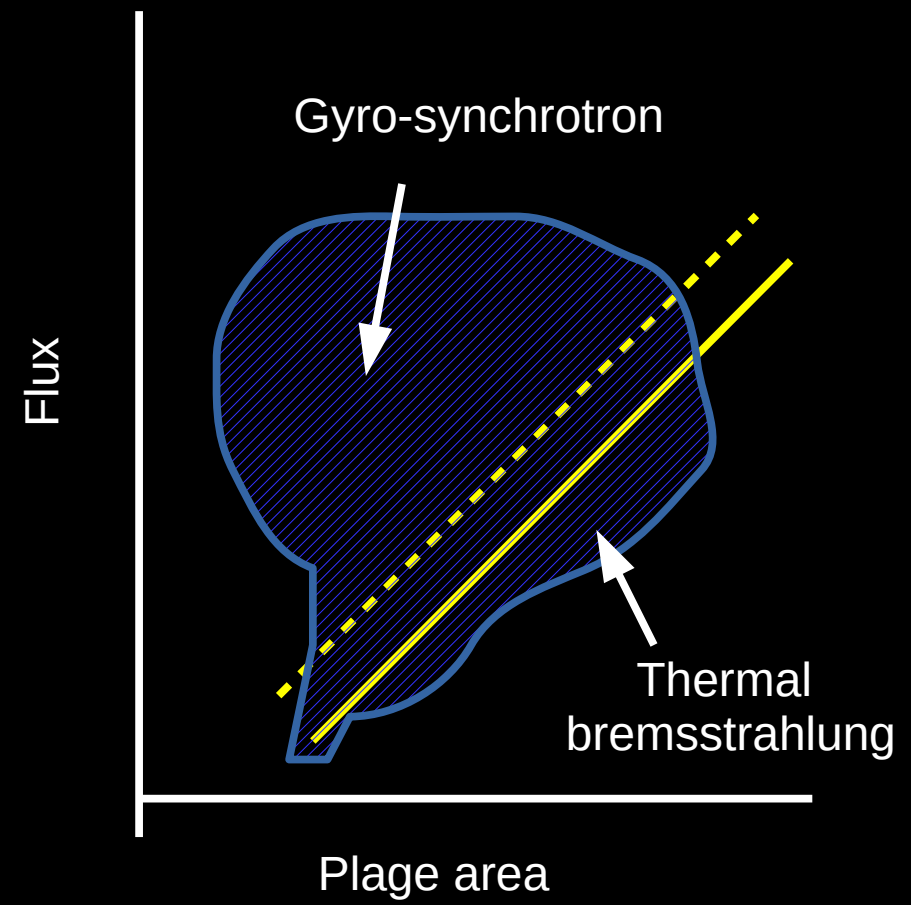
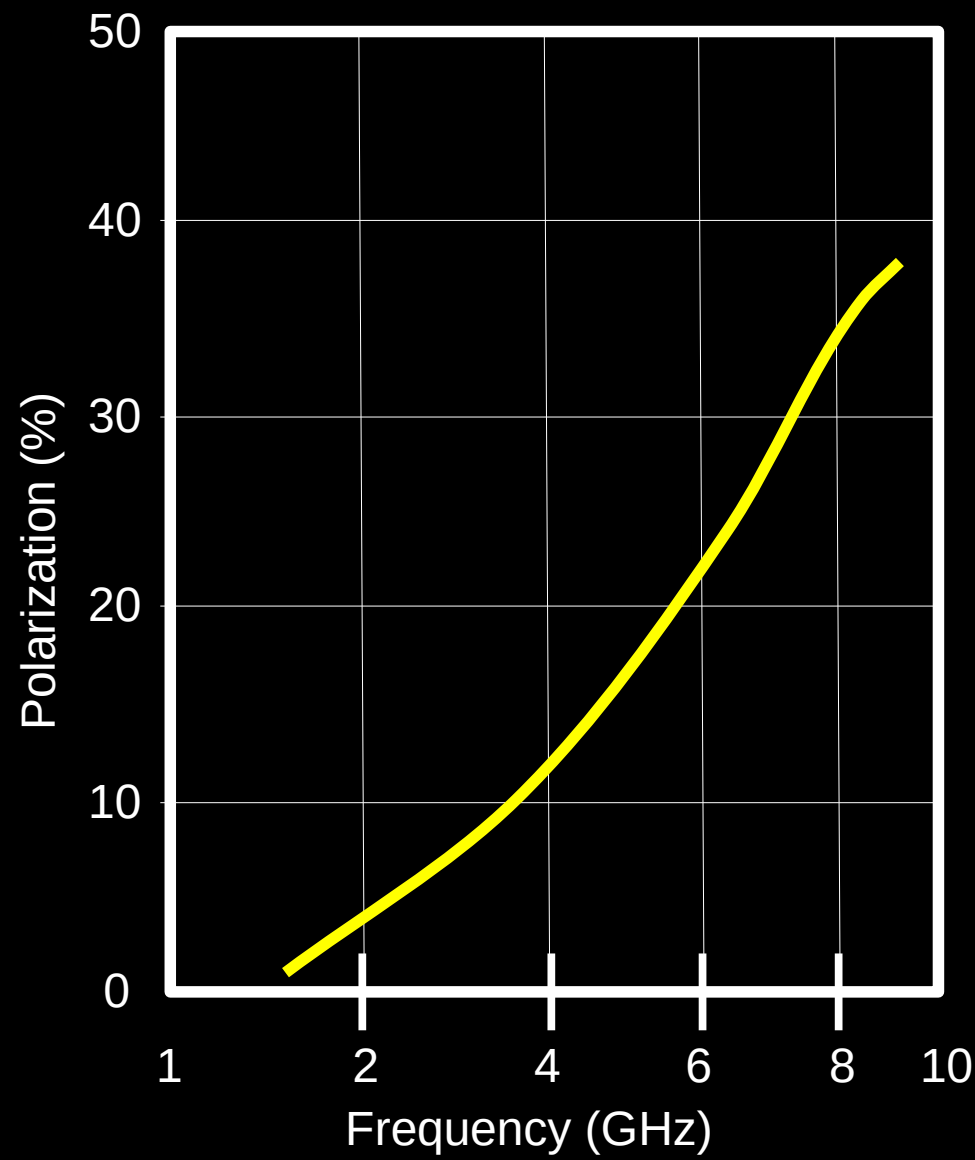
Decameter (34.5 MHz) observations

Radioheliograms made at 169 MHz / meter & decameter (34.5 MHz) wavelengths show the presence of SVC components on top of coronal loops, streamers, etc. This is in addition to those radio emission above plage areas of the chromosphere.

Sastry, Ch. V. et al., SoPh, 87, 391, 1983

Lantos, P. et al. SoPh, 112, 325, 1987

# SVC – Polarization & Nature of Emission



**Tapping et al., SoPh, 199, 217, 2001**

## **SVC – Polarization & Nature of Emission**

- 1. The electron gyro-resonance theory explains satisfactorily about the observed degree of circular polarization.**
- 2. It appears that radiation at the gyro-frequency ( $\omega_g = eB/m$ ) and its harmonics emitted by thermal electrons in a dense region over the sunspot group can account for the intensity and polarization spectrum. The mechanism requires an average magnetic field of 500 Gauss at about 20000 km above photosphere and an electron temperature of  $\sim 2 \times 10^6$  K.**

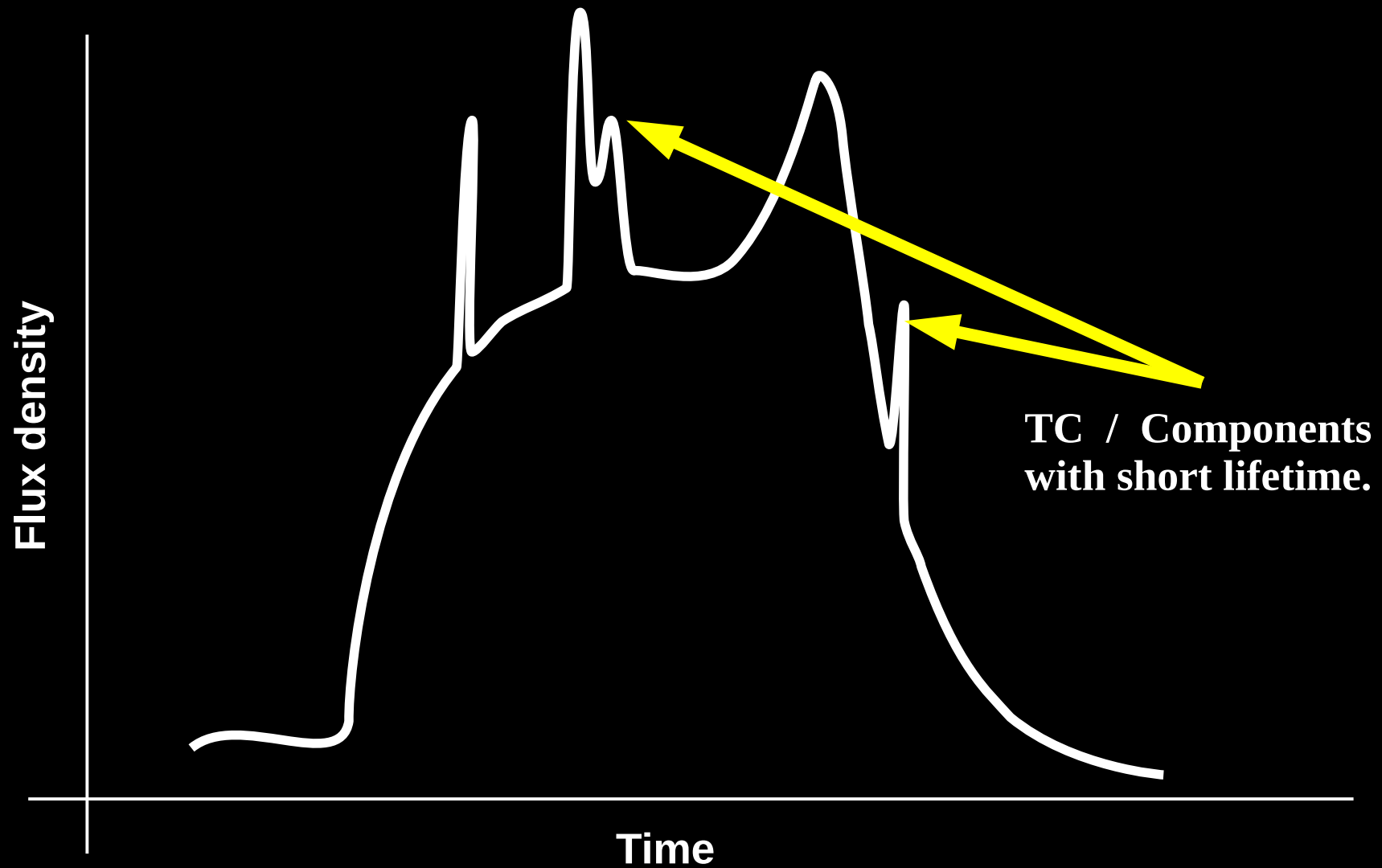
# The Transient Component

## ③

# The Transient Component

# The Transient Component

## The Transient Component / Outburst



## The Transient Component / Outburst

1. A sudden increase in the observed radio brightness ( $T_b \gg \gg 10^6 \text{ K}$ ).
2. It lasts for few seconds to minutes.
3. It is called as a radio surge or transient or outburst or simply radio burst. One can call this as a radio flare as well.

Based on the wavelength of origin they are classified into :

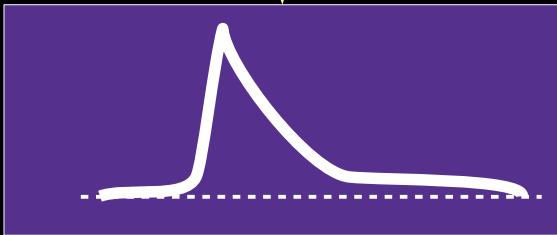
1. Centimeter wave radio bursts
2. Decimeter wave radio bursts
3. Meter & Decameter wave radio bursts
4. Hecto & kilometer wave radio bursts

Time

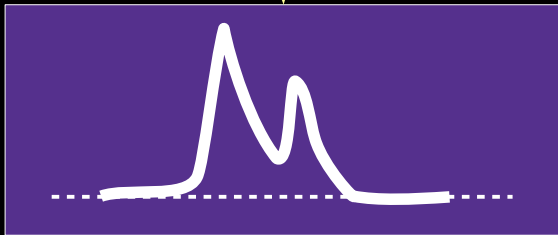
# The cm-λ radio bursts

cm-λ radio bursts

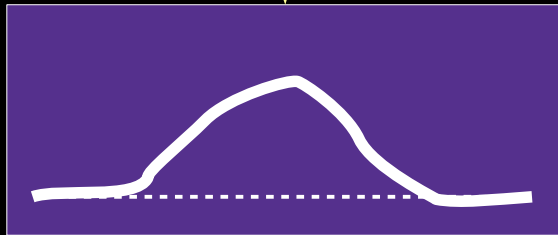
Type-A : Simple burst



Type-B : Post- burst



Type-C : Gradual rise and fall

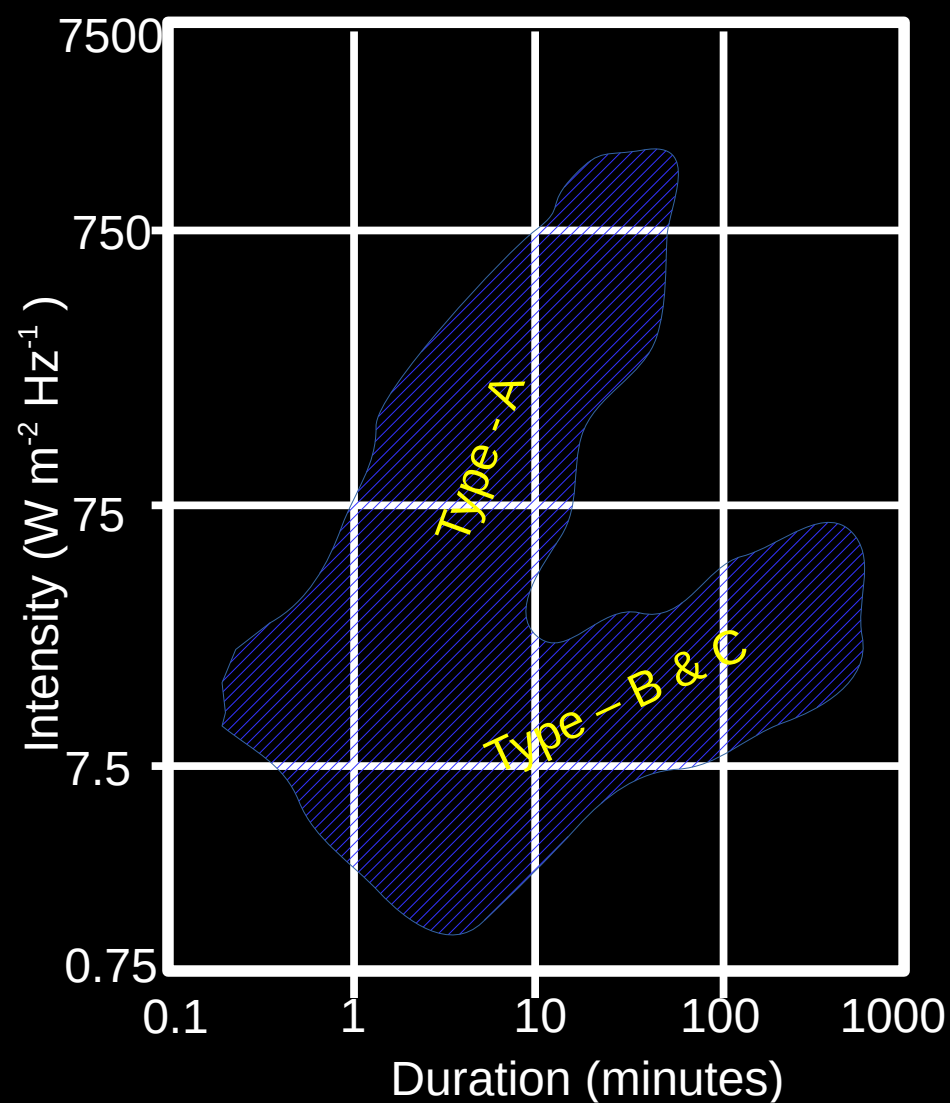
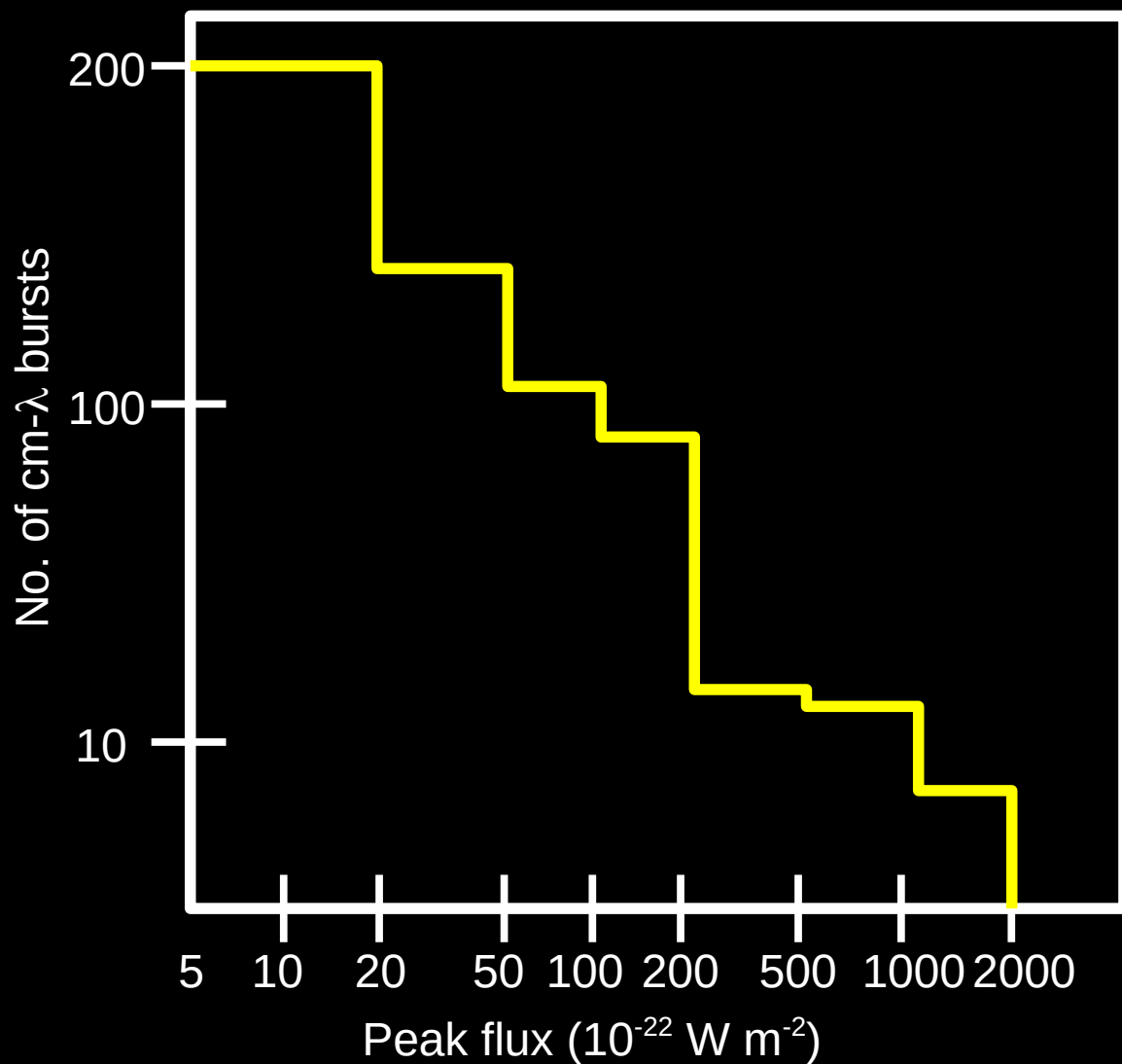


Nature → Rise very  
 Duration → 1-5 minutes  
 Polarization → partial  
 Source size → 1'.5  
 $T_b \rightarrow 10^6$  K (for weak)  
 Emission → non-thermal gyro-synchrotron

Nature → group of simple  
 Duration → several minutes  
 Polarization → partially circular  
 Source size → > 3'.0  
 $T_b \rightarrow 10^5 - 10^9$  K (strong)  
 Emission → thermal bremsstrahlung

Nature → increase and decrease gradually  
 Duration → few tens of minutes  
 Polarization → partially circular  
 Source size → < 1'.0  
 $T_b \rightarrow 10^6$  K  
 Emission → thermal bremsstrahlung

# The cm- $\lambda$ radio bursts – Flux & duration statistics



**Covington, C. Paris symposium on Radio Astronomy, 159 (1959)**

## The cm- $\lambda$ radio bursts : General Properties

1. The location of the sources : 4' – 6' above photosphere and move rarely; Size : 1' - 4'; Polarization : 5 % - 40 %.
2. Bursts that gradually rise and fall often occur near simultaneously with H-alpha flare indicate the heating and compression of the flare region.
3. The weak impulsive bursts originate in the coronal plasma of Chromospheric density with a local temperature of  $10^6$  K.
4. The strong impulsive bursts are either due to gyro-synchrotron or non-thermal bremsstrahlung by super-thermal electrons from flare ejected plasma.
5. The electrons producing cm bursts by bremsstrahlung and synchrotron also produce bremsstrahlung x-ray bursts of low and high energy.

## **The cm- $\lambda$ radio bursts : Microwave bursts**

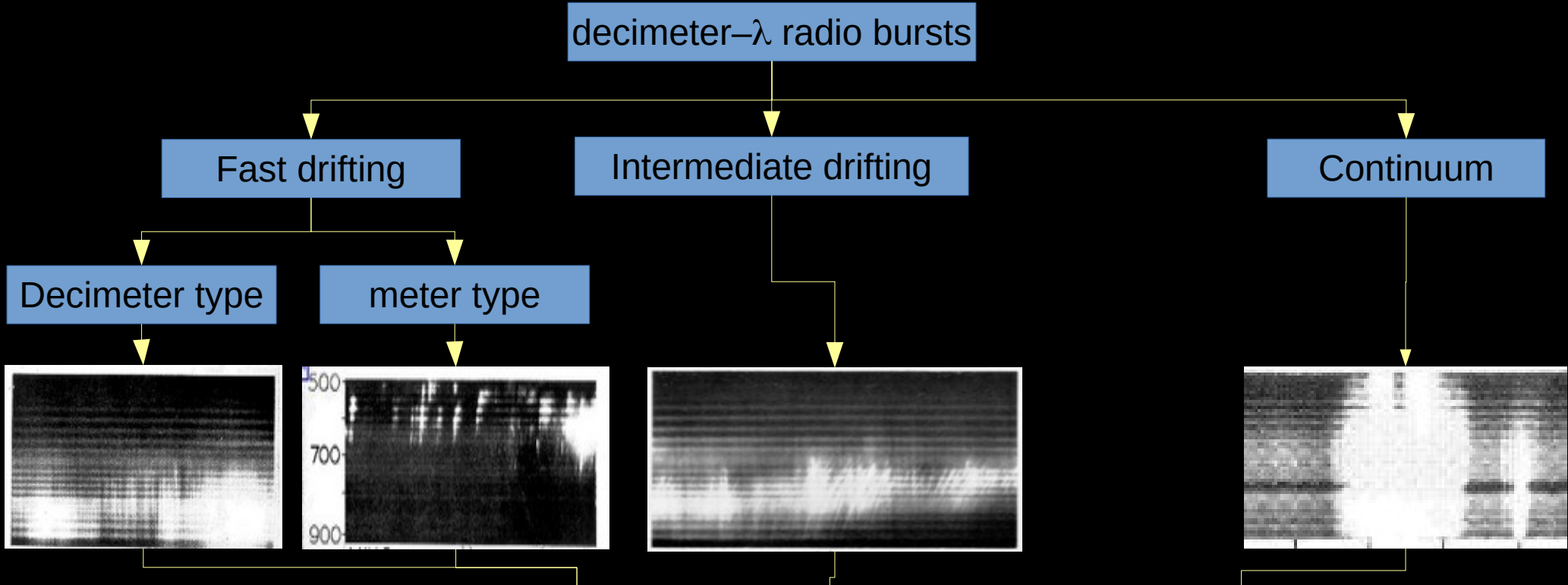
- 1. Type-A - called microwave outbursts.**
- 2. Intensity  $> 100$  times higher than usual cm bursts**
- 3. Have several peaks during the rise phase (few minutes) and follow a gradual decay for few tens of minutes to hours.**
- 4. Source size :  $1' - 2'$ . But increases after the post-burst phase to  $>3'$ .**
- 5. Temperature can go up to  $10^9$  K.**
- 6. 70 % of them are partially circularly polarized.**

---

**Many more properties  
can be discussed further**

**Limited it due to time constraint**

# The decimeter- $\lambda$ radio bursts



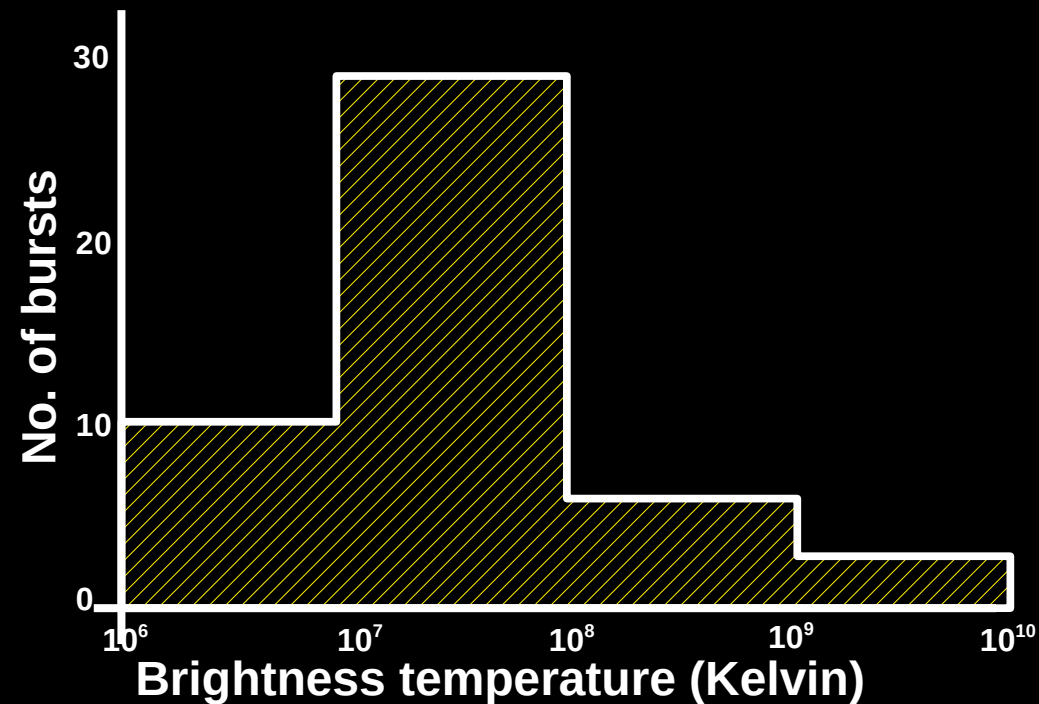
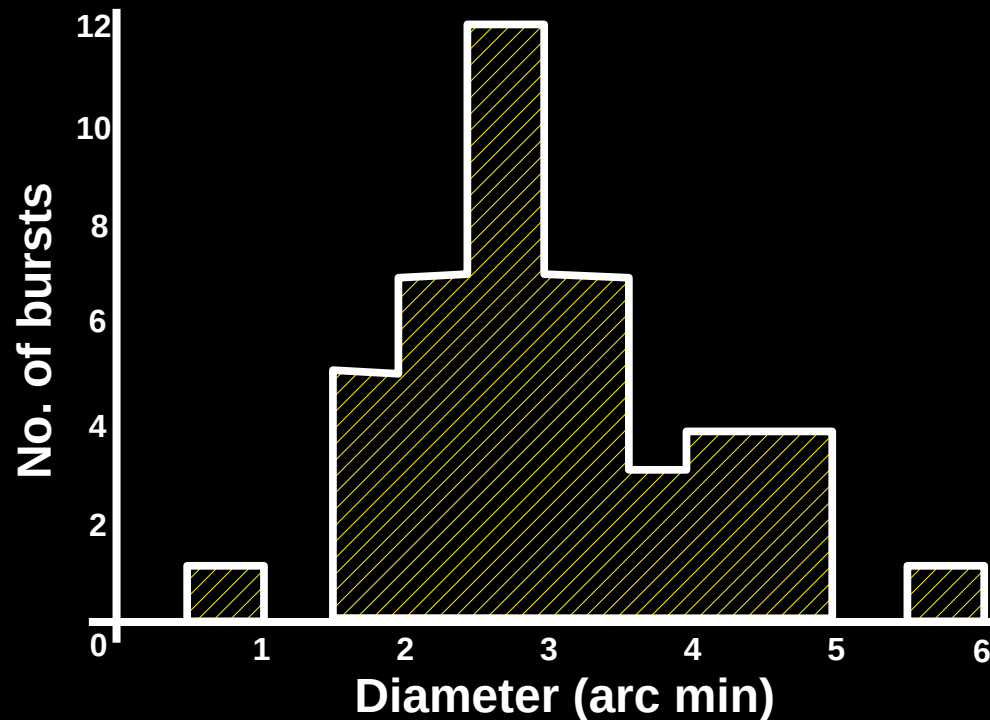
Both are fast drifting  $> 2 \text{ GHz/s}$  with shorter duration (100 MHz $\times$ 2/3)  
 Positive and reverse drifts are seen  
 Decimeter type does not extend into meter wave domain  
 (30 - 100 MHz / 3 - 60 cm)  
 Meter type continues into meter wave domain  
 Reason  $\rightarrow$  plasma oscillation like type-III

Intermediate drift rate  $< 15 \text{ GHz/s}$   
 Bandwidth  $\sim 10 \text{ MHz}$   
 Exists below 600 MHz  
 Reason  $\rightarrow$  plasma oscillations like type-II

Continuum - no drifts seen  
 Bandwidth  $\sim 500 \text{ MHz}$   
 Exists from 900 - 500 MHz  
 Reason  $\rightarrow$  plasma oscillations within specific layers

**Young et al., ApJ, 133, 243 (1961)**

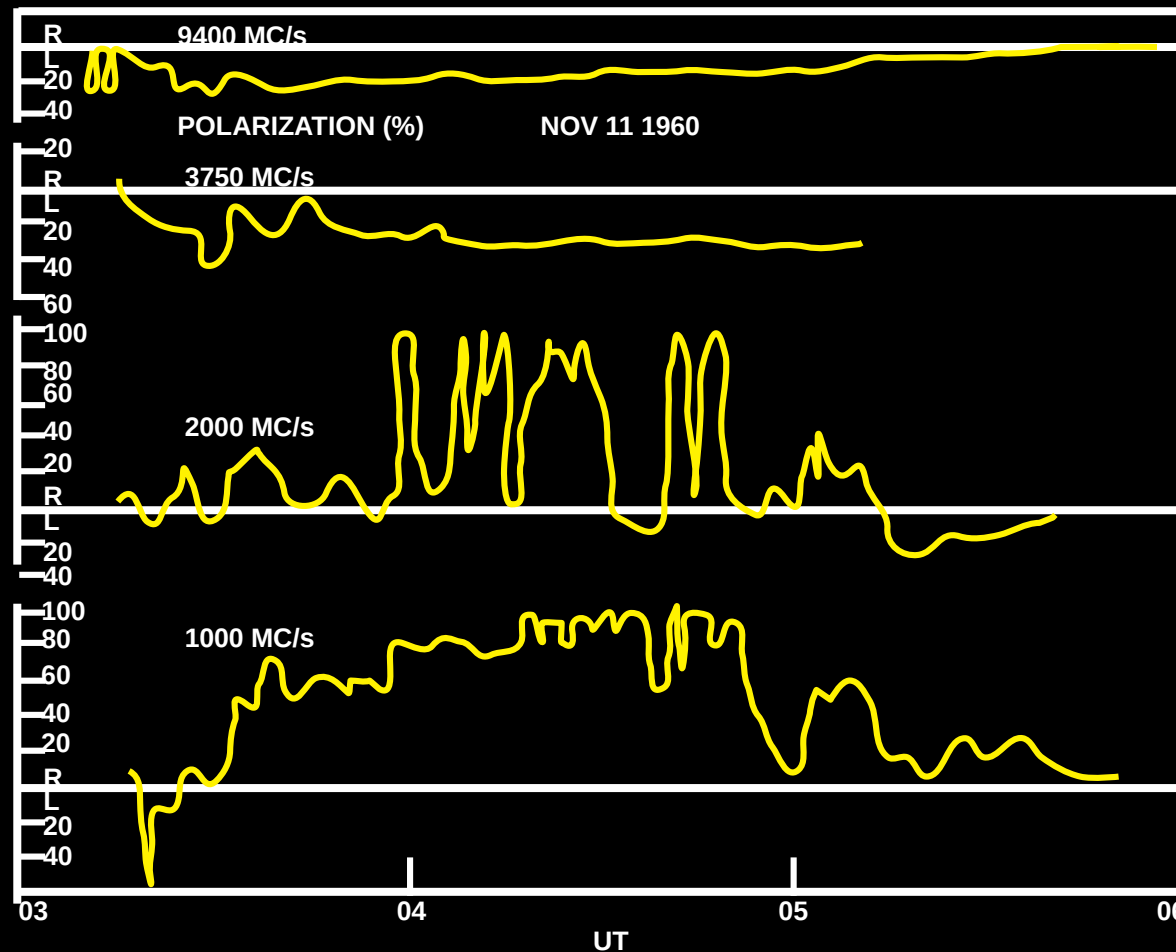
## Decimeter- $\lambda$ radio bursts : Source size & Brightness



1. Mean source diameter :  $\sim 2'$  ( $2'$ - $5'$ )
2. Mean brightness temperature :  $\sim 10^7$  °K ( $10^6$  –  $10^{10}$  °K).

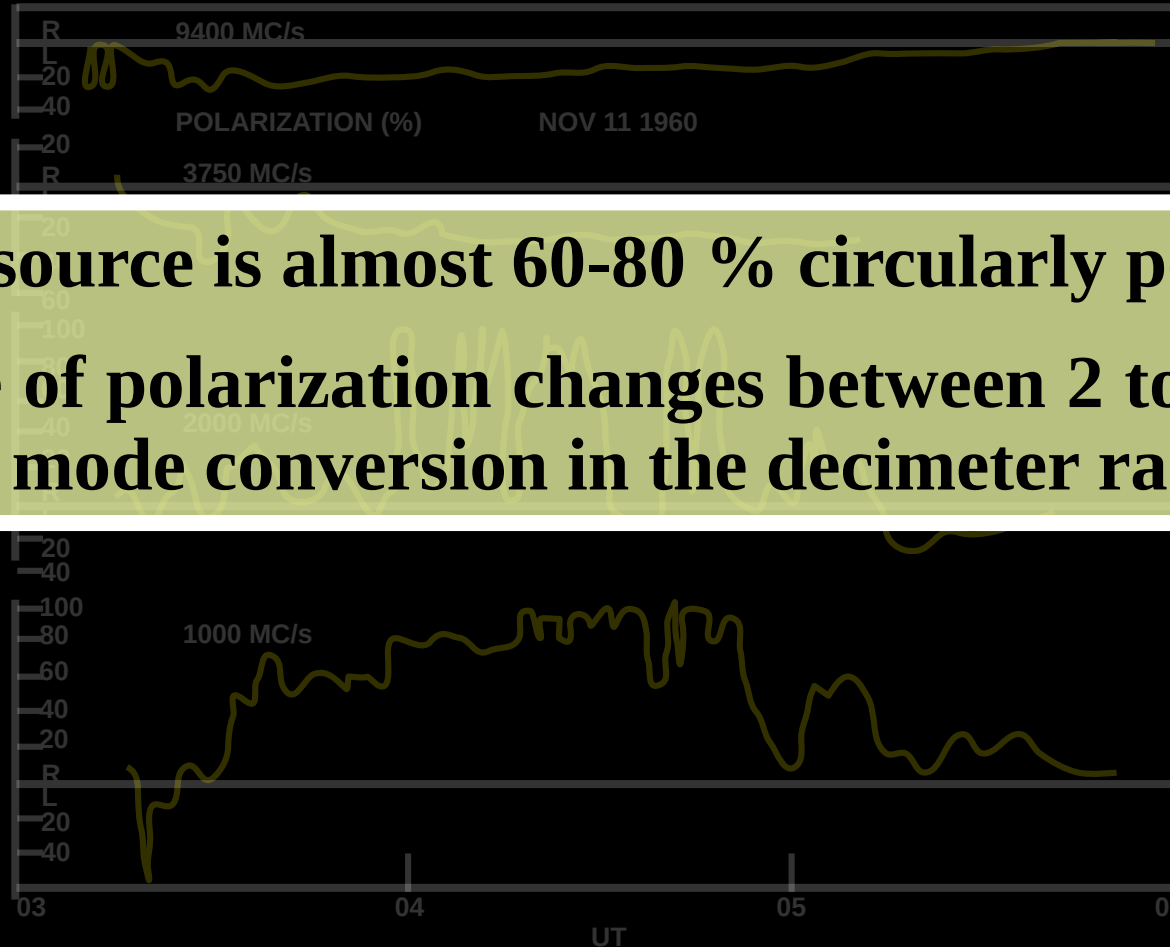
Mullaly, R. F. et al., *Au. J. Ph*, 16, 8 (1963)

# Decimeter- $\lambda$ radio bursts : Polarization



**Tanaka, H., Proc. Res. Inst. Atmosph., Nagoya Univ. Japan, 8, 1 (1961)**

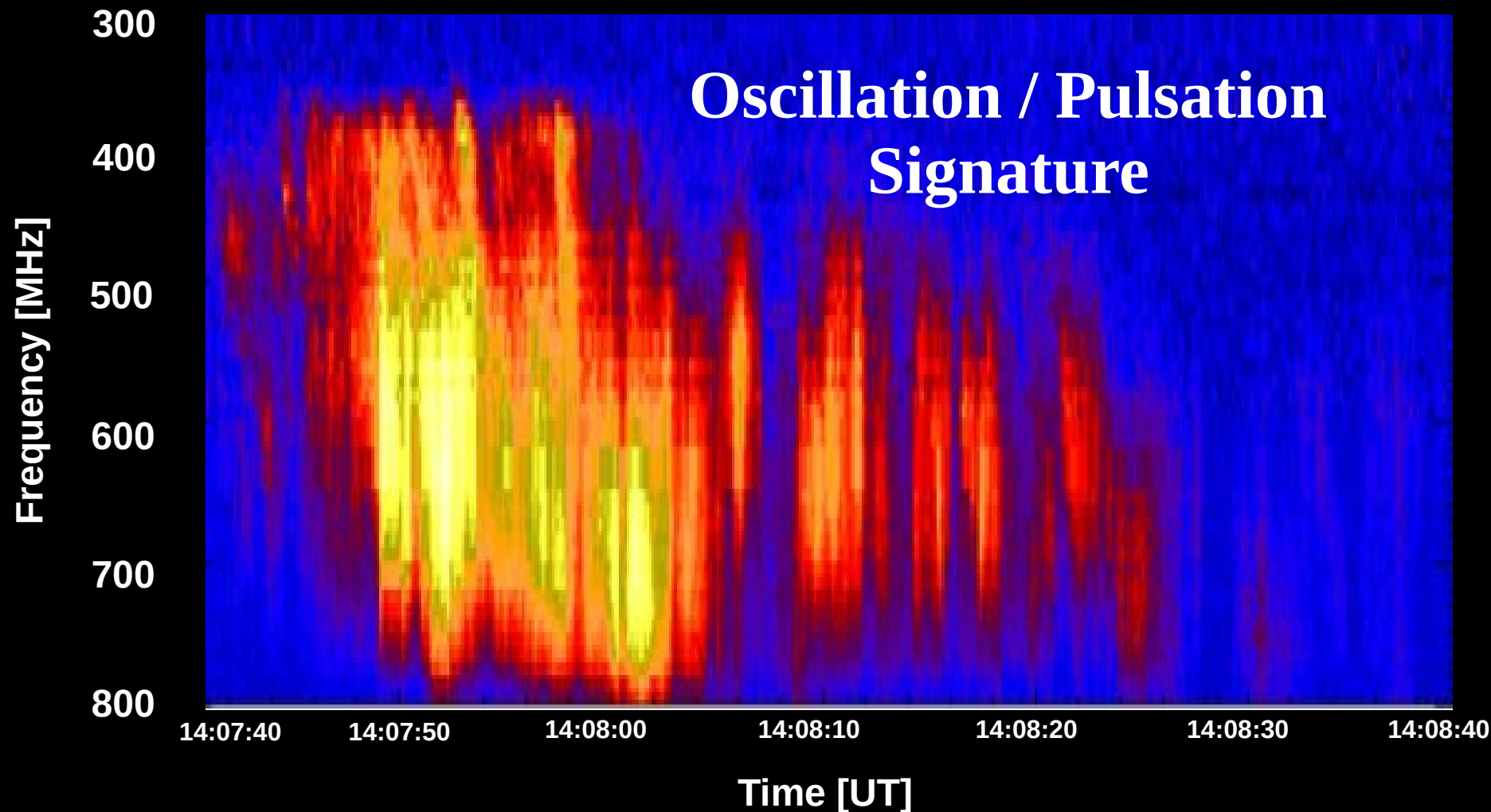
## Decimeter- $\lambda$ radio bursts : Polarization



1. The dcm source is almost 60-80 % circularly polarized.
2. The sense of polarization changes between 2 to 3.7 GHz, indicating a mode conversion in the decimeter radiation.

**Tanaka, H., Proc. Res. Inst. Atmosph., Nagoya Univ. Japan, 8, 1 (1961)**

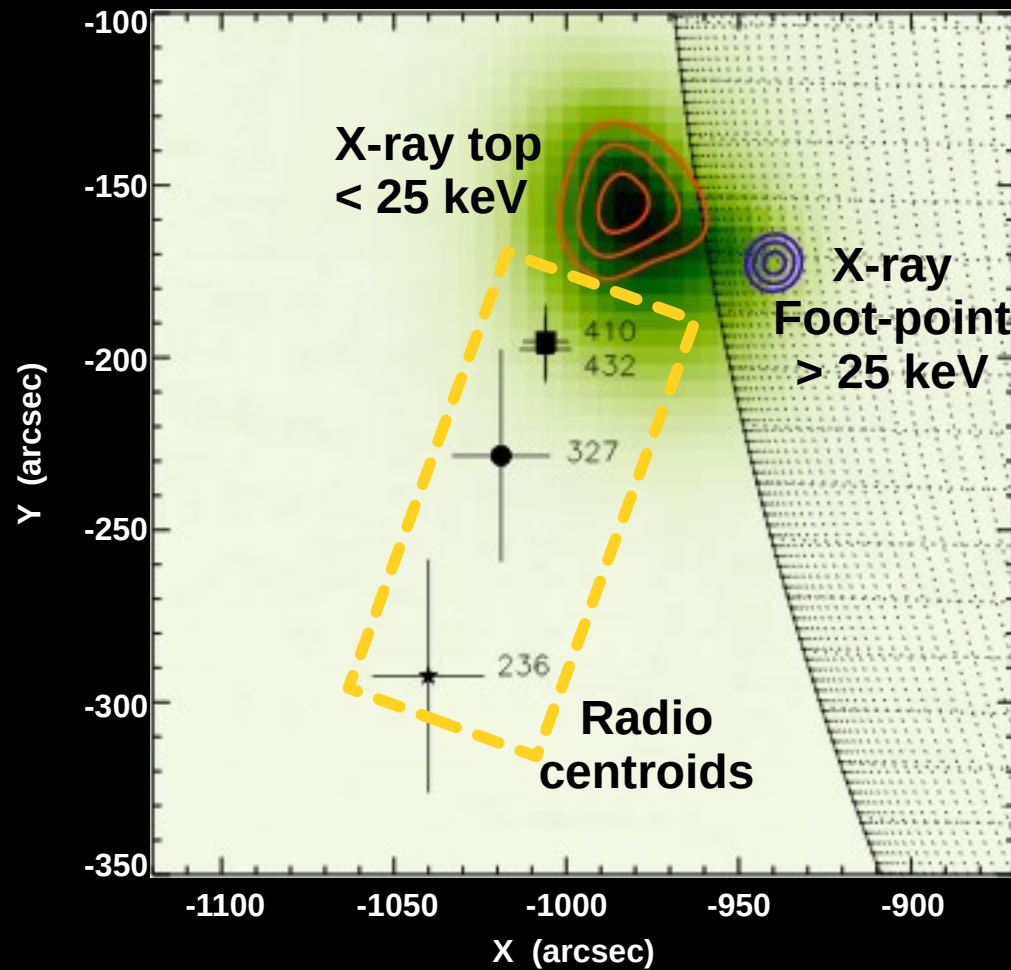
# Decimeter- $\lambda$ radio pulsations



## Radio Dynamic Spectrum

Benz, A. O. SoPh, 273, 363 (2011)

# Decimeter- $\lambda$ radio pulsations



**X-Ray & Radio  
superposition**

**Benz, A. O. SoPh, 273, 363 (2011)**

## Decimeter- $\lambda$ radio pulsations

1. X-rays and coherent radio emissions are due to particle accelerations.
2. The dcm pulsation observations combined with RHESSI X-ray and radio imaging (Nancay) observations indicate that the radio sources are in line with the X-ray source.
3. A common source responsible for X-ray and radio gave rise to pulsation in the lower atmosphere.

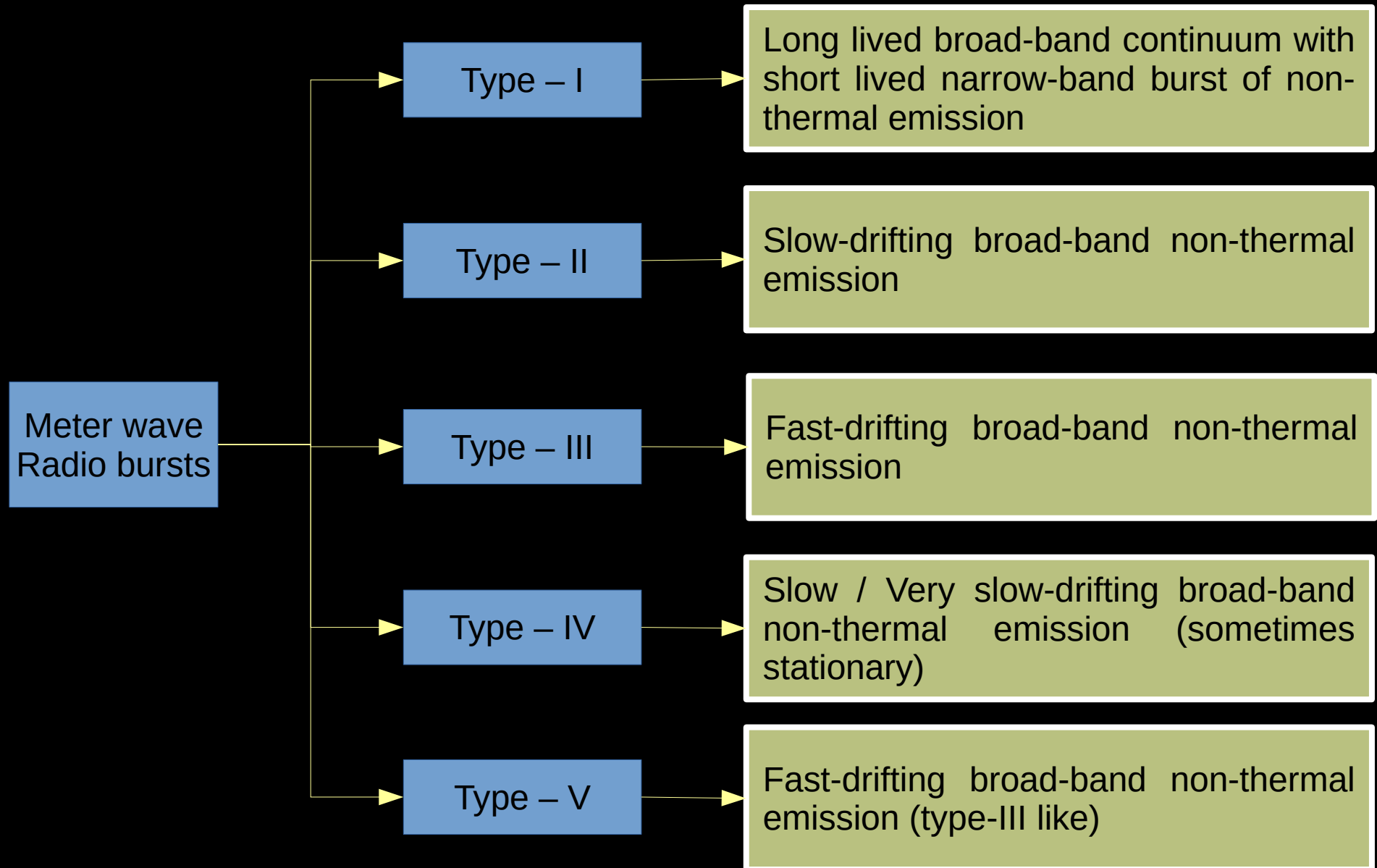
**Benz, A. O. SoPh, 273, 363 (2011)**

---

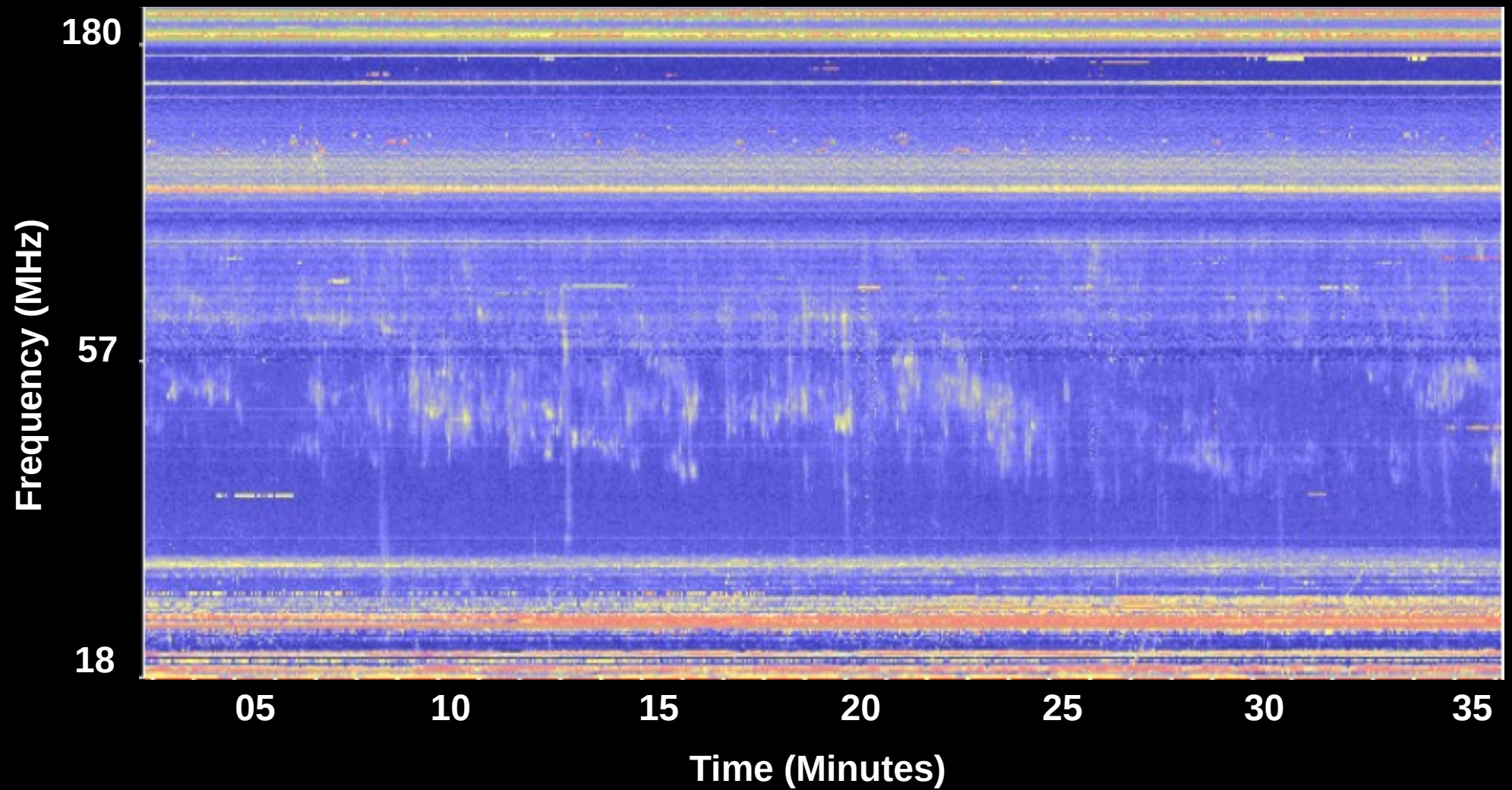
**Many other dcm- $\lambda$  bursts  
can be discussed further**

**Limited it due to time constraint**

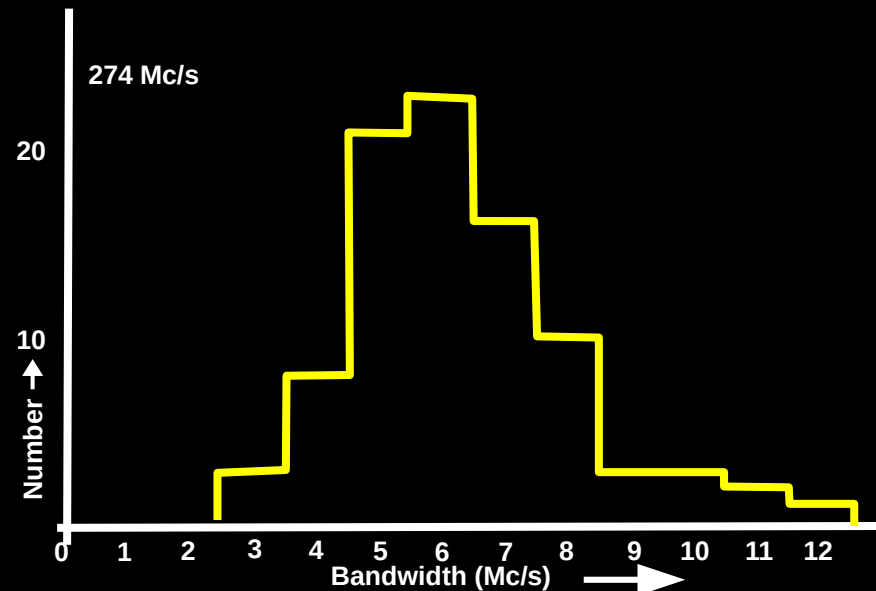
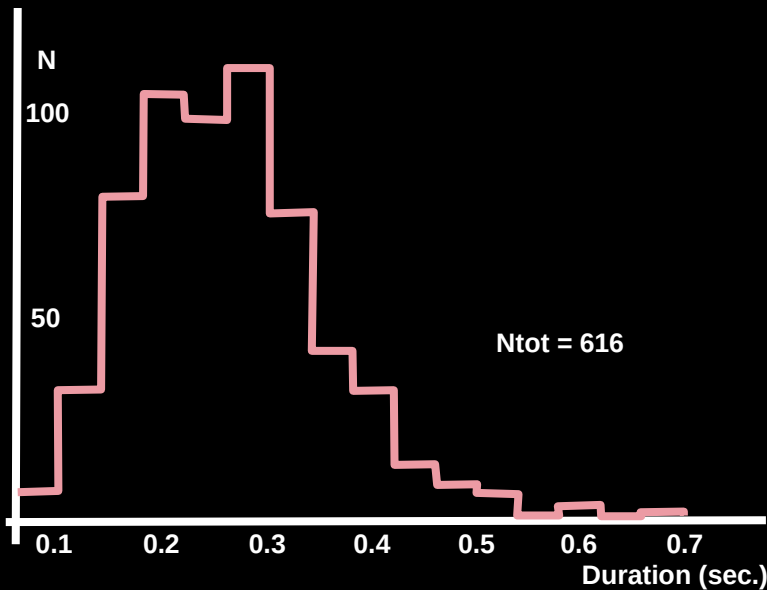
# Meter & deca-m $\lambda$ radio bursts : Classification



# Meter & deca-m $\lambda$ type-I radio burst / Noise Storms



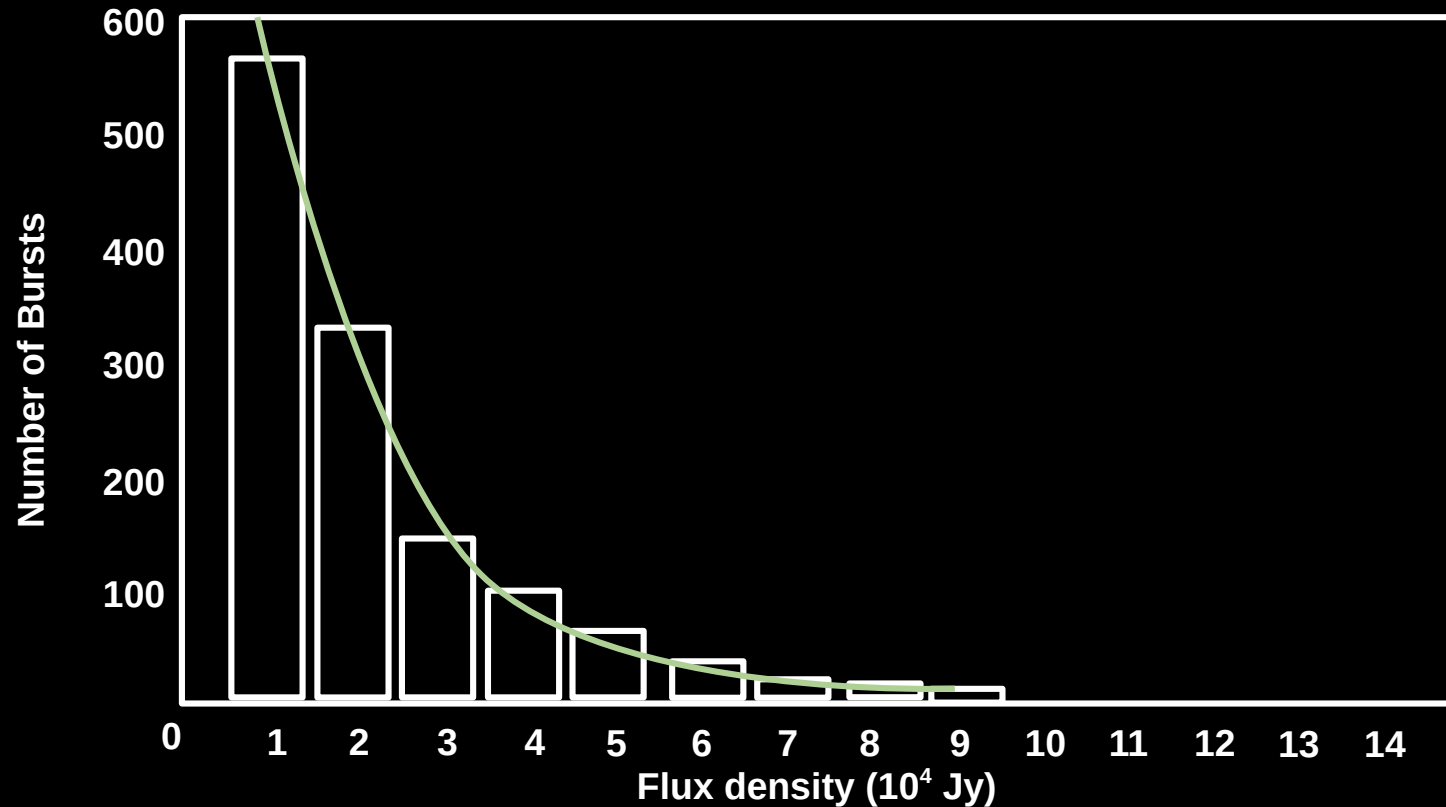
## Meter & deca-m $\lambda$ type-I – Bandwidth & lifetime



Majority of the type-I bursts have :

1. Duration in the range 0.2 – 0.4 second (274 MHz) & 1 second (77 MHz).
2. Bandwidth in the range 5 – 8 MHz.

## Meter & deca-m $\lambda$ type-I – Energy distribution

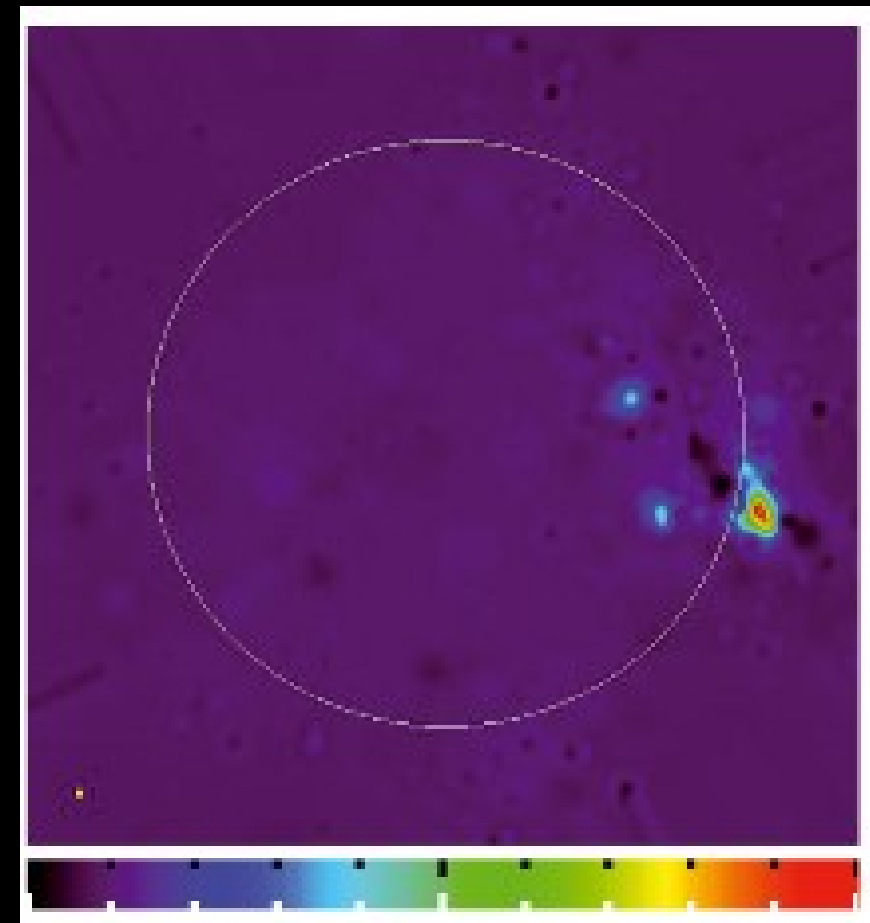
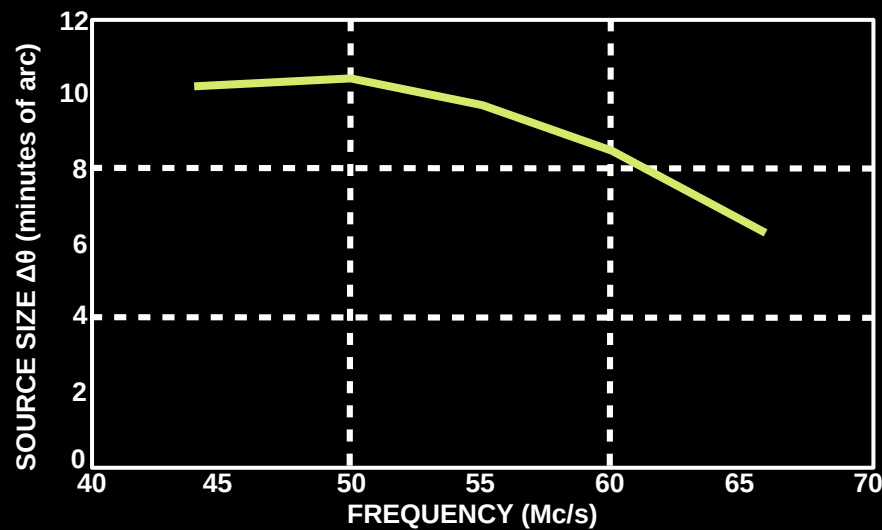
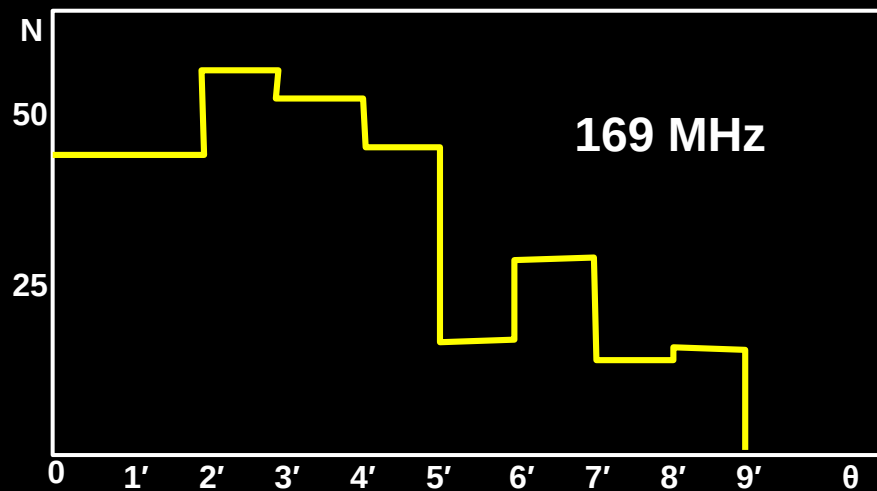


**Majority of the type-I bursts have flux density  $< 30$  kJy.**

Elgaroy, O., *Astrophysica Norvegica*, 7, 123 (1961)

Ramesh et al., *ApJ*, 89, 762 (2013)

# Meter & deca-m $\lambda$ type-I – Storm center size



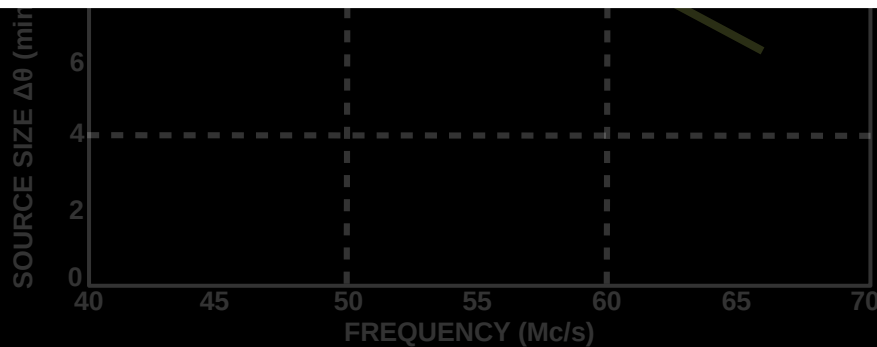
Wild, J. P., Proc. IRE, 46, 160, 1958

Mercier et al., A&A, 576, 136, (2015)

## Meter & deca-m $\lambda$ type-I – Storm center size



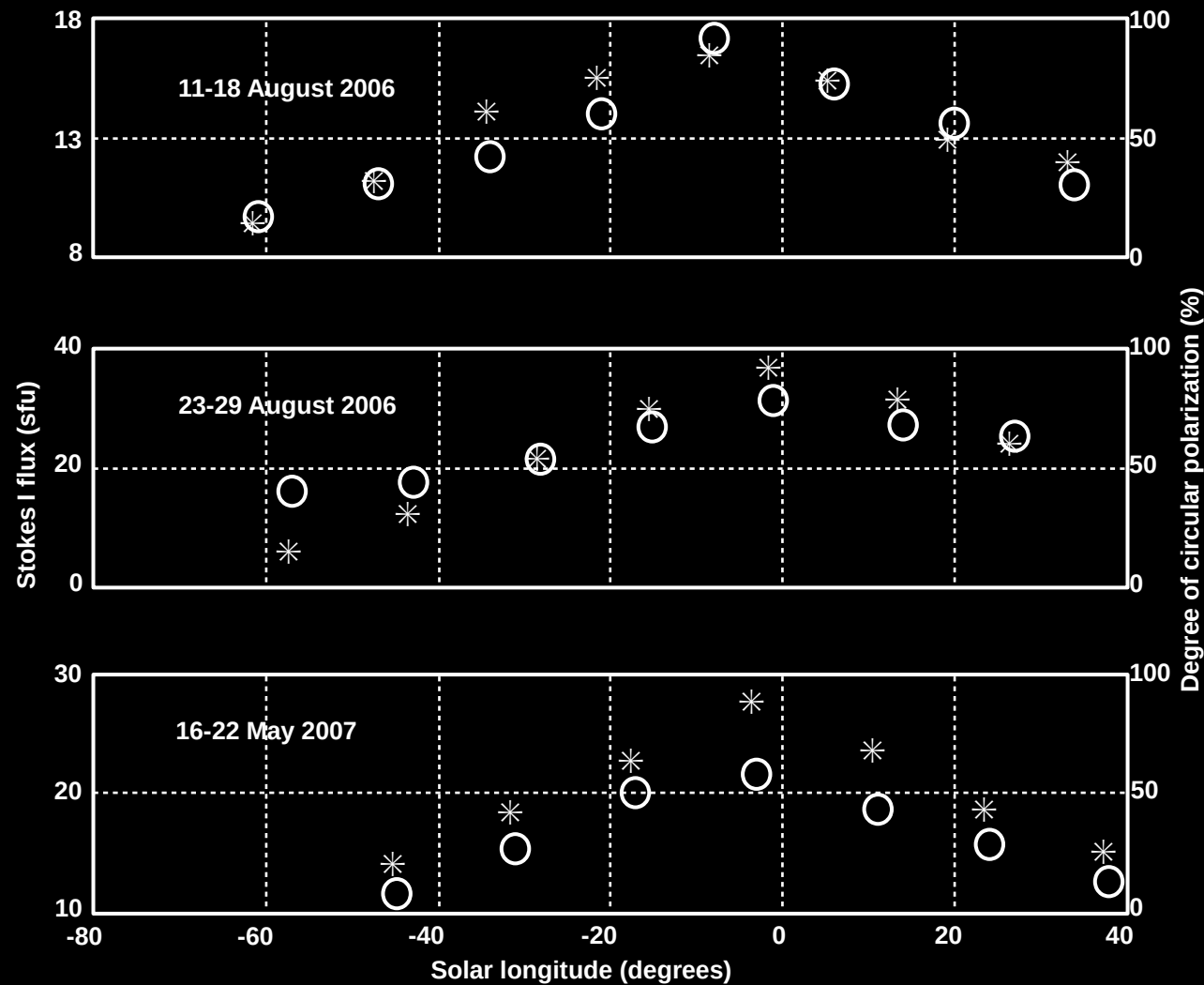
1. The overall angular size of the source varies from 30'' – 90'' with an inner core size of 30''-60'' at 237 MHz.
2. However, the source size is higher at low frequencies. And it continues to increase as a function of decreasing frequency (or increasing altitude in the atmosphere).



Wild, J. P., Proc. IRE, 46, 160, 1958

Mercier et al., A&A, 576, 136, (2015)

# Meter & deca-m $\lambda$ type-I : Polarization



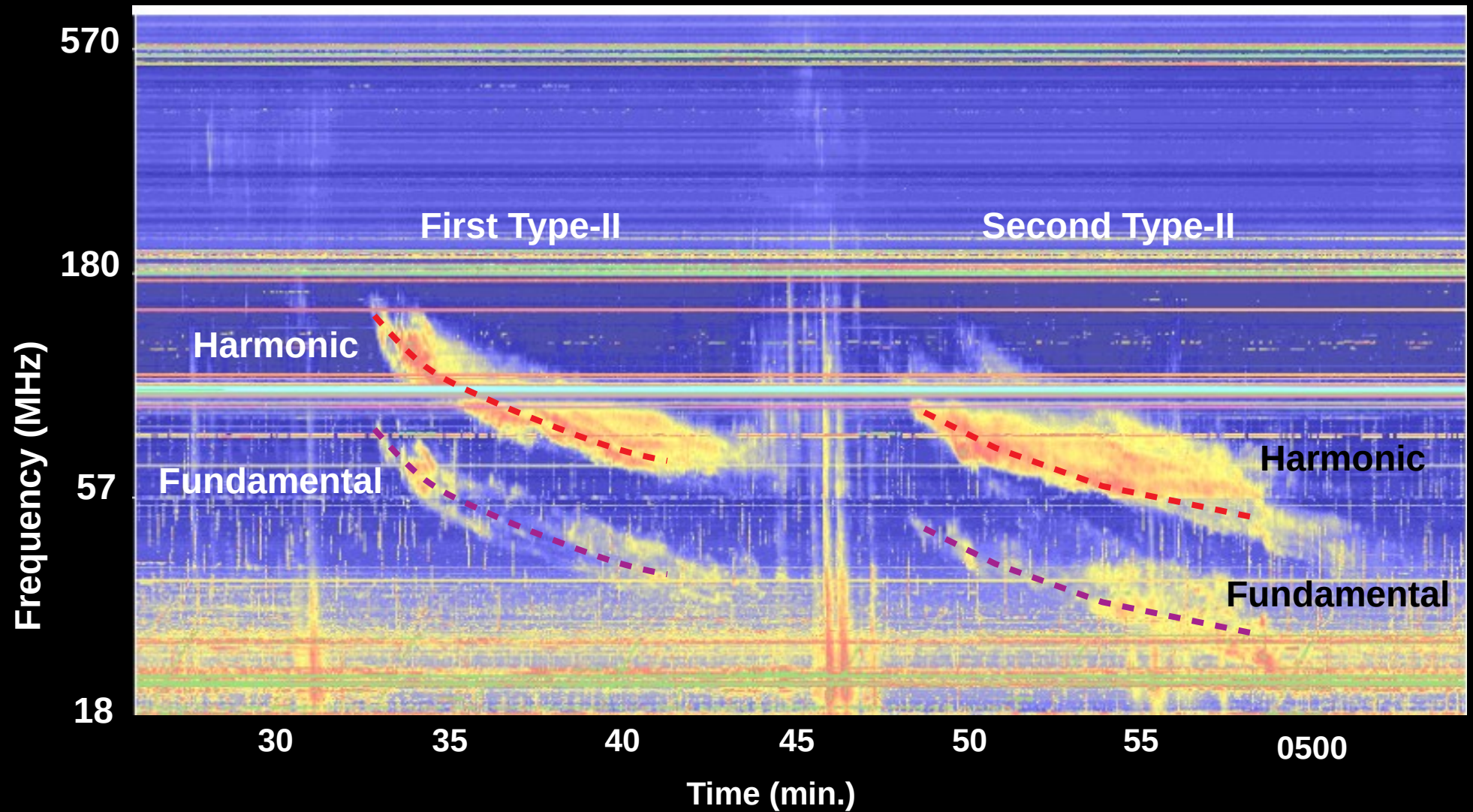
Ramesh et al., ApJ, 734, 39 (2011)

## Meter & deca-m $\lambda$ type-I : Polarization

1. The fall of polarization on either side of the disk center implies that the source is highly directive.
2. The magnetic field of the noise-storm active regions estimated are 0.6 – 1.1 G
3. The emerging magnetic flux and the changes in the existing active region magnetic fields inevitably lead to field reconnection and generation of type-I bursts – So, these are associated with these small sites of reconnection.

Ramesh et al., ApJ, 734, 39 (2011)

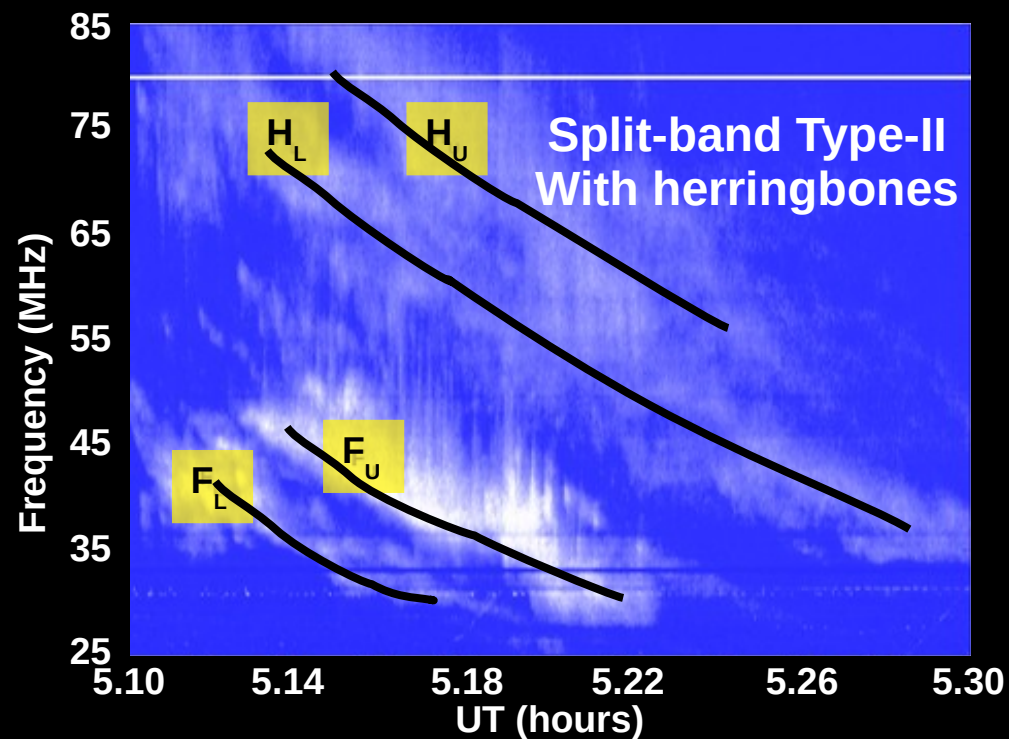
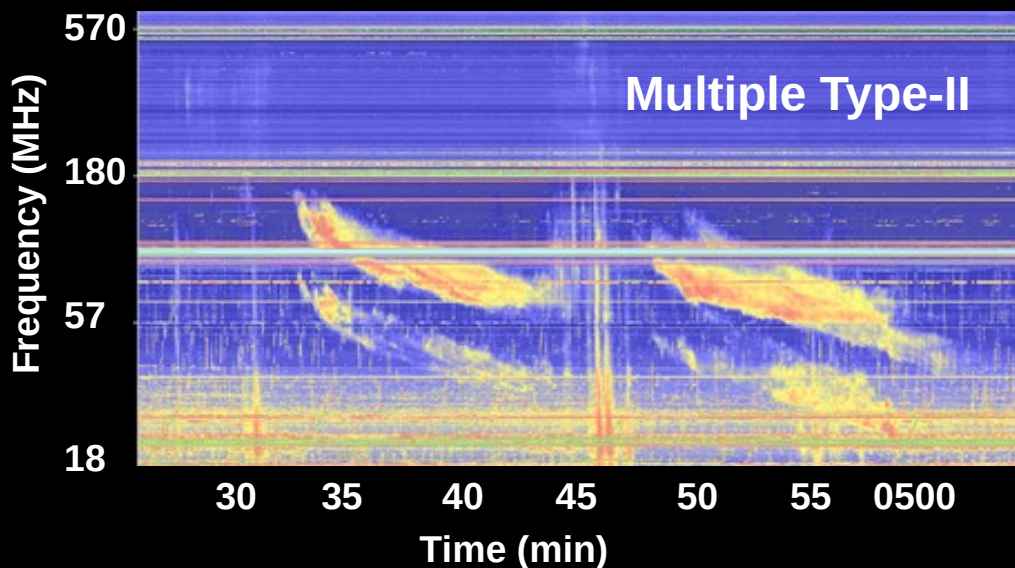
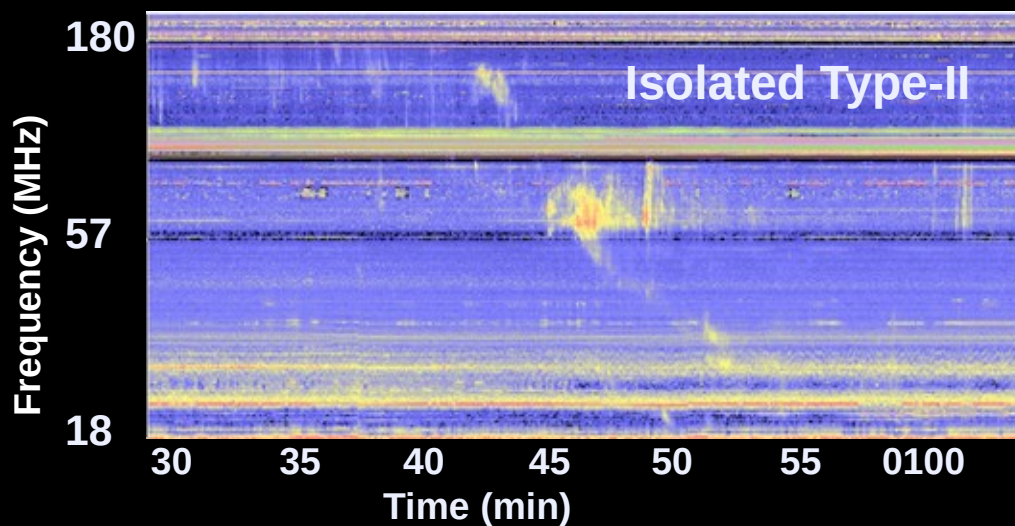
# Meter & deca-m $\lambda$ type-II radio bursts



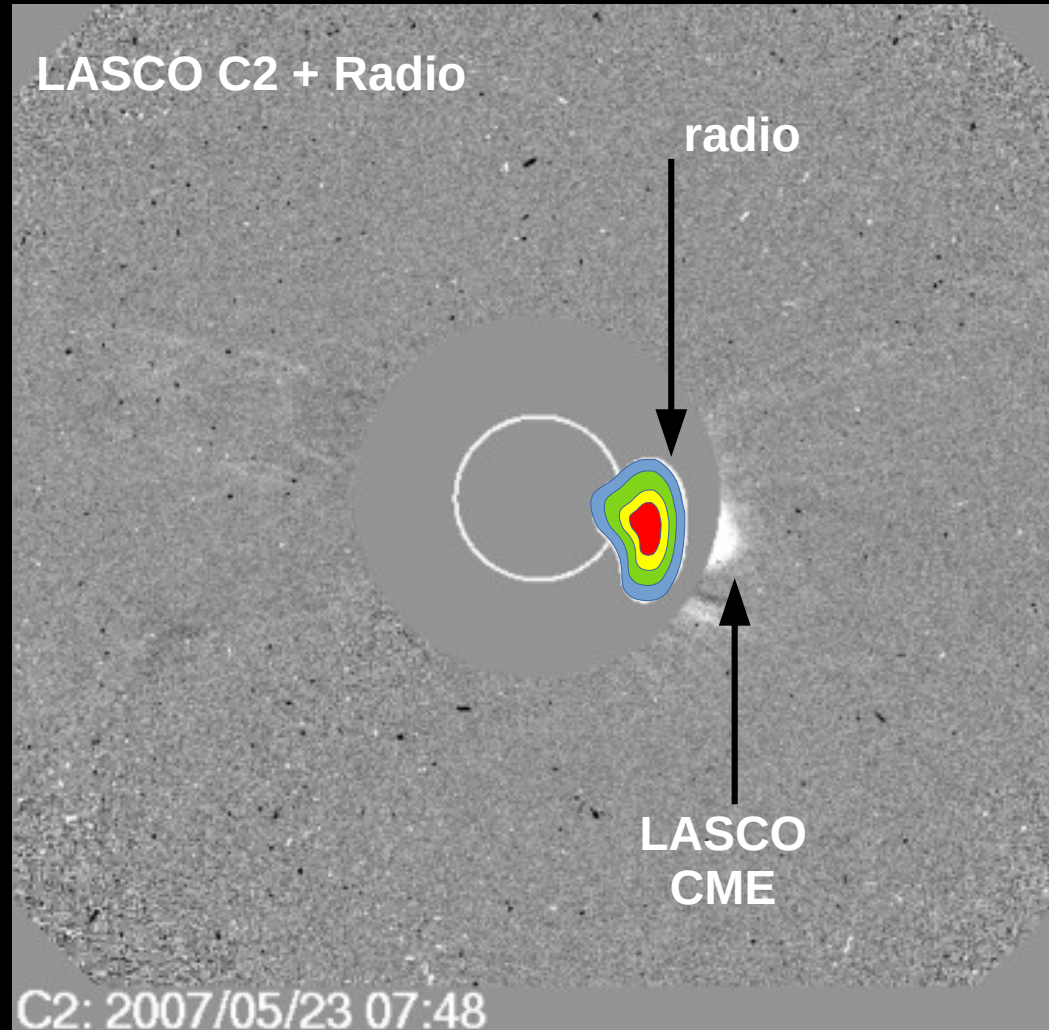
## Meter & deca-m $\lambda$ type-II radio bursts

1. This is a type of burst in which there will be a noticeable delay in the peak of emission as a function of frequency.
2. The high frequency appears first and it is followed by successive emission at lower frequencies with the drift rate of few MHz/s.
3. These are the signatures of coronal shock that are generated by the bulk motion of plasma material from the inner to the outer coronal atmosphere.
4. They generally appear in pairs, called the fundamental and harmonic with the frequency ratio 1:2.

# Meter & deca-m $\lambda$ type-II radio burst variants



# Meter & deca-m $\lambda$ type-II radio burst drivers



Ramesh et al, APJ, 752, 107 (2012)

Gopalswamy et al, AIPC, 264, 267 (1992)

## Meter & deca-m $\lambda$ type-II radio burst drivers

LASCO C2 + Radio

radio

1. The superposition of type-II radio emission and the WL running difference image clearly establishes their association between them.
2. This indicates that the CME is the driver of the type-II radio burst. When a CME travels in a plasma medium with a speed exceeding the local Alfvén speed, it creates shocks which in turn triggers a type-II burst.

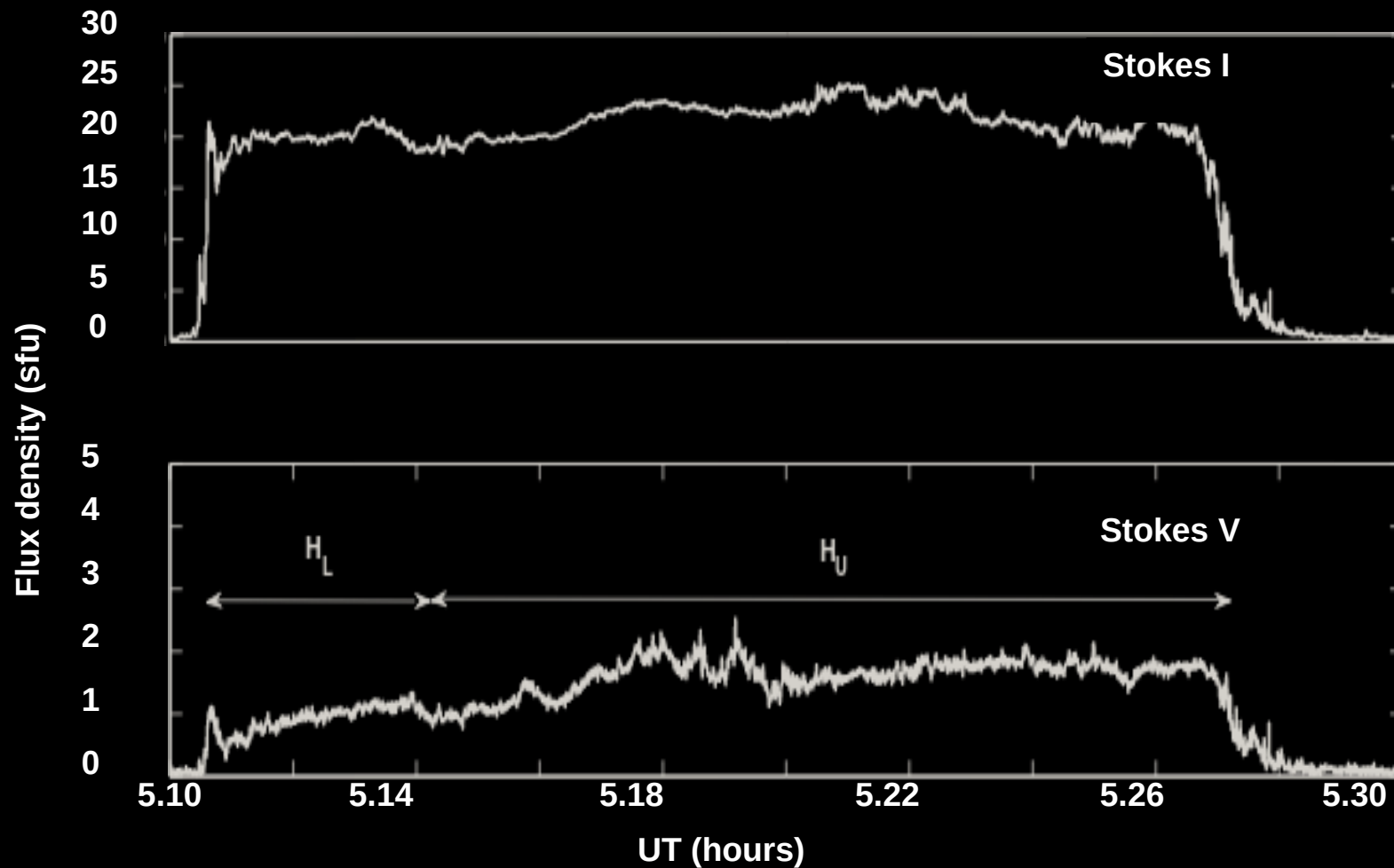
CME

C2: 2007/05/23 07:48

Ramesh et al, APJ, 752, 107 (2012)

Gopalswamy et al, AIPC, 264, 267 (1992)

# Meter & deca-m $\lambda$ type-II : Polarization

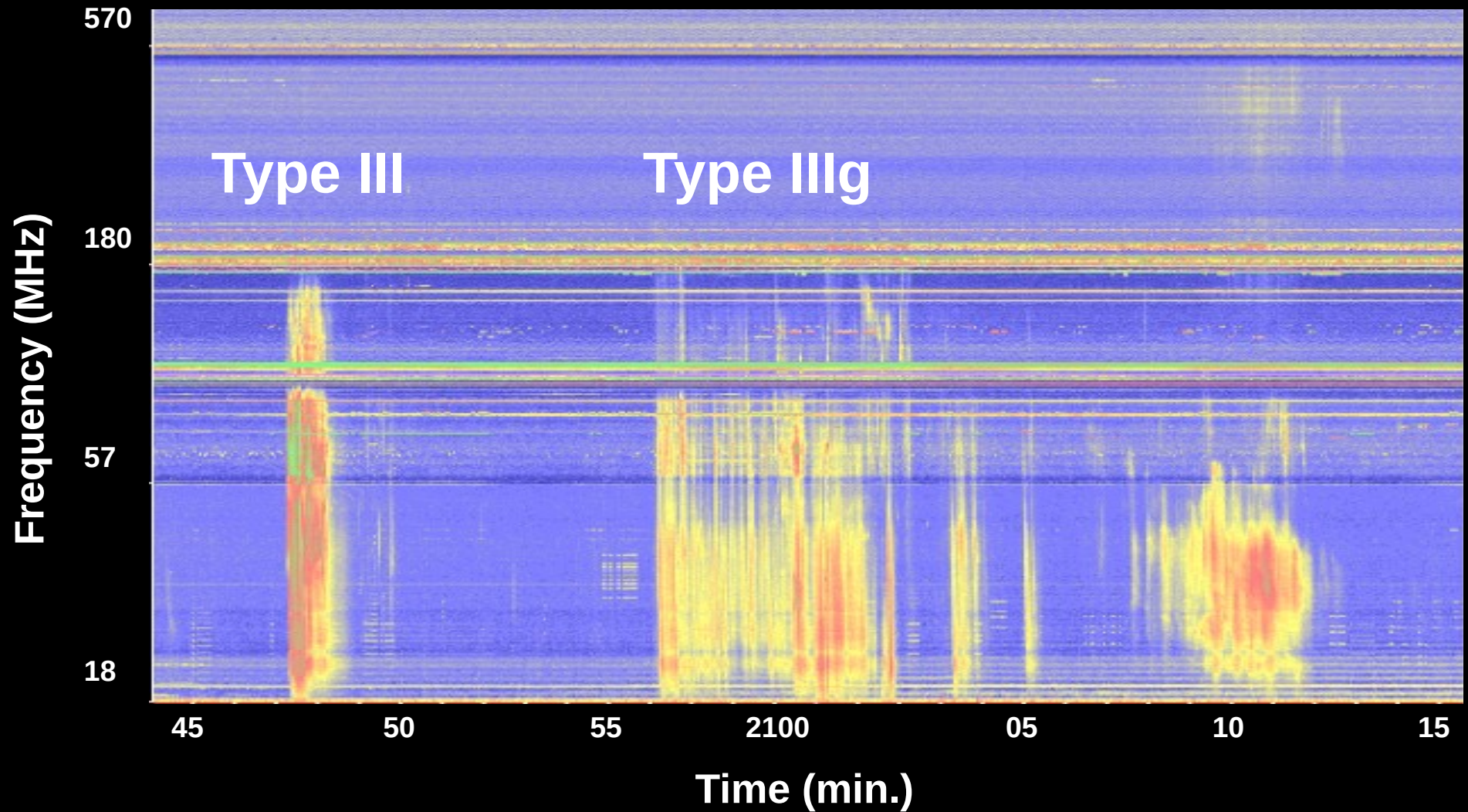


Ramesh et al, ApJ, 752, 107 (2012)

## Meter & deca-m $\lambda$ type-II : Polarization

1. Type-II burst intensities were found to lie in the range  $\sim 10^{-21} - 10^{-18}$  Watt/ m<sup>2</sup> / Hz.
2. Type-II bursts are weakly polarized ( $\sim 10\%$  at 80 MHz).

# Meter & deca-m $\lambda$ type-III radio bursts

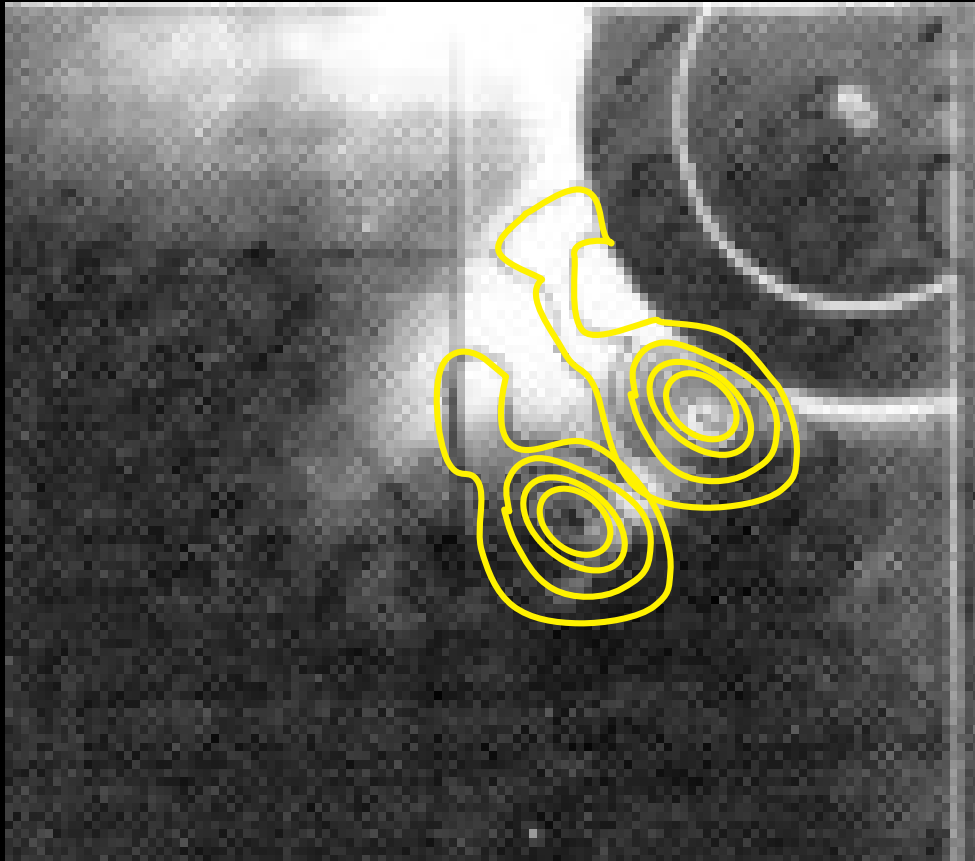


## Meter & deca-m $\lambda$ type-III radio bursts

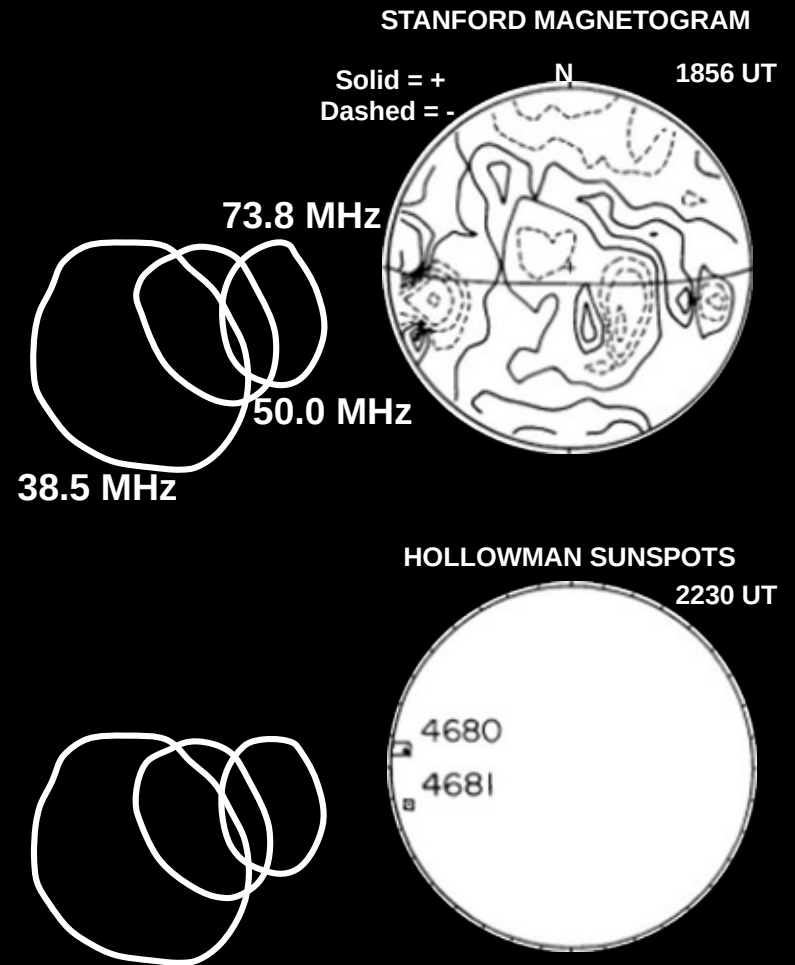
1. This type is a fast drifting broad band emission; their average drift rate is  $\sim 100$  MHz/s.
2. They occur isolated and sometime in groups; they have both fundamental and harmonic components.
3. Their frequency range is  $\sim$  GHz -  $\sim$  kHz.
4. The high energy electrons released in the aftermath of a flare (X-ray/EUV/H-alpha) travels outward along open magnetic field lines cause type-III.
5. The emission is weakly polarized ( $<15\%$ ) but occasionally observed to have about 50% (if fundamental)

Time (min.)

# Meter & deca-m $\lambda$ type-III : Source regions



**Radio contour on WL  
Coronagraph image.**



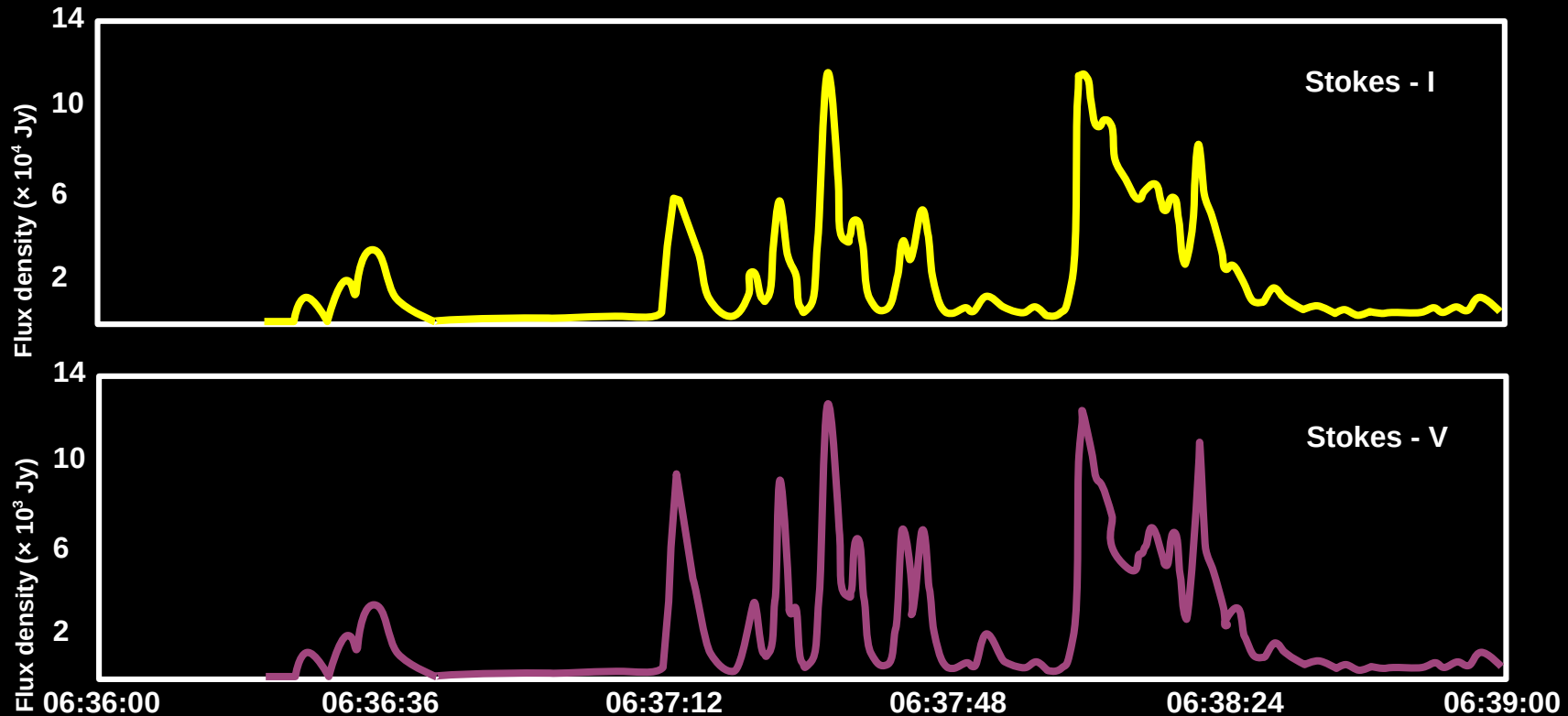
**Gopalswamy et al., SoPh, 108, 333 (1987)**

## Meter & deca-m $\lambda$ type-III : Source regions

1. Type-III originate from coronal streamers since they have open magnetic field lines on their top.
2. The increasing structure as a function of frequency signifies, the electrons propagate along radial open magnetic field lines.

**Gopalswamy et al., SoPh, 108, 333 (1987)**

## Meter & deca-m $\lambda$ type-III : Polarization

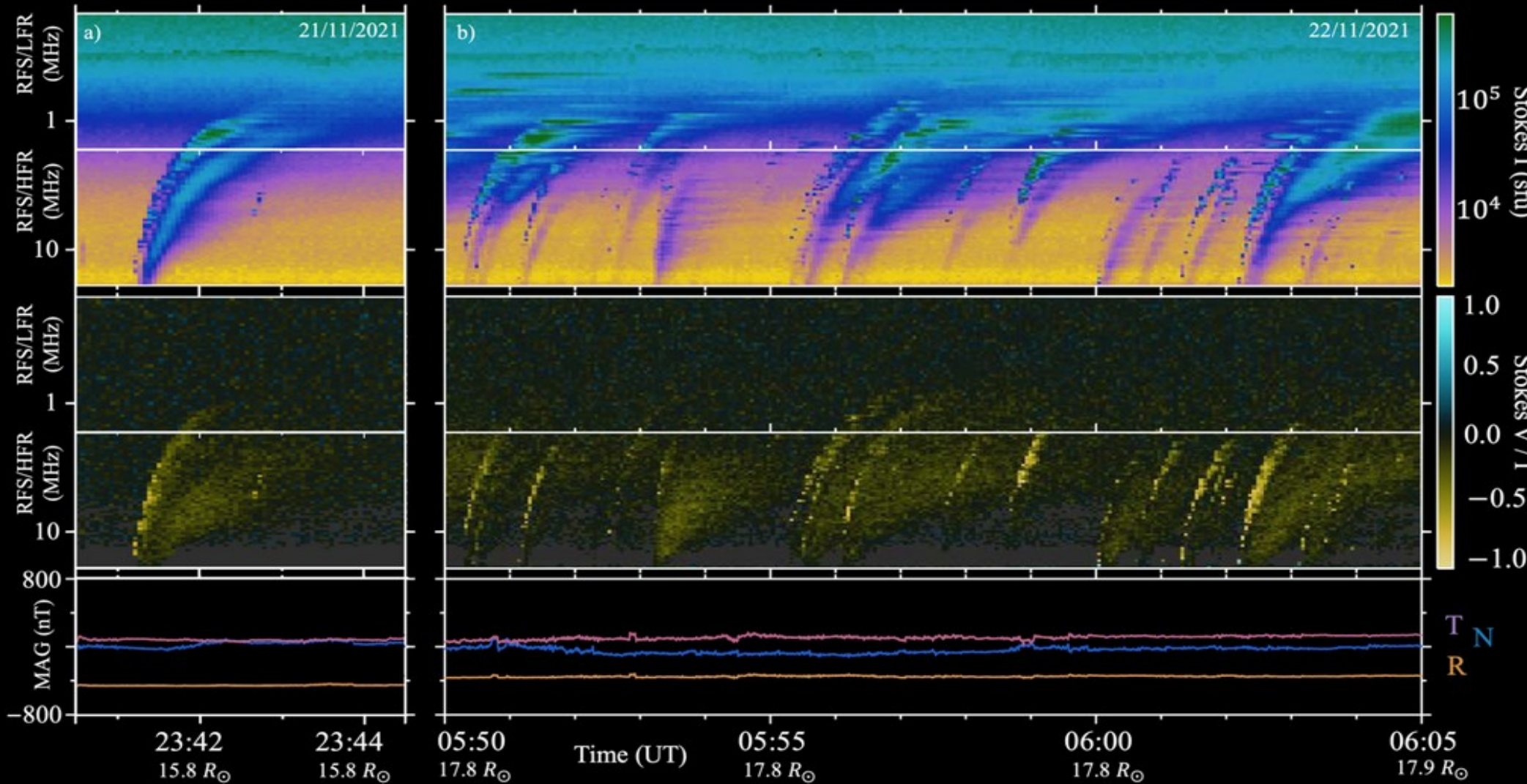


1. Type-IIIs are weakly polarized  $< 15\%$  and occasionally go up to  $50\%$ .
2. Linear polarization of type-IIIs are observed for a very low bandwidth of few kHz.

Sasikumar Raja, ApJ, 775, 38 (2013)

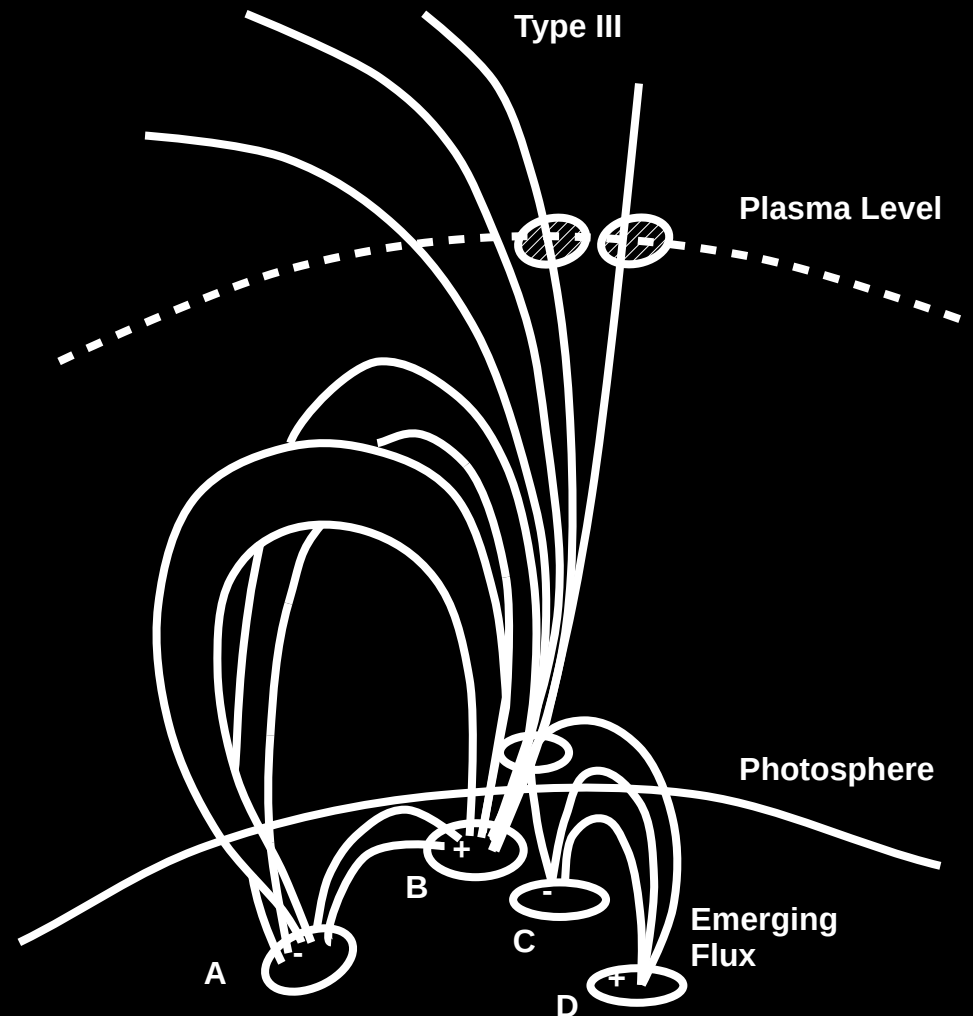
Cohen, ApJ, 130, 221 (1959)

# Meter & deca-m $\lambda$ type-III : Polarization



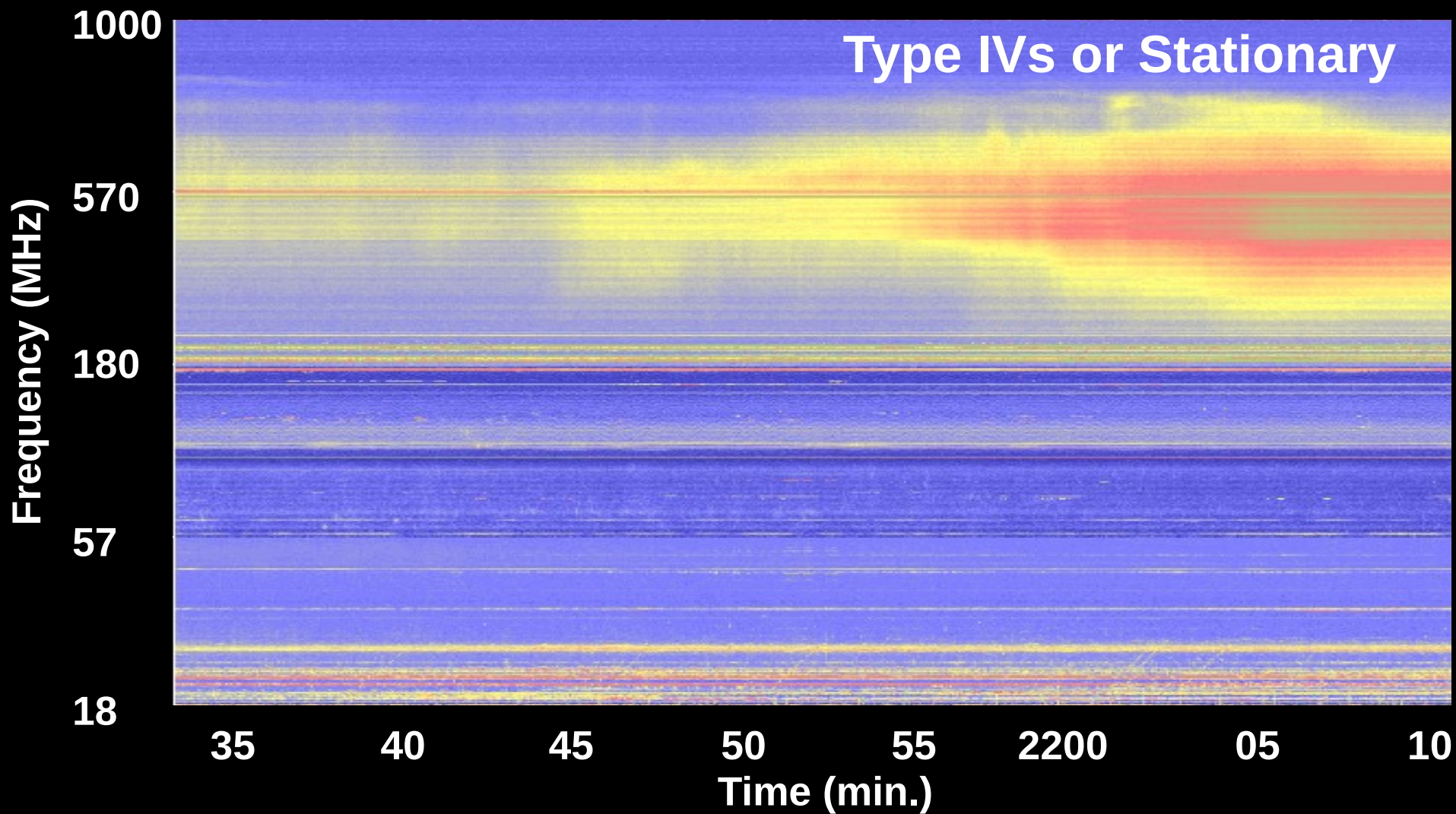
Jebaraj et al., ApJL, 955, 20 (2023)

# Meter & deca-m $\lambda$ type-III : Schematic

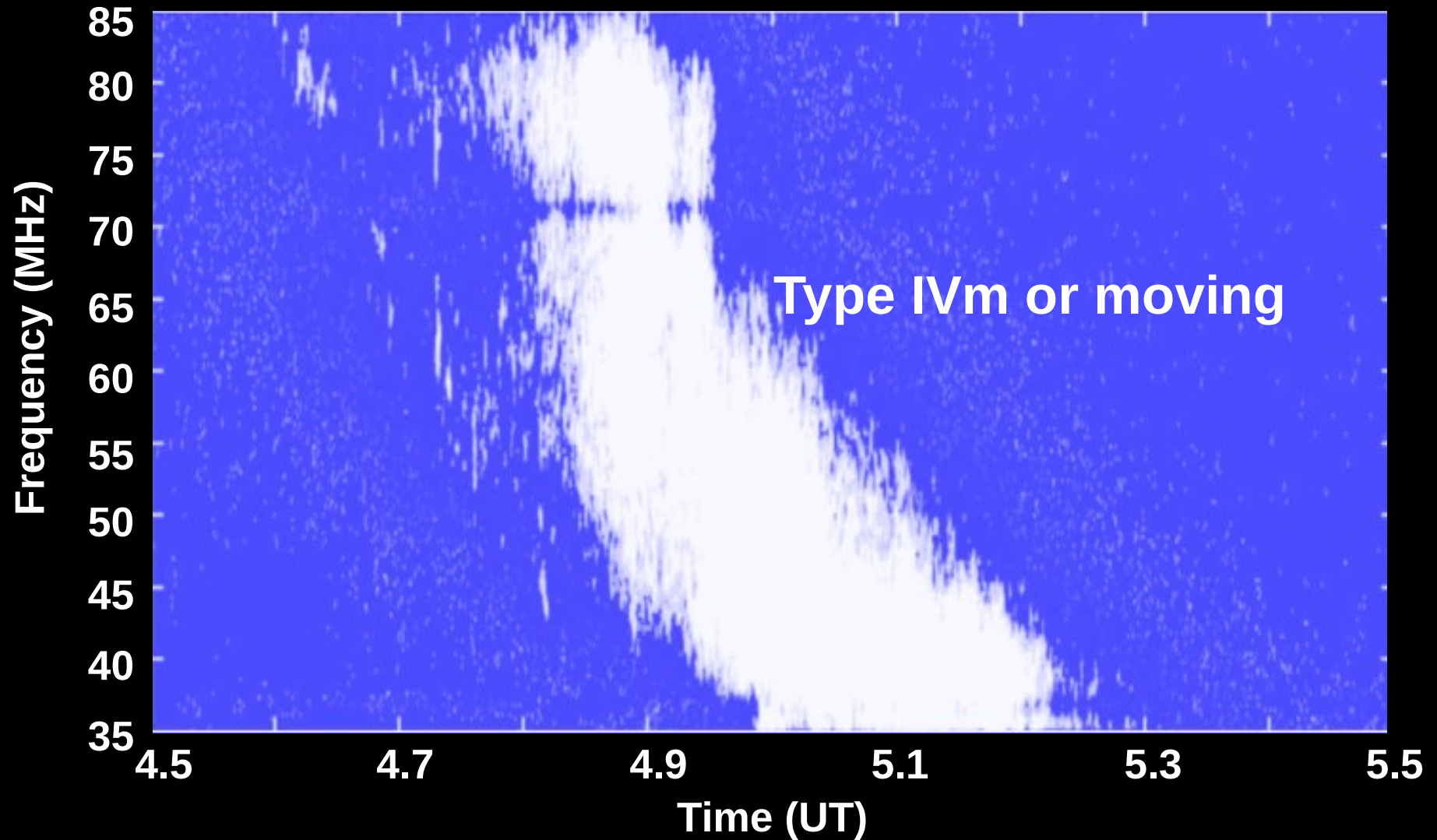


Gopalswamy et al., SoPh, 111, 347 (1987)

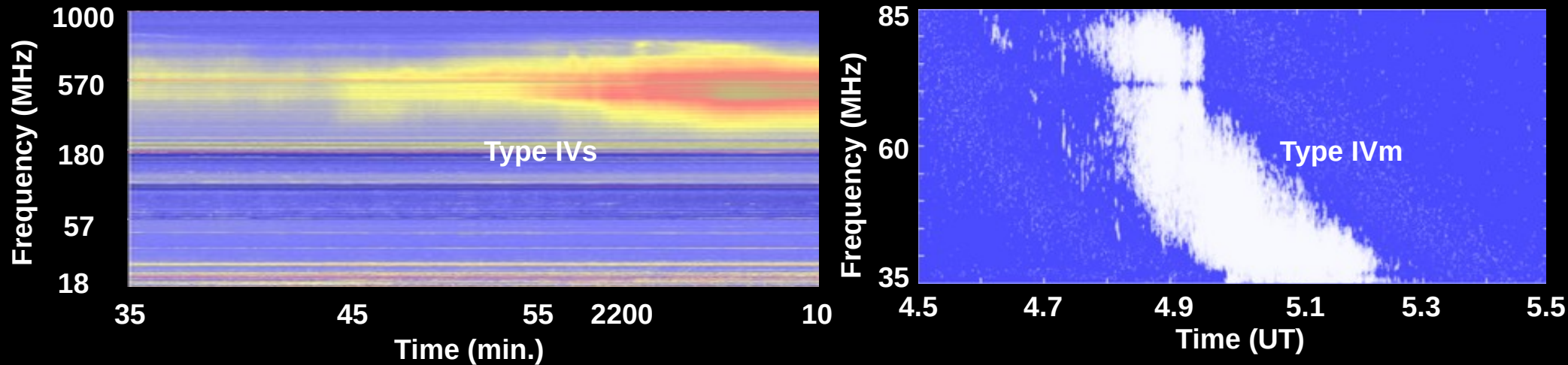
# Meter & deca-m $\lambda$ type-IV radio burst



## Meter & deca-m $\lambda$ type-IV radio burst

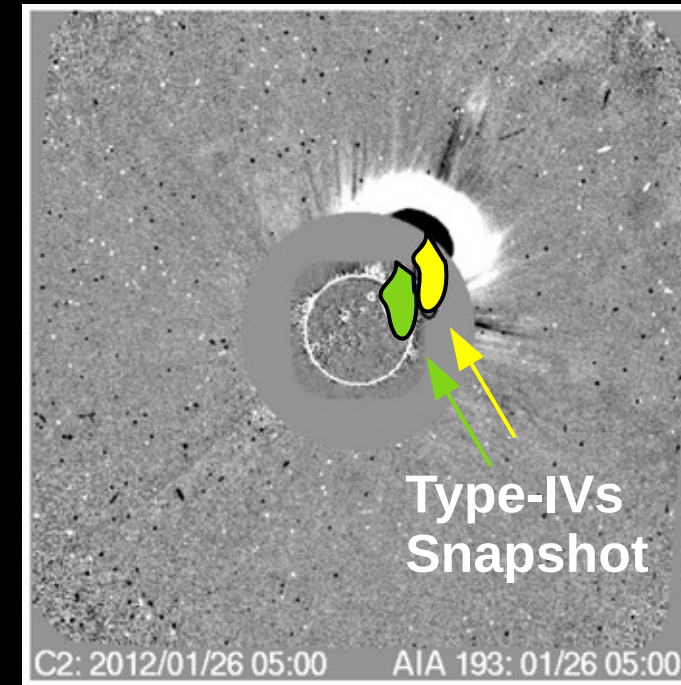
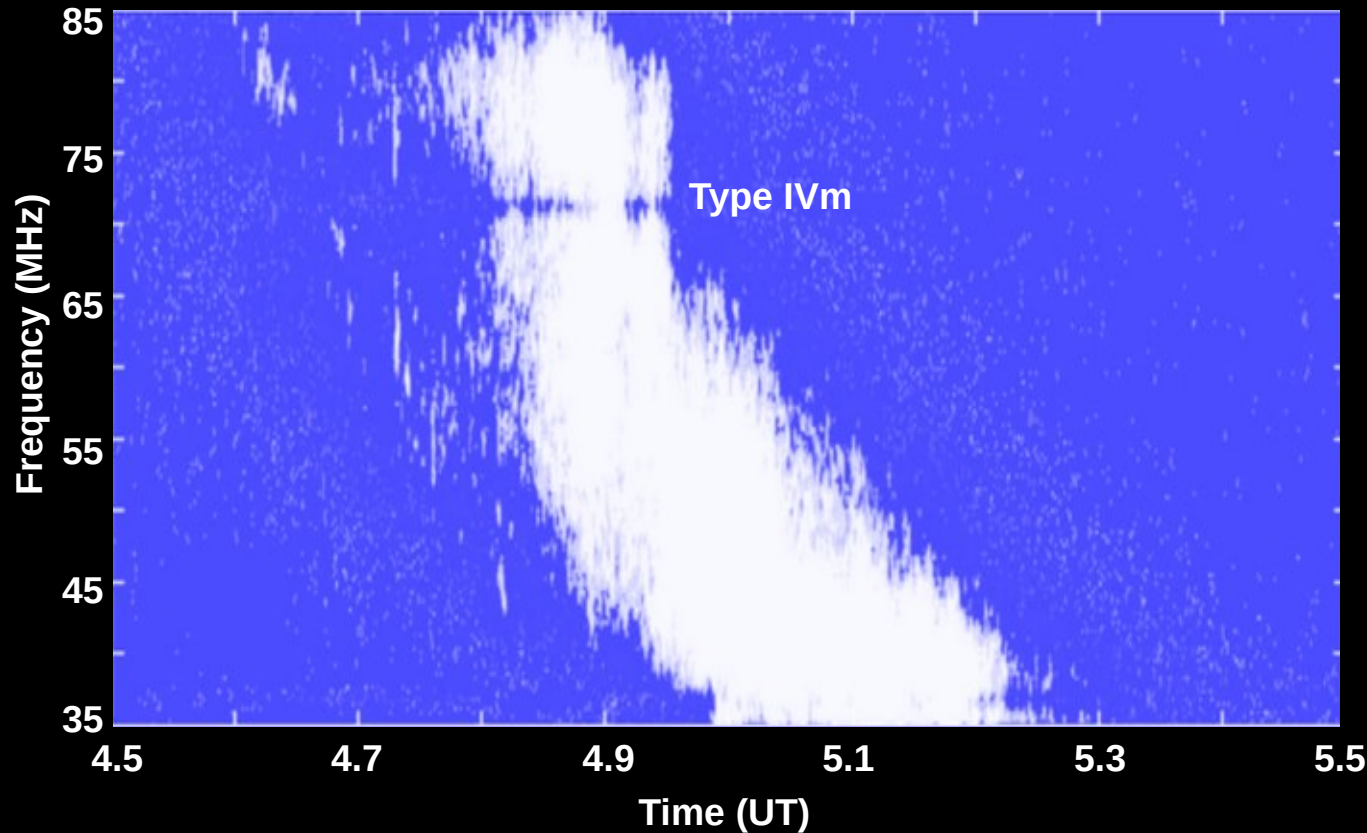


## Meter & deca-m $\lambda$ type-IV radio burst



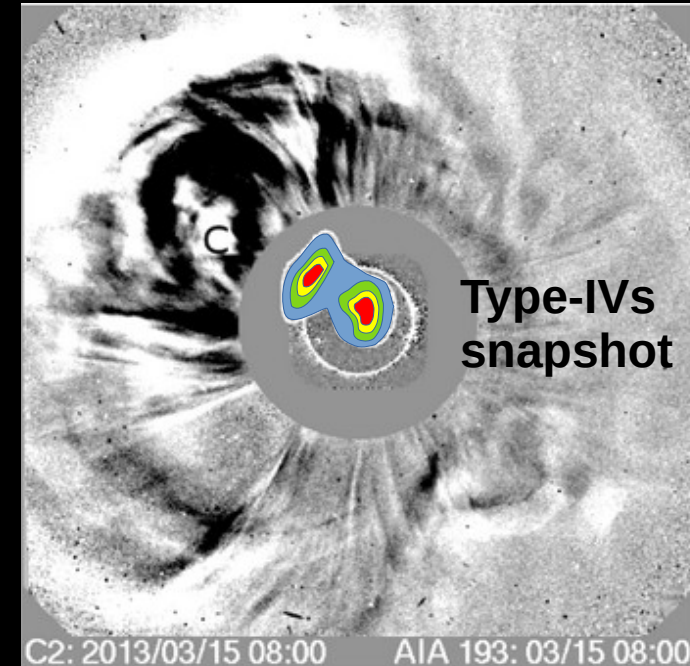
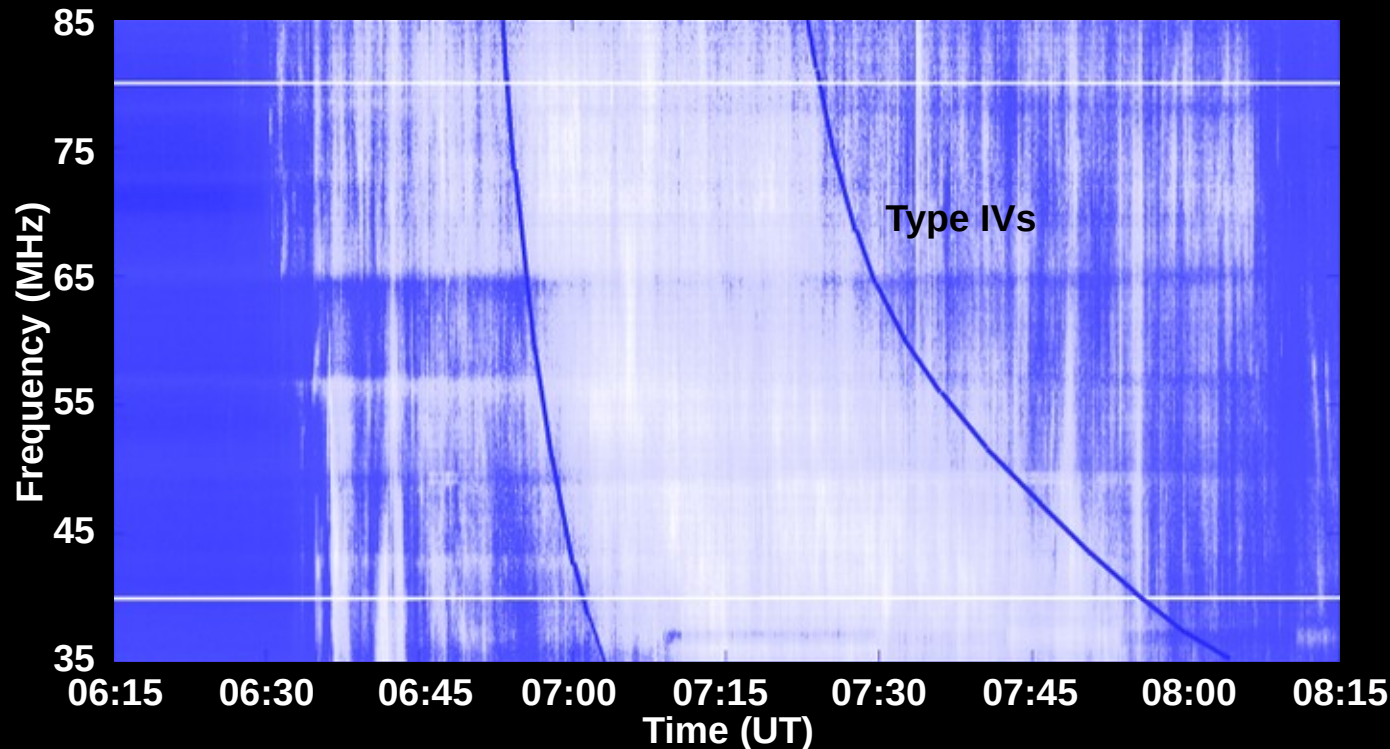
1. These are similar to type-II burst but the bandwidth at an instant is broader than type-II. It lasts up to several tens of minutes to hours.
2. Their size is about 10' (at 170 MHz) and shows a drift of about 6'-8' over 10 minutes. They appear to move faster during the initial phase and gradually reduces as a function of time.
3. The brightness temperature is about  $10^{10} - 10^{12}$  K ( $10^{-19}$  Watt/ m<sup>2</sup>/Hz). They do not drift further like type-II and type-III.
4. These are weakly circularly polarized (~10 %) and sometimes unpolarized.

## Meter & deca-m $\lambda$ type-IVm : Sources



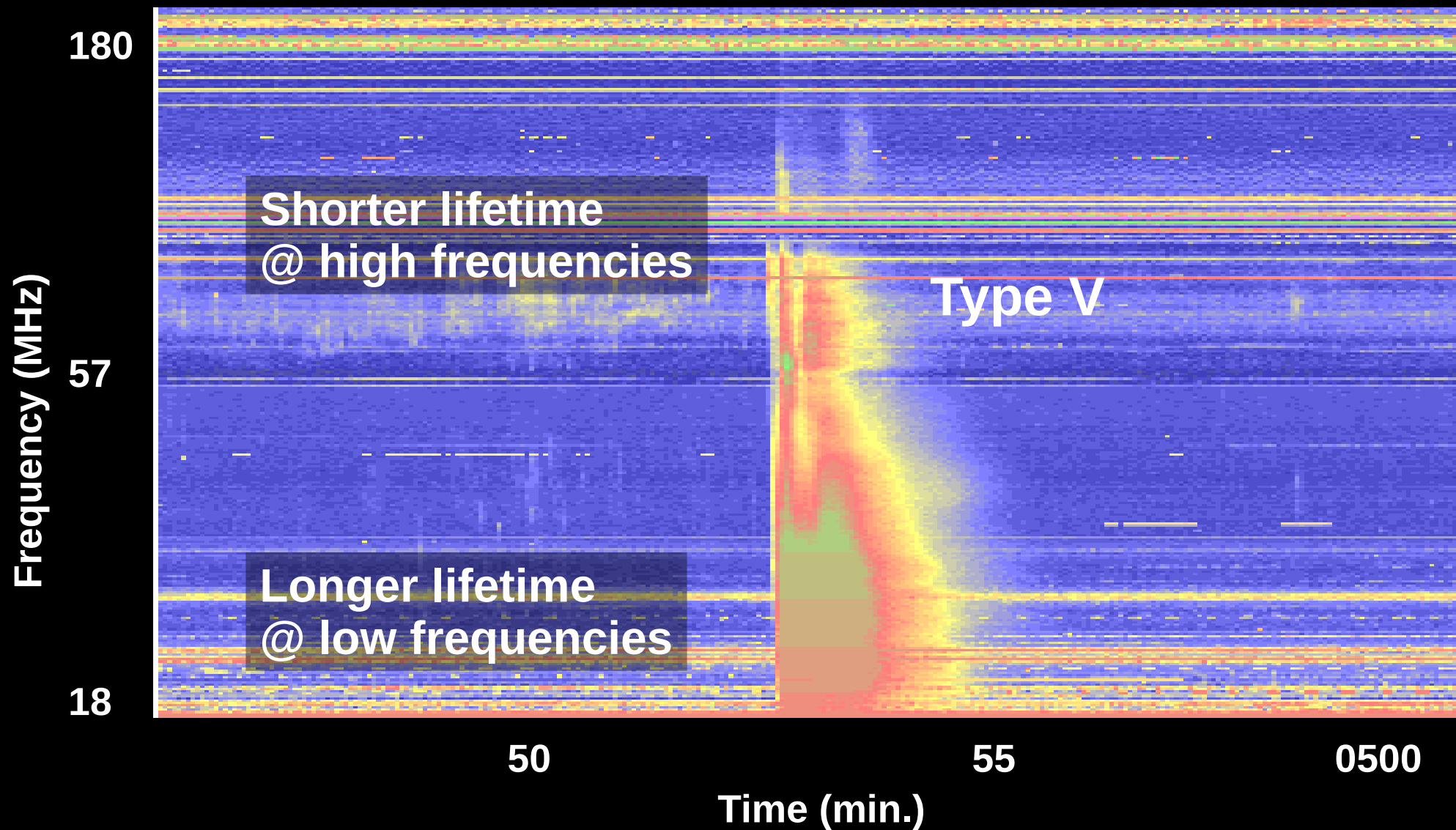
**1. Radio spectral and imaging observations show the type-IVm are generally due to plasma emission associated with the flanks / legs of the CMEs. Hence the drift rate is lower than that of the CME leading edge.**

## Meter & deca-m $\lambda$ type-IVs : Sources



**Radio spectral and imaging observations show the type-IVs are generally due to gyro-synchrotron emission associated with the core of the CMEs. Hence the drift rate is lower than that of the CME leading edge / flank.**

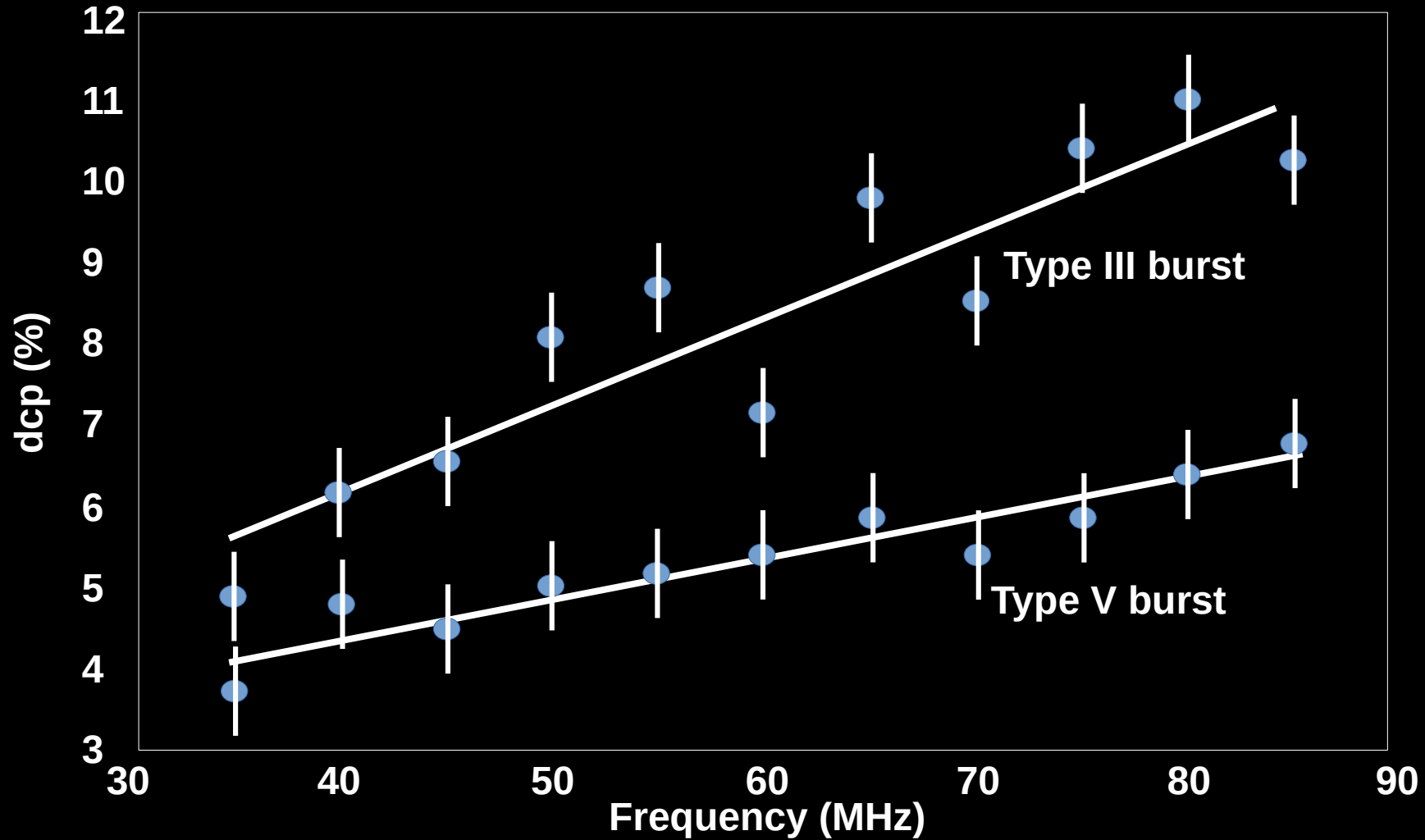
# Meter & deca-m $\lambda$ type-V radio bursts



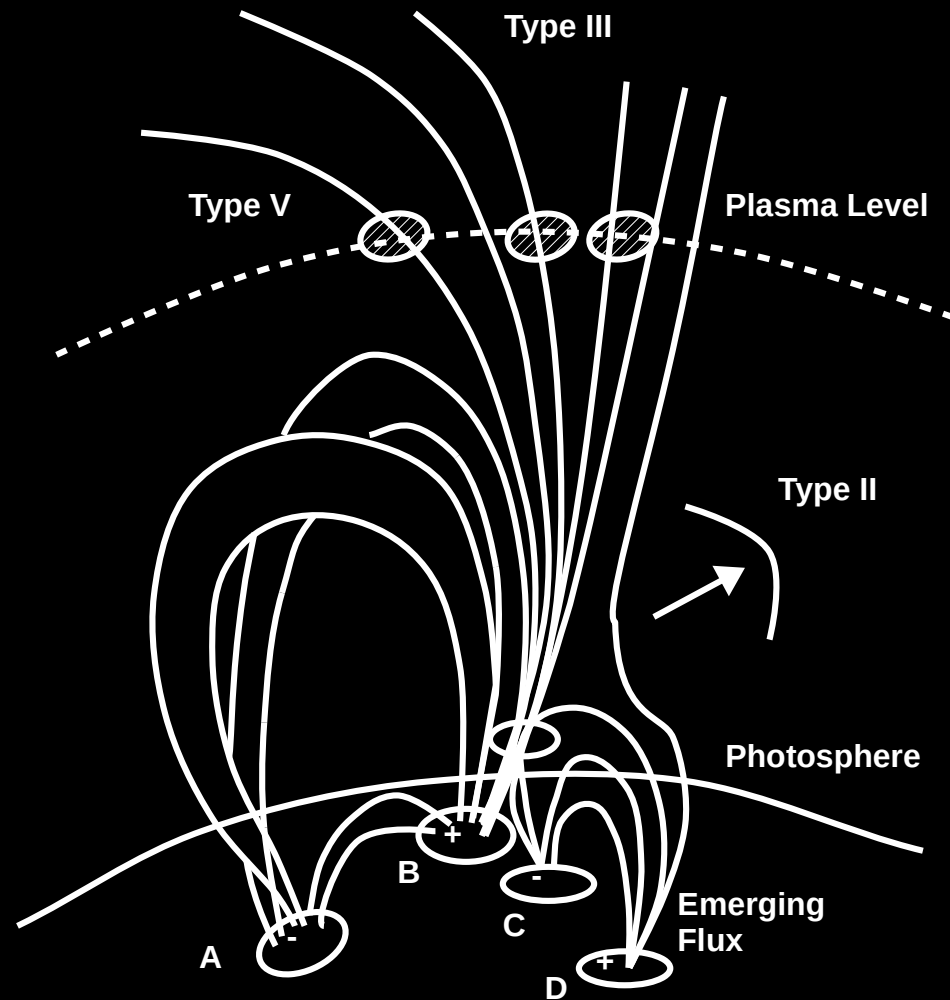
## Meter & deca-m $\lambda$ type-V radio bursts

1. Type-V occur very rarely and they always follow type-III.
2. Their duration as like type III vary as a function of frequency.
3. The emission is due to plasma mechanism like type-III bursts. The electrons that travel along curved magnetic field lines are responsible for type-V bursts.
4. Both type-III and type-V can have the same velocity of propagation, i.e. at 0.3 – 0.5 c.

# Meter & deca-m $\lambda$ type-V : Polarization

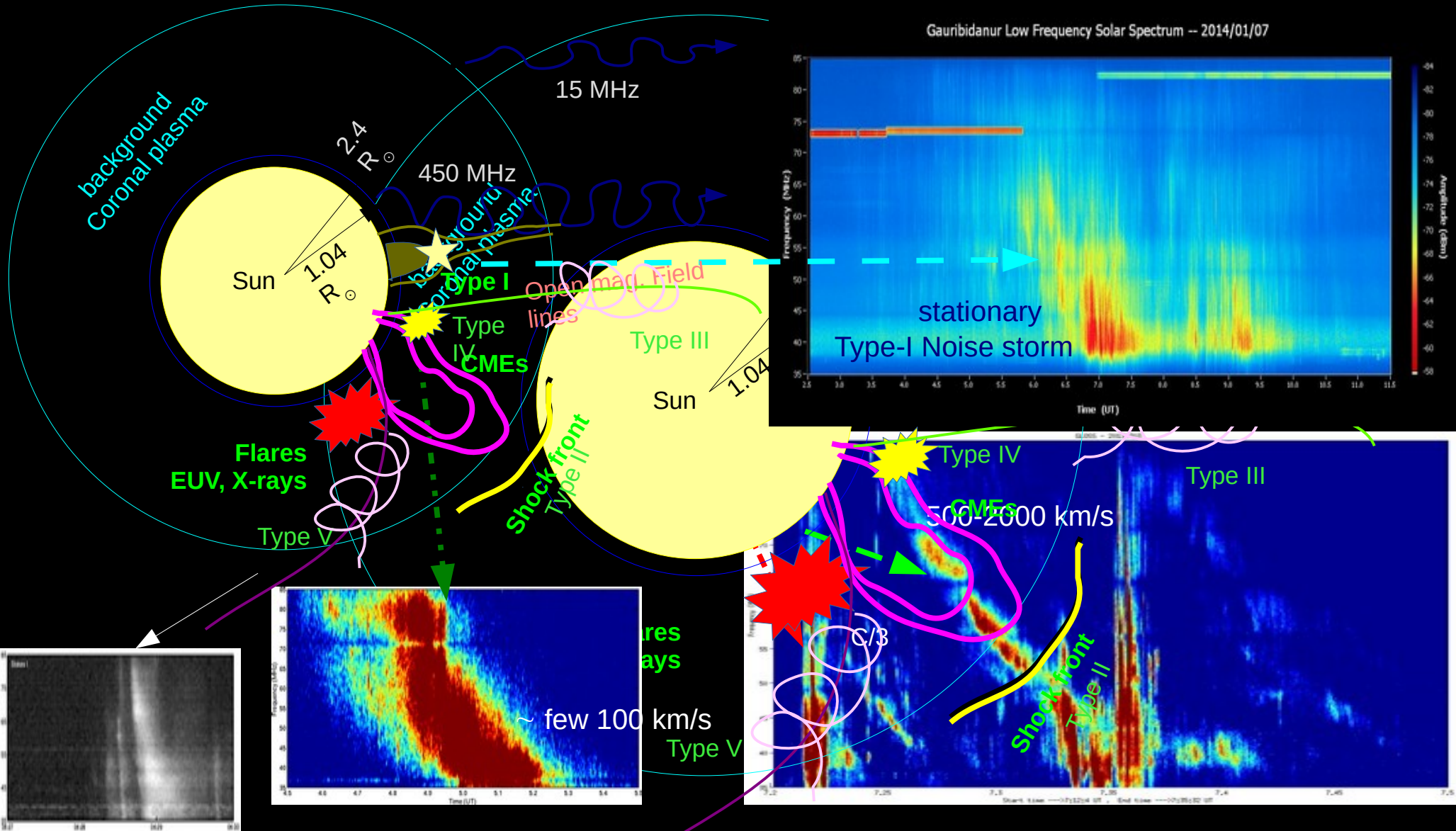


# Meter & deca-m $\lambda$ type-V : Schematic



**Gopalswamy et al., SoPh, 111, 347 (1987)**

# Meter & deca-m $\lambda$ burst summary

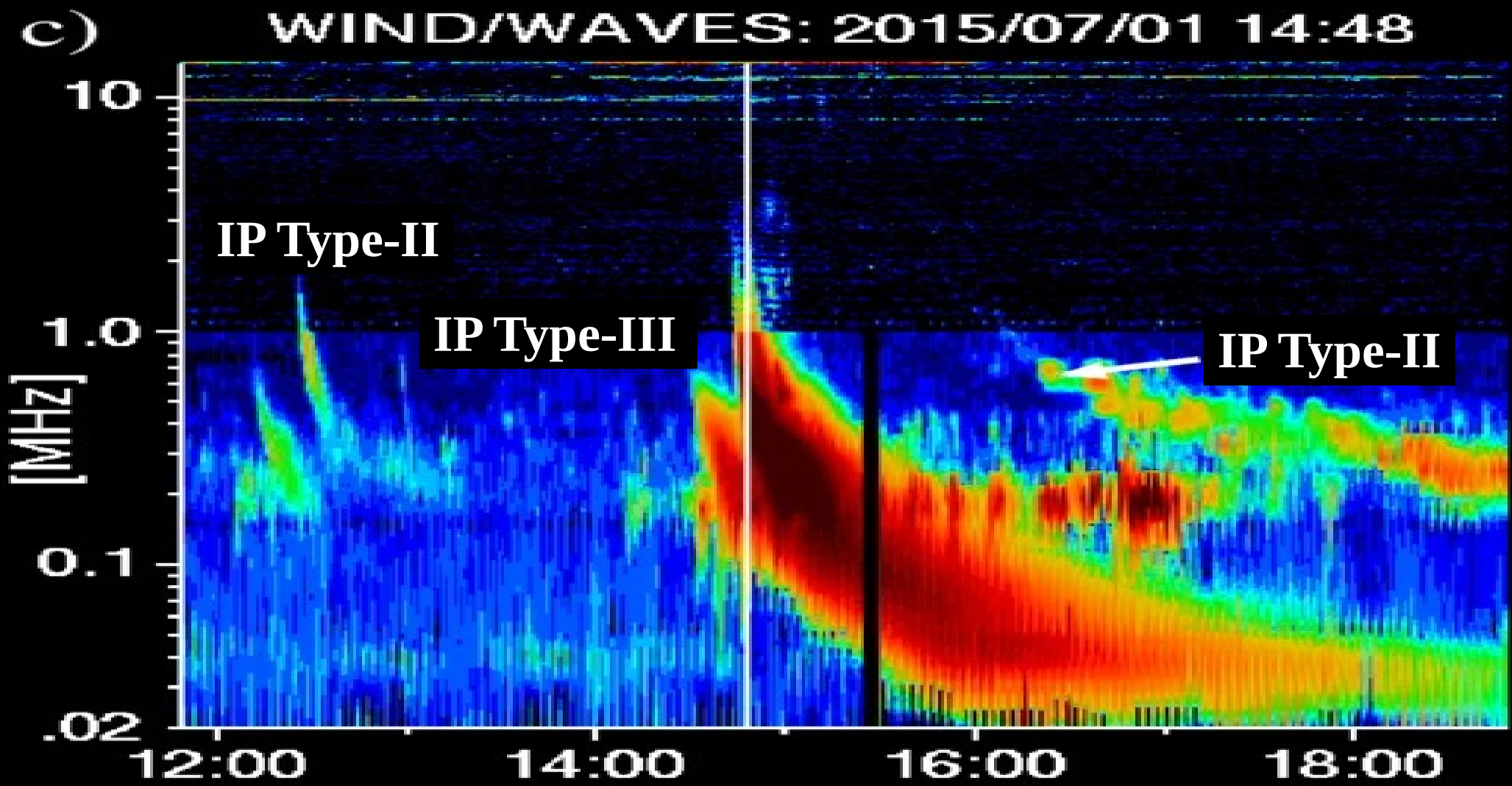


---

**Many more meter-deca-m  $\lambda$  bursts can be discussed further**

**Limited it due to time constraint**

# Hecto-m & km $\lambda$ / IP radio bursts



Pohjolainen et al. *SoPh*, 296, 81 (2021)

## Hecto-m & km $\lambda$ / IP radio bursts

- 1. Interplanetary type-III bursts are similar to meter-deca meter type-III. When they reach the Earth's atmosphere they live longer.**
- 2. Unless the spectra are continuous in the deca-meter to hecto-meter domain, it would be difficult to identify IP type-III bursts.**
- 3. IP type-II bursts are driven by shocks that are generated by Interplanetary CMEs (ICMEs).**

---

**Since CMEs and flares are also transients, can they be observed in radio ??**

**Yes... Radio Imaging of transients**

1

---

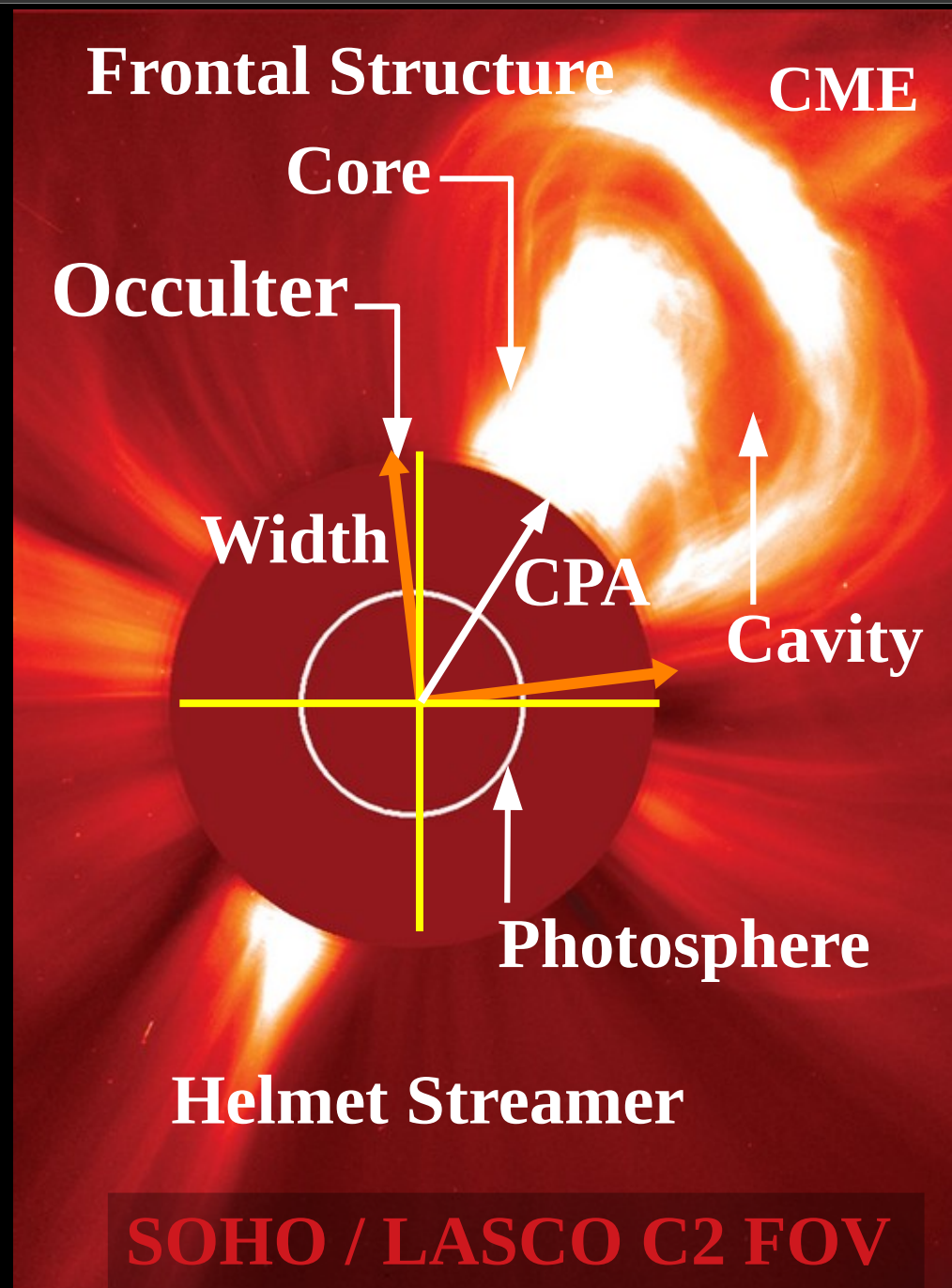
# CME associated Radio signatures

---

# Coronal Mass Ejection (CME)

A discrete brightening observed in the field of view of a white-light coronagraph.

It always moves outward from the Sun into the heliosphere over a time-scale of several hours to ~ days.



SOHO / LASCO C2 FOV

Webb, D. et al., LRSP, 9, 3 (2012)

## Coronal Mass Ejection (CME)

It is a large scale plasma entrained on an expanding magnetic field (flux rope).

One can identify the CME features clearly from the running difference images and its propagation from the time-lapse movies.



**Webb, D. et al., LRSP, 9, 3 (2012)**

---

# Can CMEs be observed in Radio ??

---

## Two Possibilities :

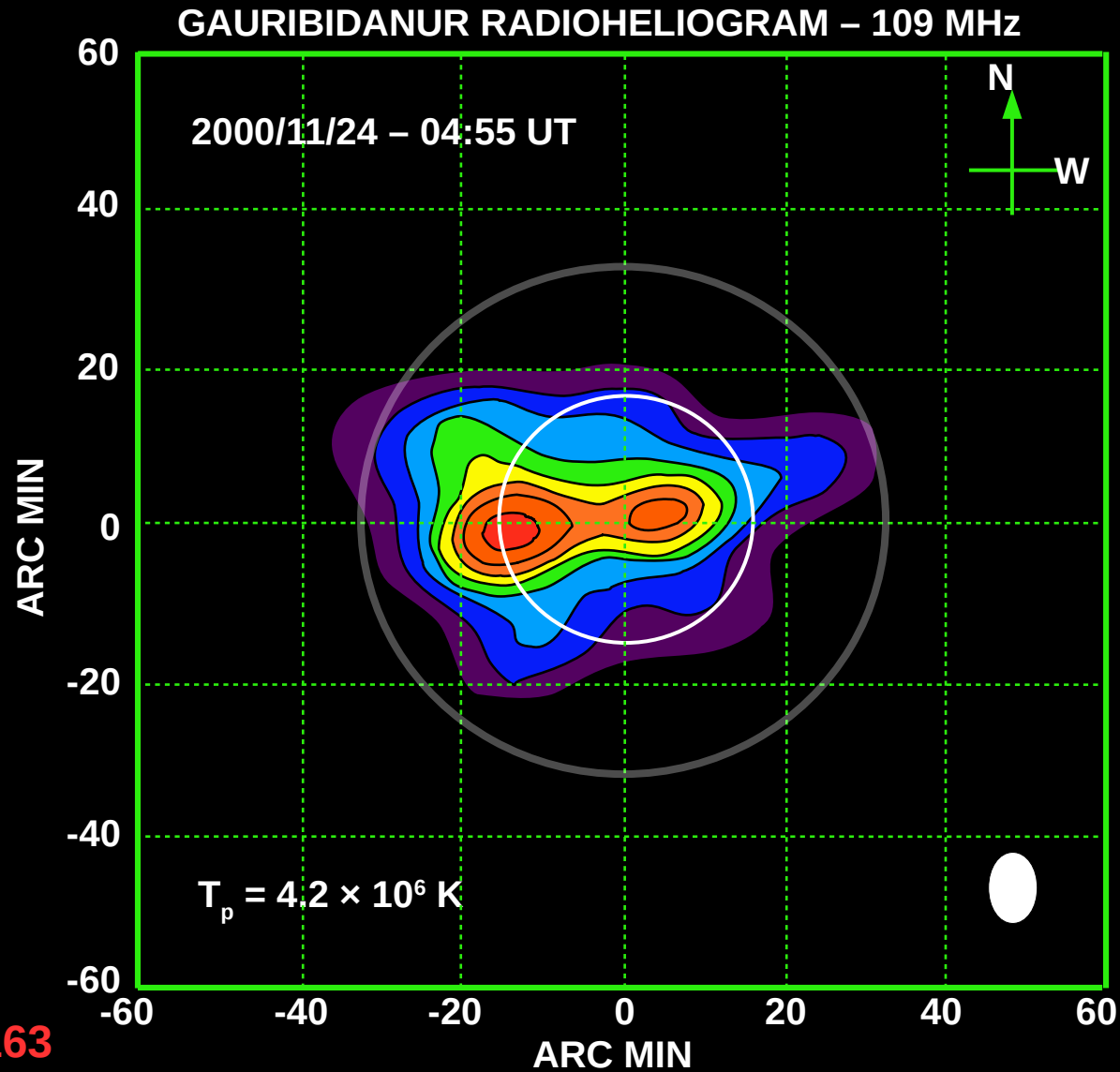
---

**CME → Thermal ✓**  
**CME → Non-thermal**

---

# CME → Mass + Sky-plane Speed

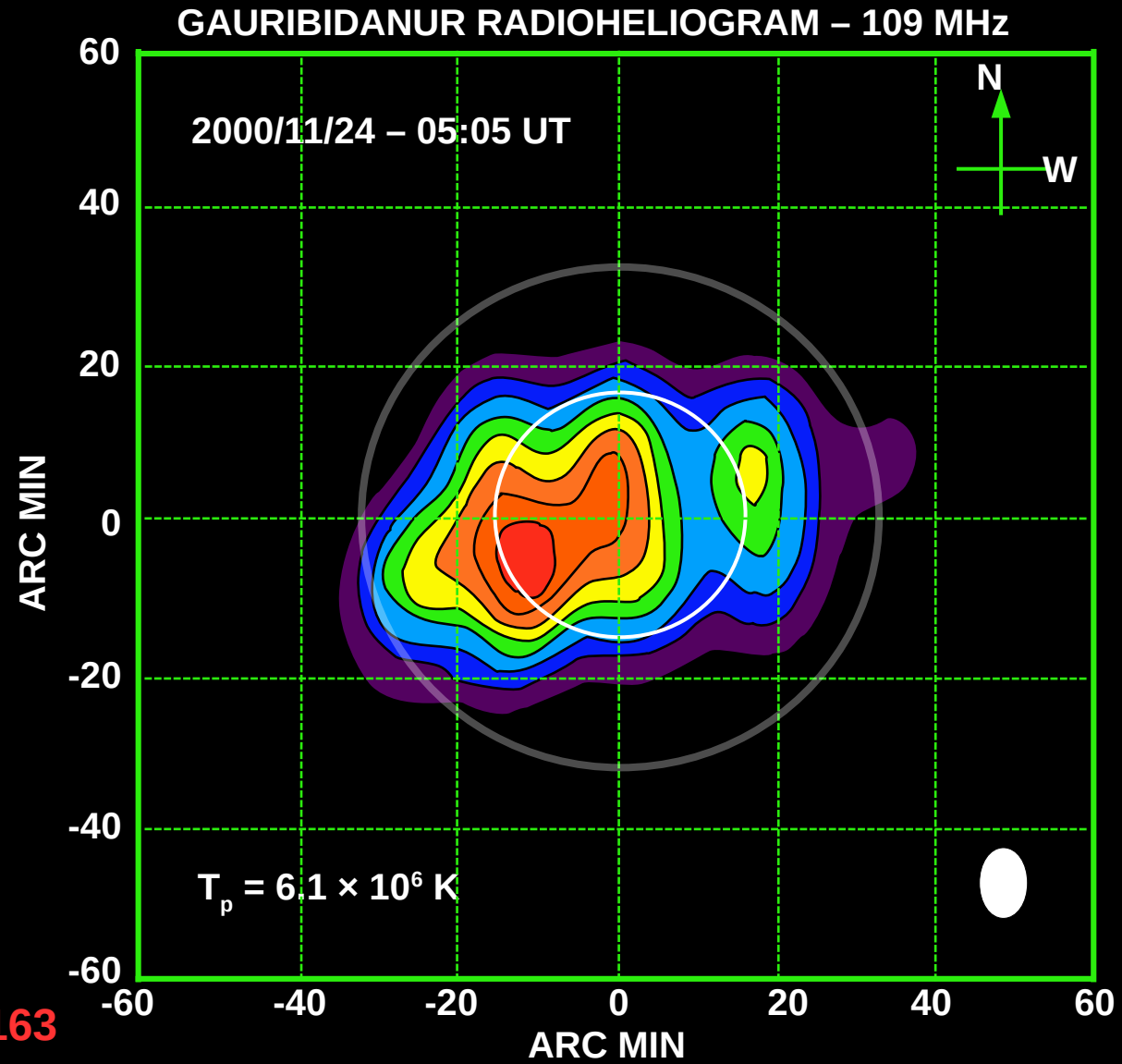
<u>Radio Observation Summary</u>
Radio Telescope : GRAPH
Nov. 24, 2000 – 04:55 UT
f = 109 MHz
$\Omega_{res} = 7' \times 11'$
$T_b = 4.2 \times 10^6 \text{ K}_{\leftarrow \dots}$
$T_b \text{ (interval)} = 0.5 \times 10^6 \text{ K}_{\leftarrow \dots}$
Dynamic Range : $\approx 20 \text{ dB}$
Red : Maximum Temperature
Violet : Minimum Temperature



Ramesh, R. et al. *ApJL*, 2003, 591, 2, 163

# CME → Mass + Sky-plane Speed

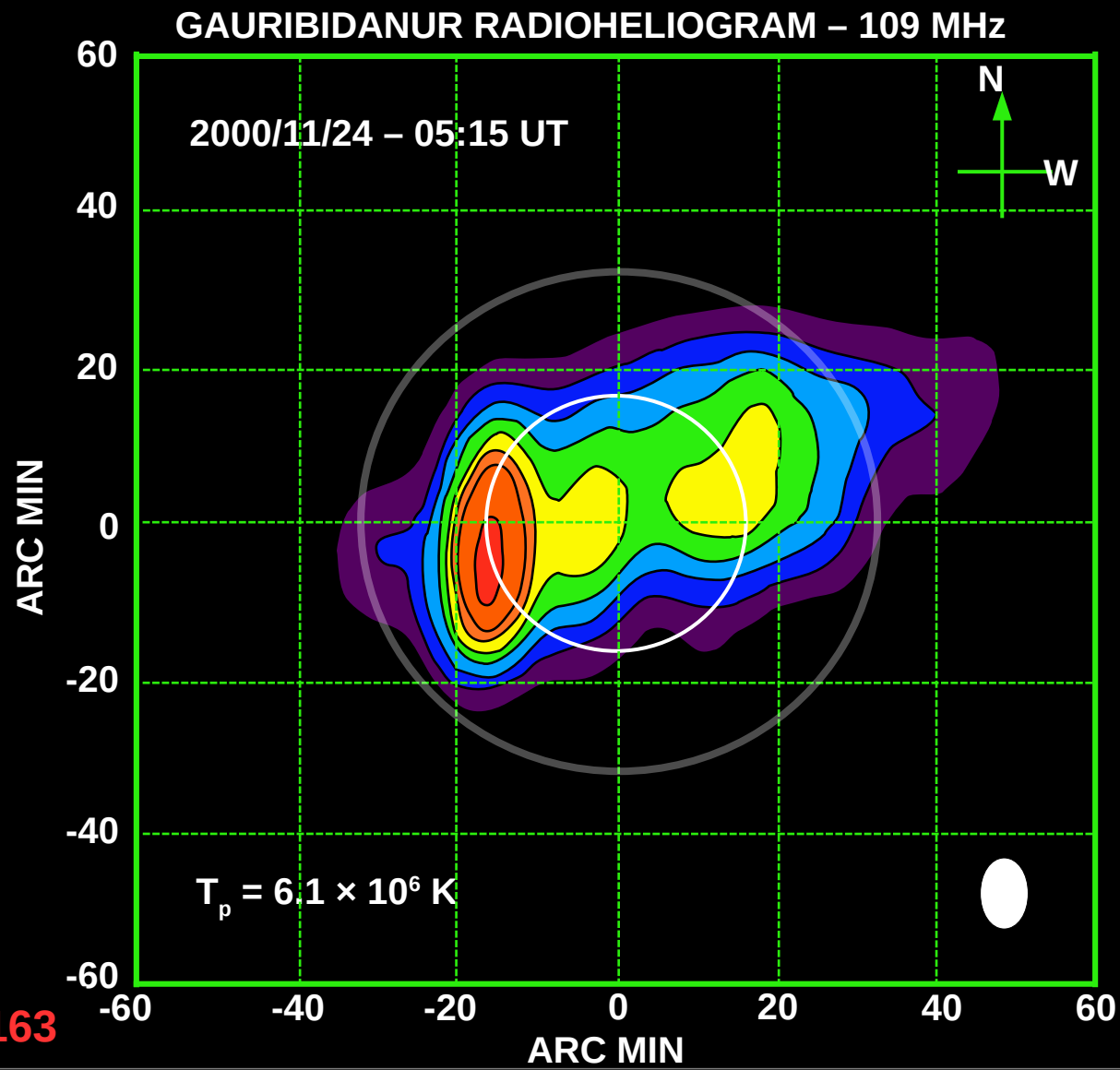
<u>Radio Observation Summary</u>
Radio Telescope : GRAPH
Nov. 24, 2000 – 05:05 UT
f = 109 MHz
$\Omega_{res} = 7' \times 11'$
$T_b = 6.1 \times 10^6 K_{\leftarrow \dots}$
$T_b$ (interval) = $0.6 \times 10^6 K_{\leftarrow \dots}$
Dynamic Range : $\approx 20$ dB
Red : Maximum Temperature Violet : Minimum Temperature



Ramesh, R. et al. ApJL, 2003, 591, 2, 163

# CME → Mass + Sky-plane Speed

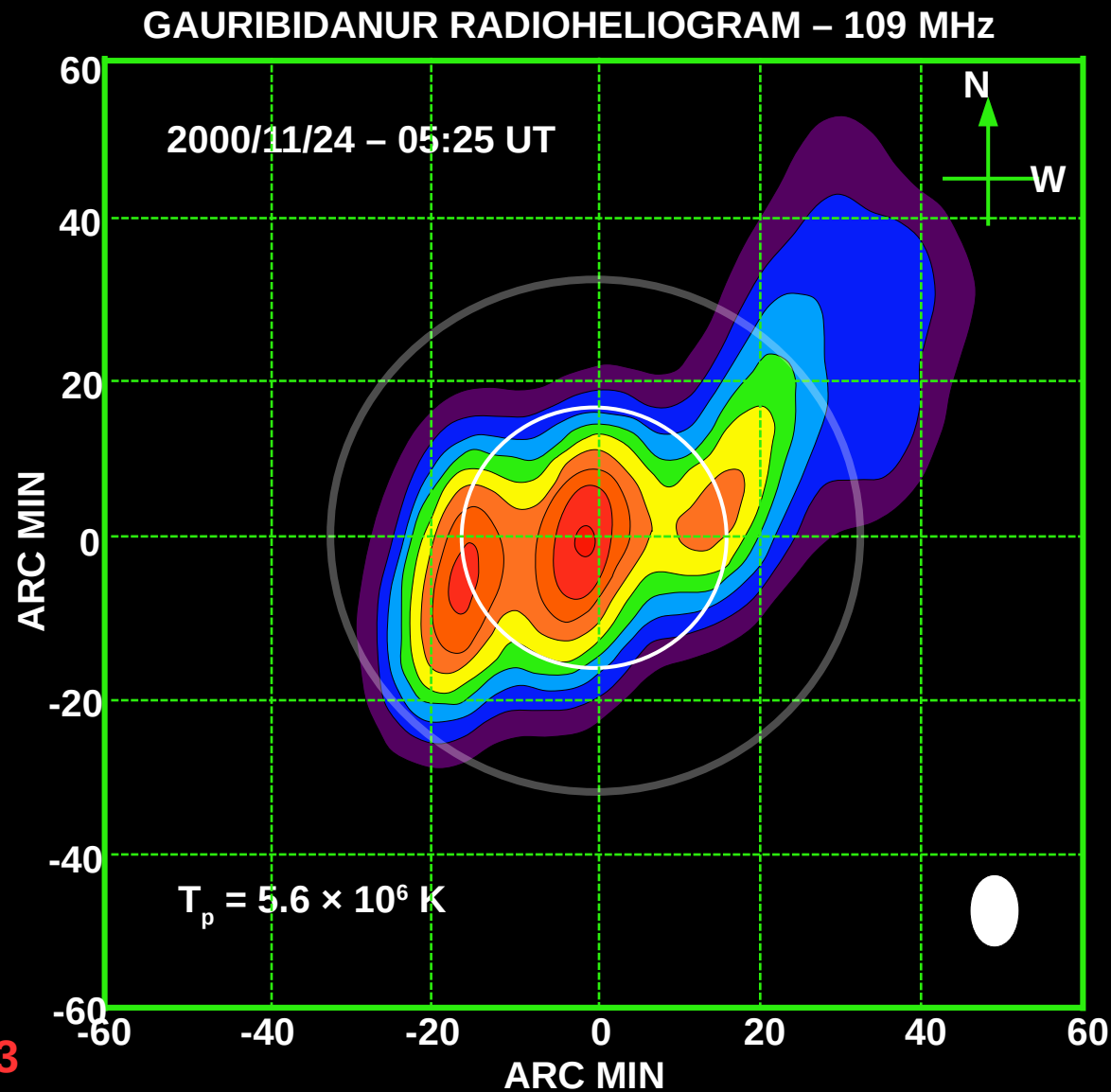
<u>Radio Observation Summary</u>
Radio Telescope : GRAPH
Nov. 24, 2000 – 05:15 UT
f = 109 MHz
$\Omega_{res} = 7' \times 11'$
$T_b = 6.1 \times 10^6 \text{ K}_{\leftarrow \dots}$
$T_b \text{ (interval)} = 0.6 \times 10^6 \text{ K}_{\leftarrow \dots}$
Dynamic Range : $\approx 20 \text{ dB}$
Red : Maximum Temperature Violet : Minimum Temperature



Ramesh, R. et al. *ApJL*, 2003, 591, 2, 163

# CME → Mass + Sky-plane Speed

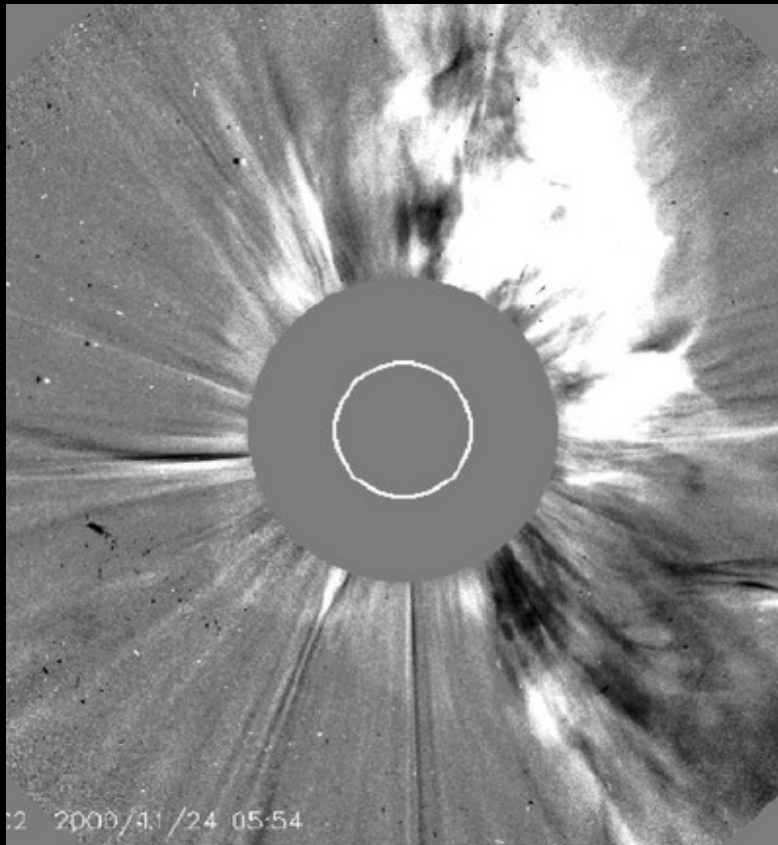
<u>Radio Observation Summary</u>
Radio Telescope : GRAPH
Nov. 24, 2000 – 05:25 UT
f = 109 MHz
$\Omega_{res} = 7' \times 11'$
$T_b = 5.6 \times 10^6 \text{ K}_{\leftarrow}$
$T_b \text{ (interval)} = 0.5 \times 10^6 \text{ K}_{\leftarrow}$
Dynamic Range : $\approx 20 \text{ dB}$
Red : Maximum Temperature Violet : Minimum Temperature



Ramesh, R. et al. *ApJL*, 2003, 591, 2, 163

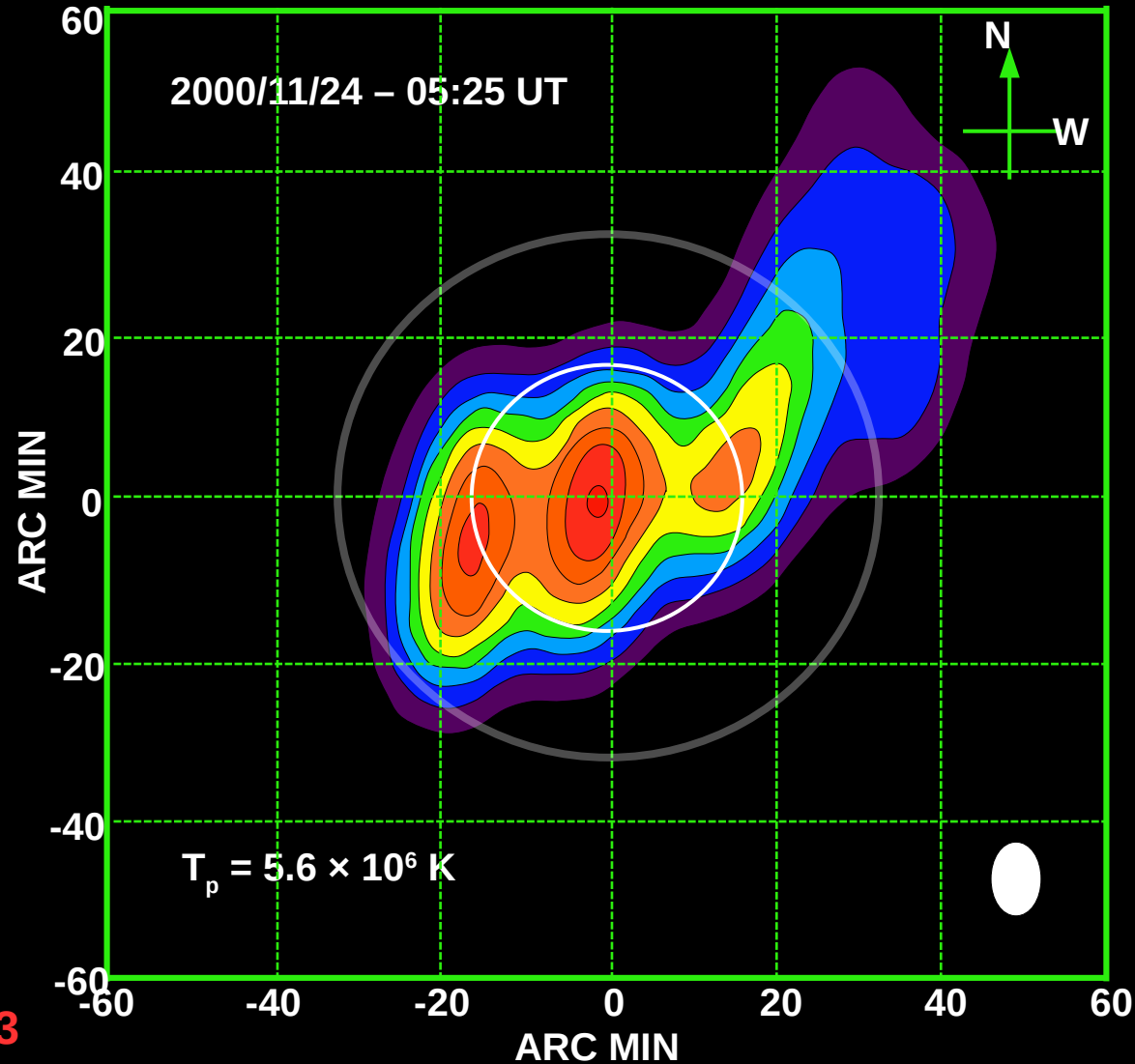
# CME → Mass + Sky-plane Speed

LASCO C2



RDI

GAURIBIDANUR RADIOHELIOGRAM – 109 MHz



Ramesh, R. et al. *ApJL*, 2003, 591, 2, 163

# CME → Mass + Sky-plane Speed

Radio Analysis Summary

**GRAPH DIFF IMAGE**

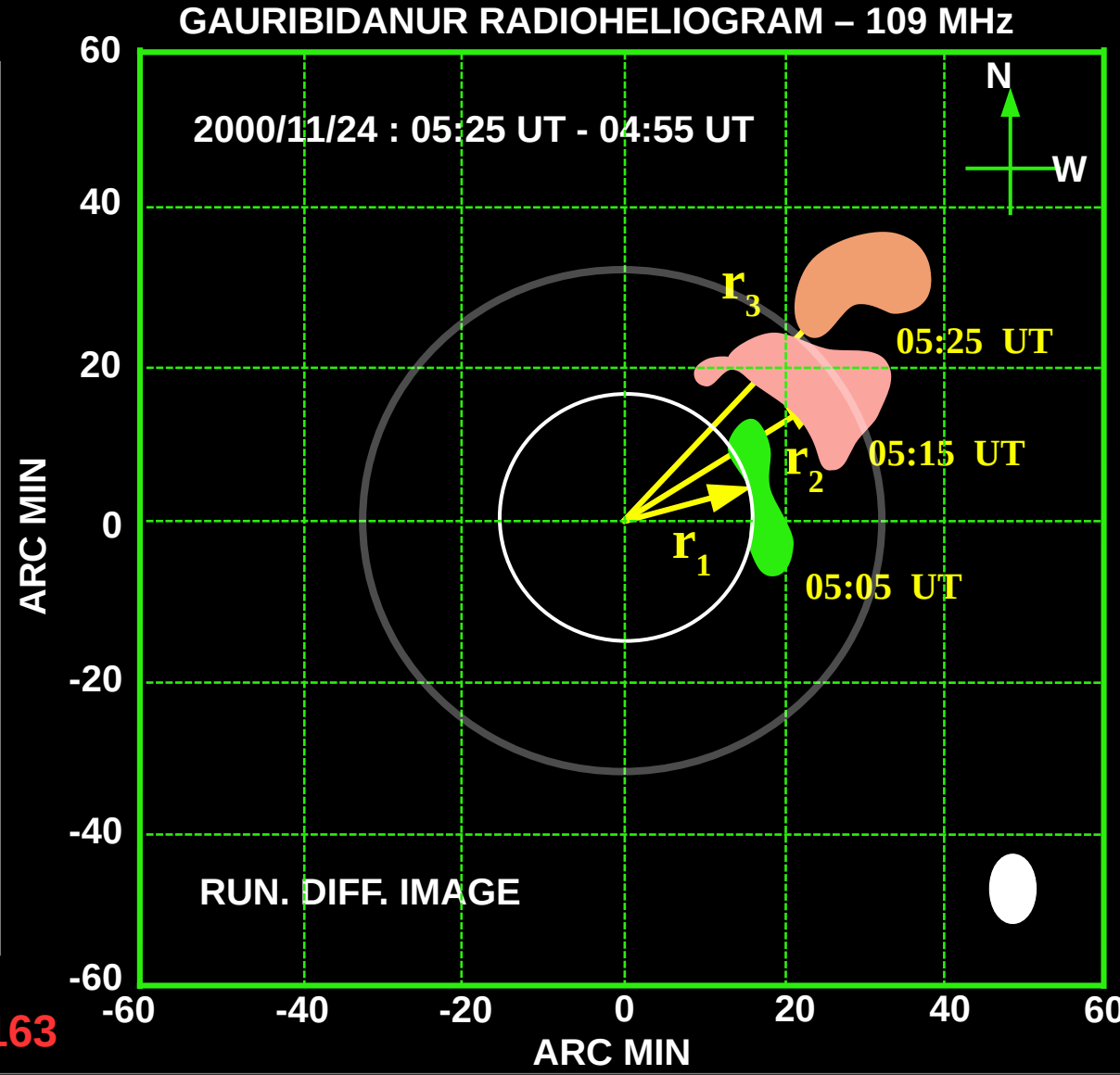
Nov. 24, 2000  
05:25 – 04:55 UT

f = 109 MHz

Difference Images were made  
@ t = 5:05, 5:15, 5:25 UT

$$v_1 = (r_2 - r_1) / (t_2 - t_1)$$

$$v_2 = (r_3 - r_2) / (t_3 - t_2)$$

$$a = (V_2 - V_1) / (t_{m2} - t_{m1})$$


Ramesh, R. et al. ApJL, 2003, 591, 2, 163

# CME → Mass + Sky-plane Speed

## Radio Analysis Summary

Time (UT)	P.A. (deg)	$T_{\text{CME}}$ (K)	$N_e$ (cm <sup>-3</sup> )	Mass (g)	Speed (km/s)
04:55					
05:05	282	$3.3 \times 10^5$	$12.4 \times 10^7$	$2.7 \times 10^{16}$	
05:15	308	$2.8 \times 10^5$	$4.5 \times 10^7$	$3.8 \times 10^{16}$	$1087 \pm 73$
05:25	318	$1.9 \times 10^5$	$2.8 \times 10^7$	$4.4 \times 10^{16}$	$1185 \pm 73$
				Acceleration	$157 \pm 120 \text{ m/s}^2$

Ramesh, R. et al. *ApJL*, 2003, 591, 2, 163

---

**Radio data can be used to estimate  
the mass & speed of CMEs  
in the sky plane  
similar to WL coronagraph data**

---

---

**Since CMEs travel in 3D space,  
do the 2D image data help to  
infer whether a CME  
would reach the Earth or not ??**

---

# CME Modeling

- 1 Epi-polar geometry & tie-Pointing technique
- 2 Forward modeling & Reverse reconstruction
- 3 Polarization ratio technique
- 4 GCS modeling

**2D WL, EUV, etc. observations → 3D reconstruction**

# CME Modeling

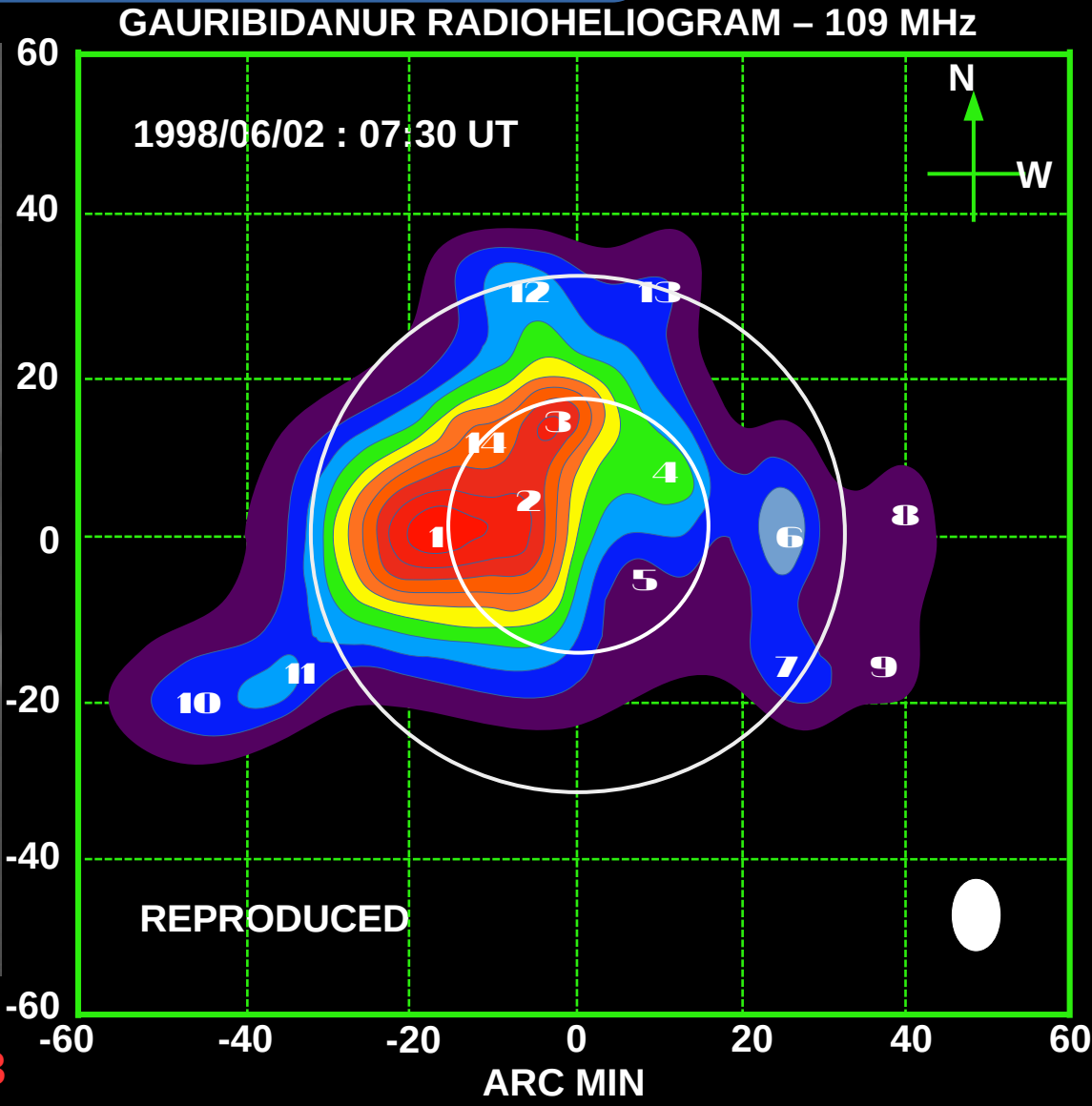
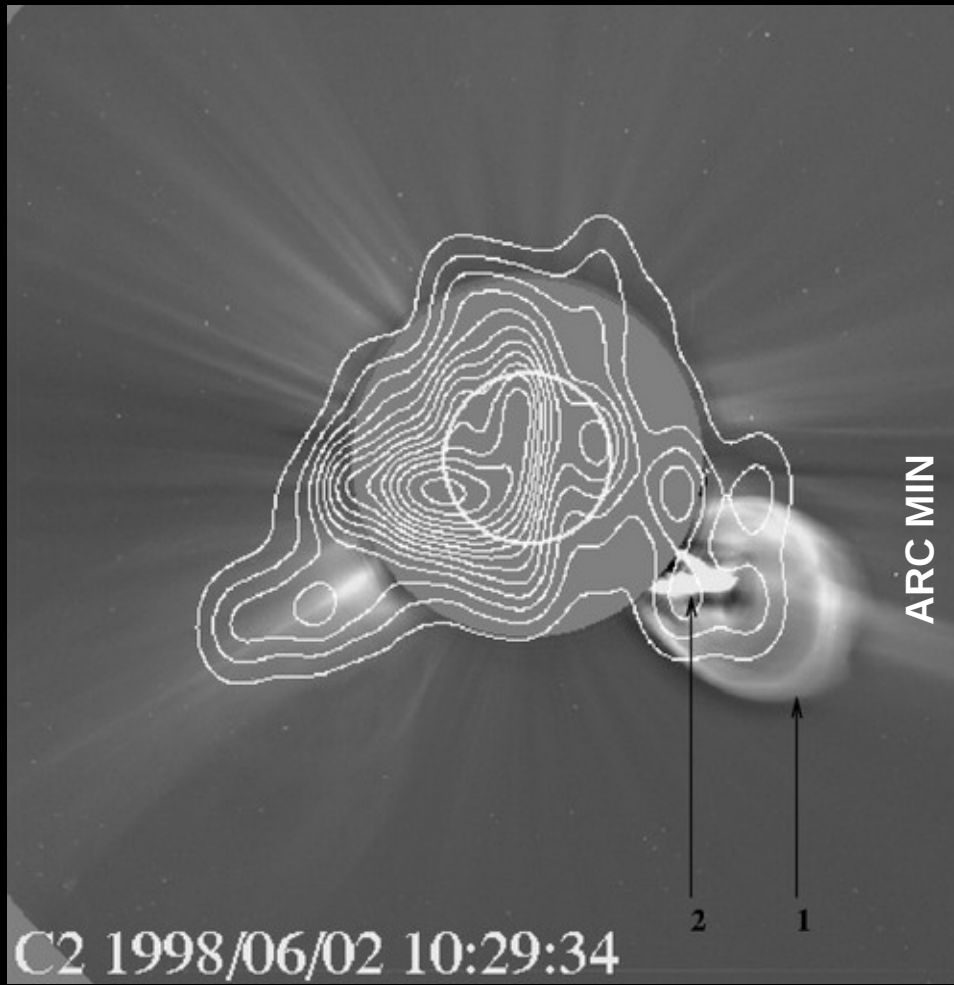
**2D Radio observations → 3D reconstruction**

---

**Ray-Tracing technique**

---

# CME → True Mass



Kathiravan, C. et al. ApJL, 2002, 567, 1, 93

# CME → True Mass

## Radio Analysis Summary

Source	Location (Sol. Rad.)	Size (Sol. Rad.)	Density factor
S6	1.50, 1.70, -0.06	0.2,0.22,0.64	10
S7	1.70, 1.72, -1.22	0.22, 0.29, 0.29	17
S8	1.70, 2.48, -0.03	0.26, 0.29, 0.50	20
S9	1.70, 2.44, -1.22	0.22, 0.29, 0.50	20
	<b>Average Density</b>	$2.65 \times 10^7 \text{ cm}^{-3}$	
	<b>Total Mass</b>	$2.02 \times 10^{15} \text{ g}$	<b>&lt; LASCO (1/4)</b>

**Kathiravan, C. et al. ApJL, 2002, 567, 1, 93**

---

**Radio reconstruction method  
can be used to estimate  
the true mass of CMEs  
similar to other techniques**

---

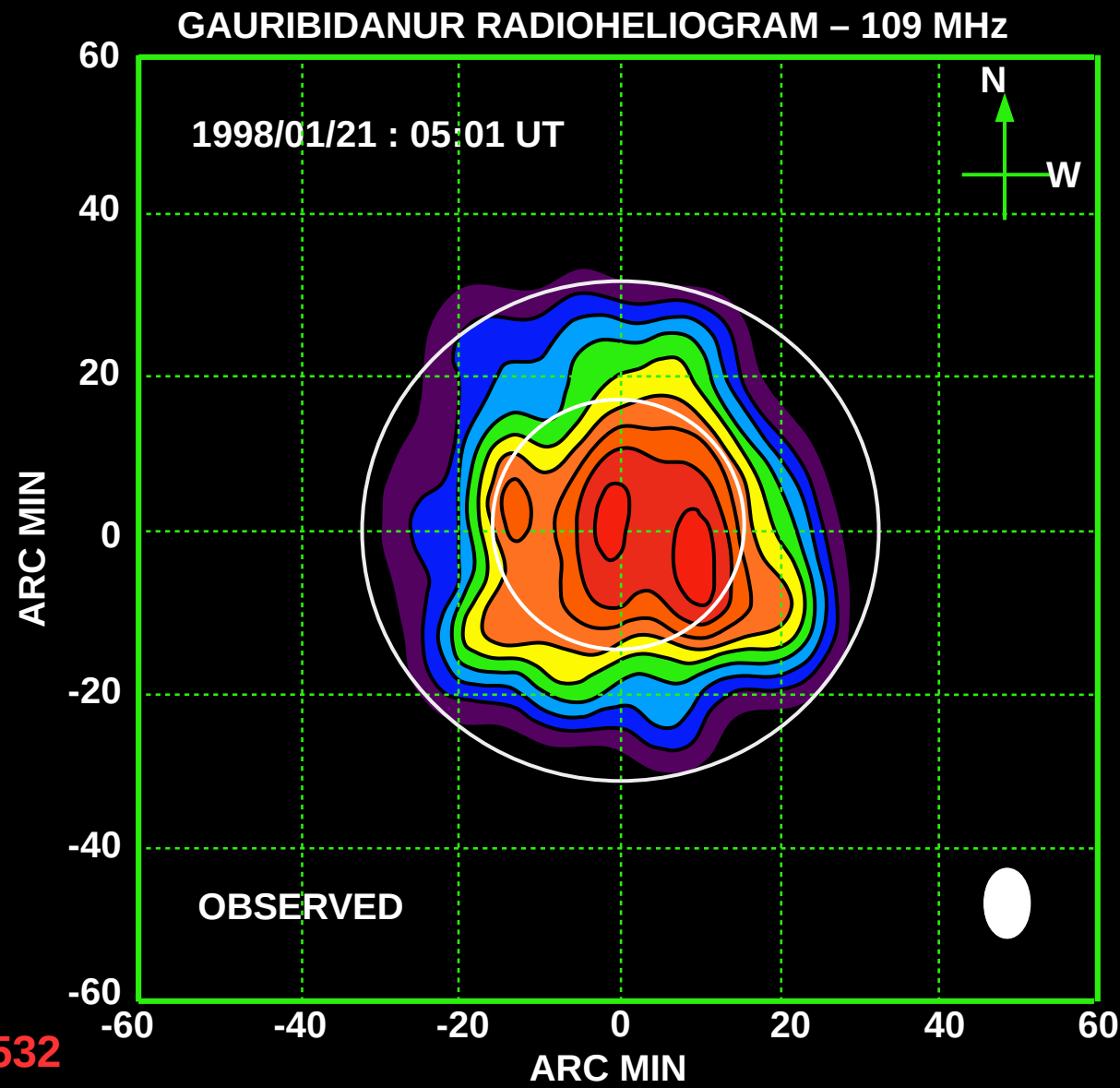
---

**Since CME related  
Structures are identified,  
Can they be used to find  
the true / 3D Speed ??**

---

# CME → True Speed

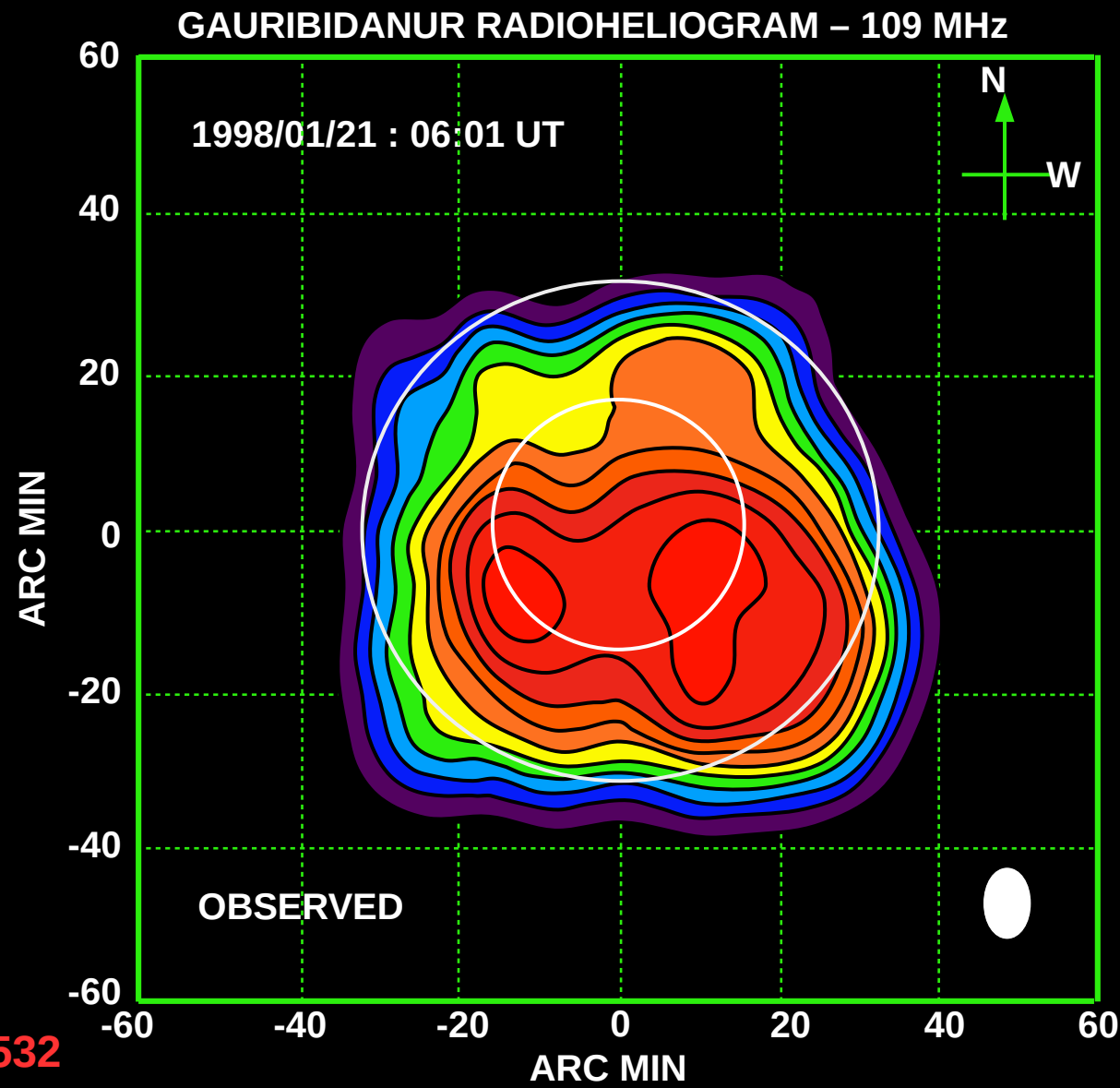
<u>Radio Observation Summary</u>
Rad. Tele. : GRAPH
Jan. 21, 1998 – 05:01 UT
$f = 109 \text{ MHz}$
$\Omega_{\text{res}} = 7' \times 11'$
$T_b = 1.2 \times 10^6 \text{ K}_{\leftarrow \dots}$
$T_b \text{ (interval)} = 0.1 \times 10^6 \text{ K}_{\leftarrow \dots}$
Dynamic Range : $\approx 20 \text{ dB}$
Red : Maximum Temperature
Violet : Minimum Temperature



Kathiravan, C. et al. *ApJ*, 2004, 610, 1, 532

# CME → True Speed

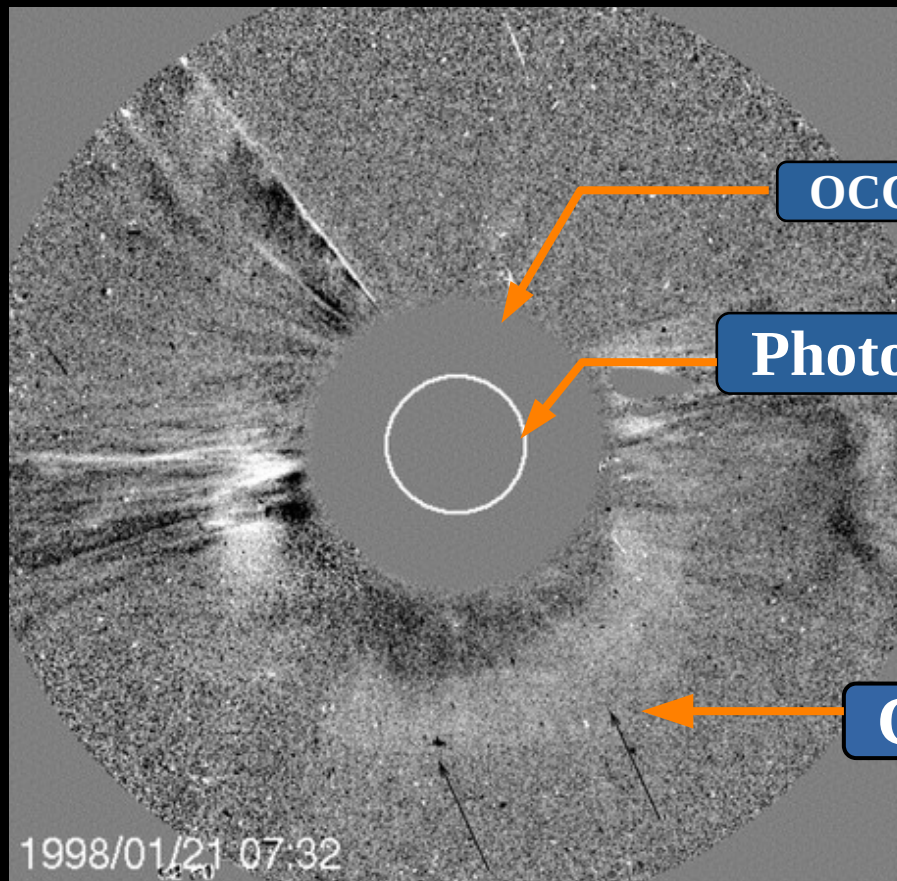
<u>Radio Observation Summary</u>
Radio Telescope : GRAPH
Jan. 21, 1998 – 06:01 UT
$f = 109 \text{ MHz}$
$\Omega_{\text{res}} = 7' \times 11'$
$T_b = 1.0 \times 10^6 \text{ K}_{\leftarrow \dots}$
$T_b \text{ (interval)} = 0.1 \times 10^6 \text{ K}_{\leftarrow \dots}$
Dynamic Range : $\approx 20 \text{ dB}$
Red : Maximum Temperature
Violet : Minimum Temperature



Kathiravan, C. et al. *ApJ*, 2004, 610, 1, 532

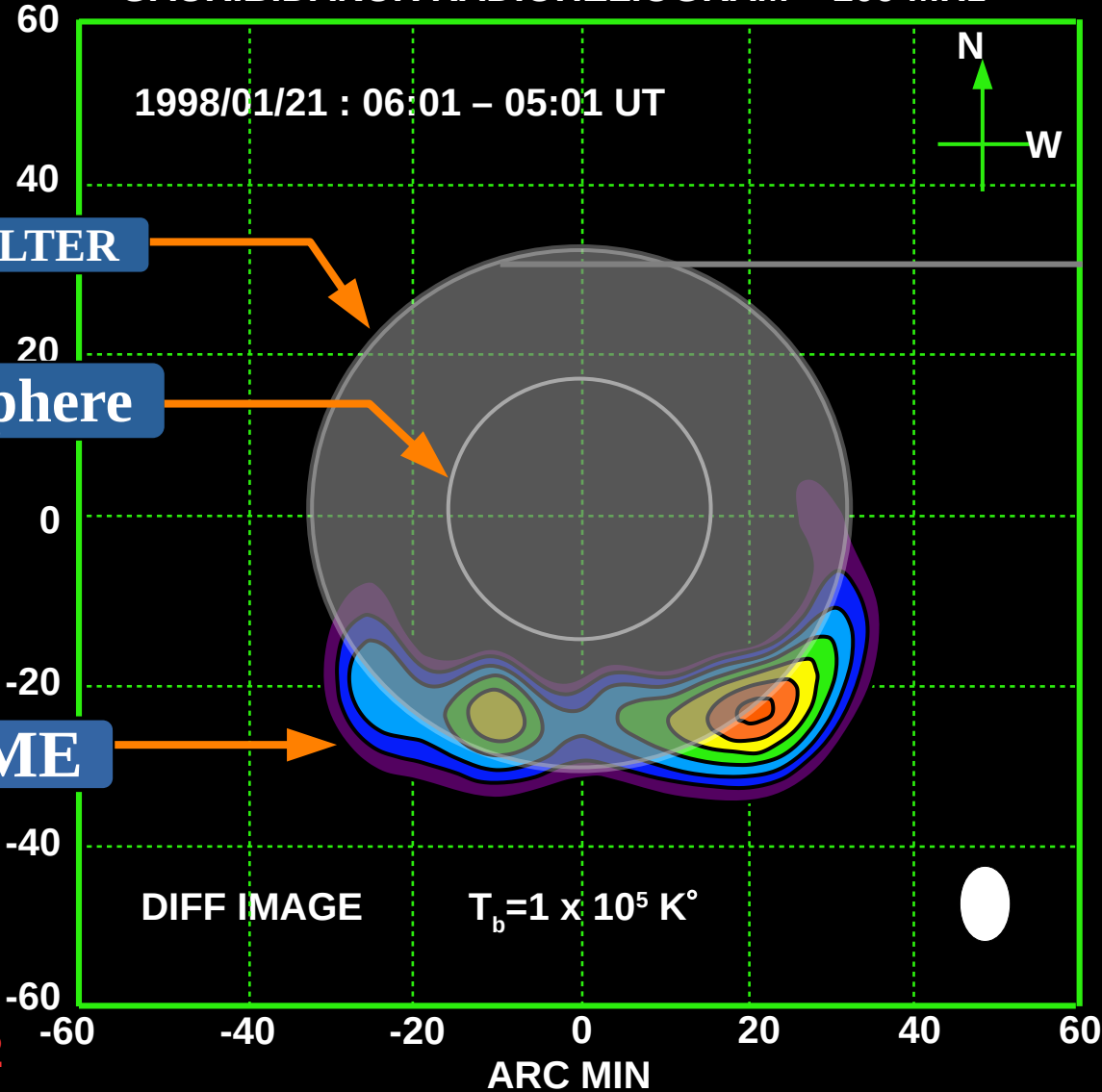
# CME → True Speed

**LASCO C2**



**RDI**

**GAURIBIDANUR RADIOHELIOGRAM – 109 MHz**



OCCULTER

Photosphere

CME

**Kathiravan, C. et al. ApJ, 2004, 610, 1, 532**

# CME → True Speed

Radio Analysis Summary

$V_{los} = 318 \text{ km/s}$   
 $V_{pos} = 485 \text{ km/s}$   
 $V_{tot} = 580 \text{ km/s}$   
 $Mass = 6.4 \times 10^{15} \text{ g}$

$$M_{CME} = M_8 + \dots + M_{13}$$

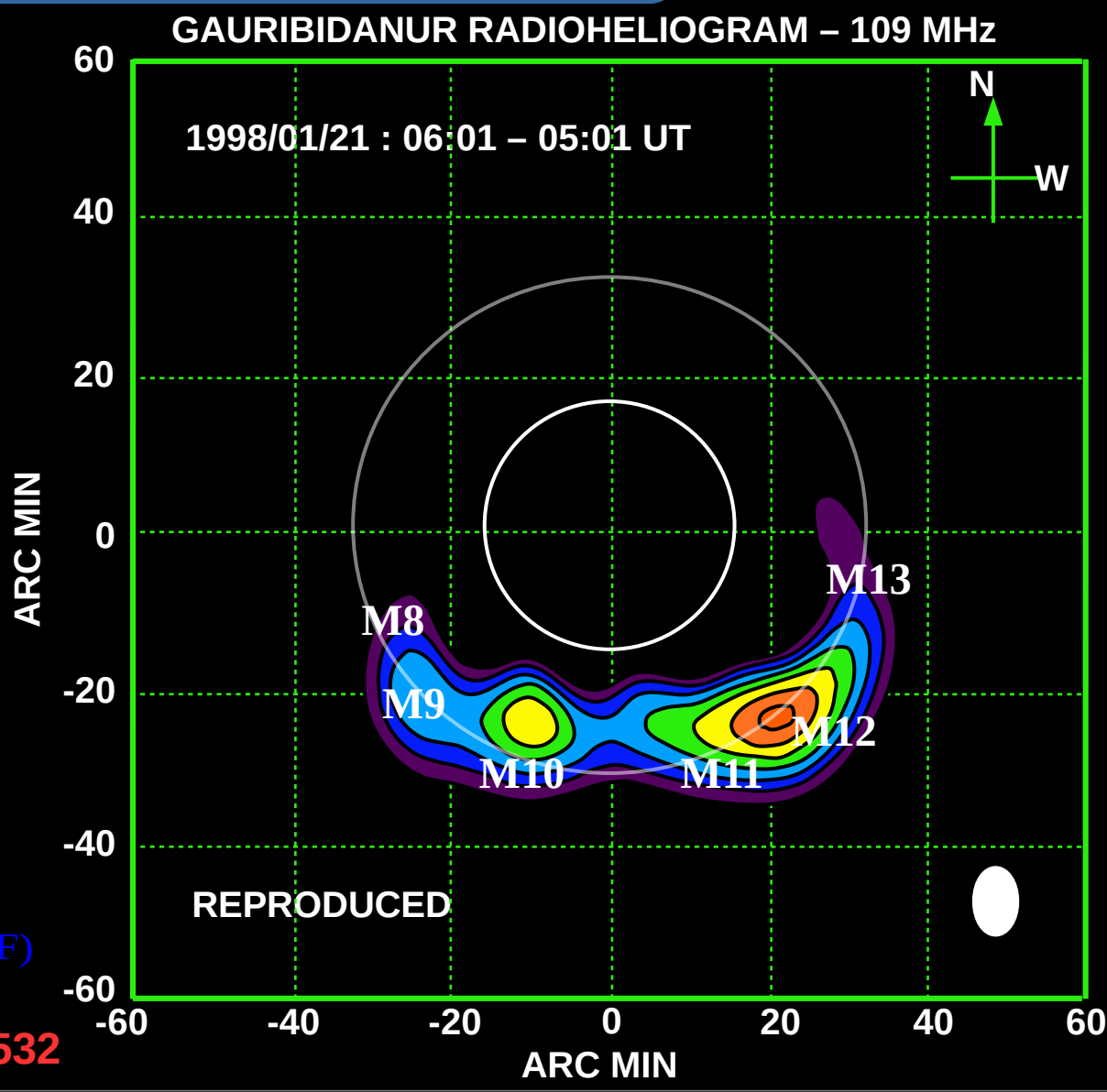
$$\vec{R}_{CME} = \frac{1}{M_{CME}} (M_8 \vec{r}_8 + \dots + M_{13} \vec{r}_{13})$$

$$\vec{R}_{CME} = 1.16 \vec{x} + 0.52 \vec{y} - 1.54 \vec{z}$$

$$\vec{R}_{H\alpha} = 0.51 \vec{x} - 0.18 \vec{y} - 0.84 \vec{z}$$

where

- $M_{CME}$  → Mass of radio CME
- $\vec{R}_{CME}$  → Position vector of CME centroid
- $\vec{R}_{H\alpha}$  → Position vector of solar filament (DSF)



**Kathiravan, C. et al. ApJ, 2004, 610, 1, 532**

---

**Radio reconstruction method  
can be used to estimate  
the true speed (3D) of CMEs  
similar to other techniques**

---

---

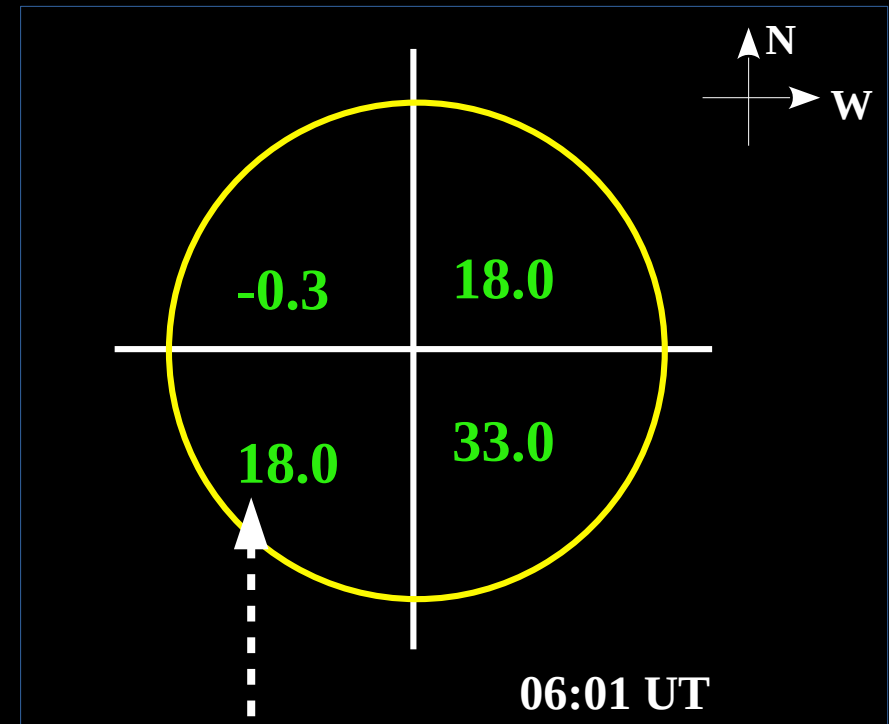
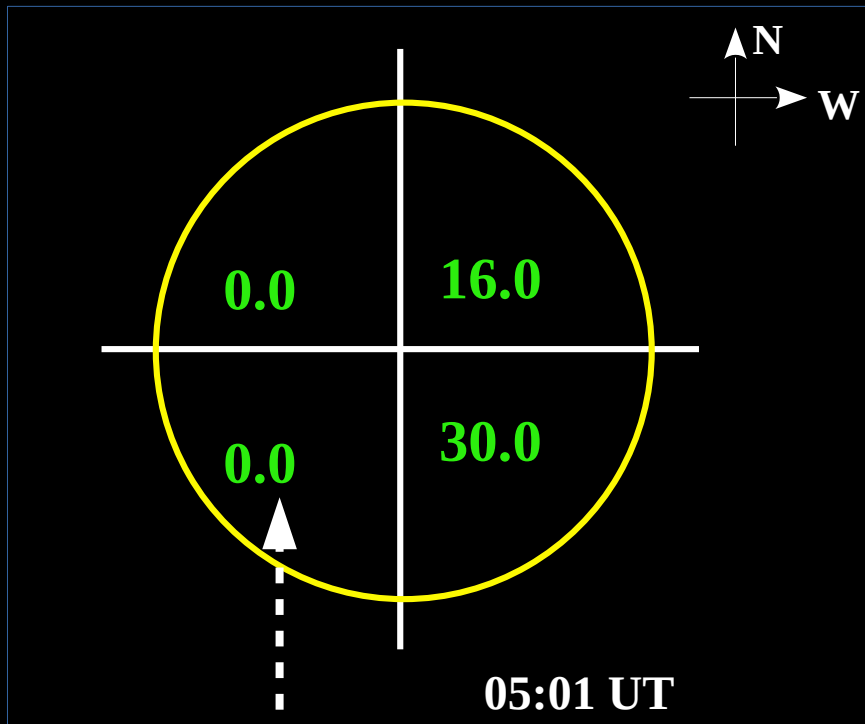
**Can we say anything  
about CME precursor  
using the disk info ??**

---

# CME → Pre-eruption Signature

**Before CME onset**

**After CME onset**



$$\Gamma_{SE} = 18$$

Mass Injection Rate =  $8.8 \times 10^{15}$  gm/hr  
 CME mass =  $6.5 \times 10^{15}$  g

Kathiravan, C. et al., ApJL, 2005, 627, 1, 77

## Two Possibilities :

---

**CME → Thermal**

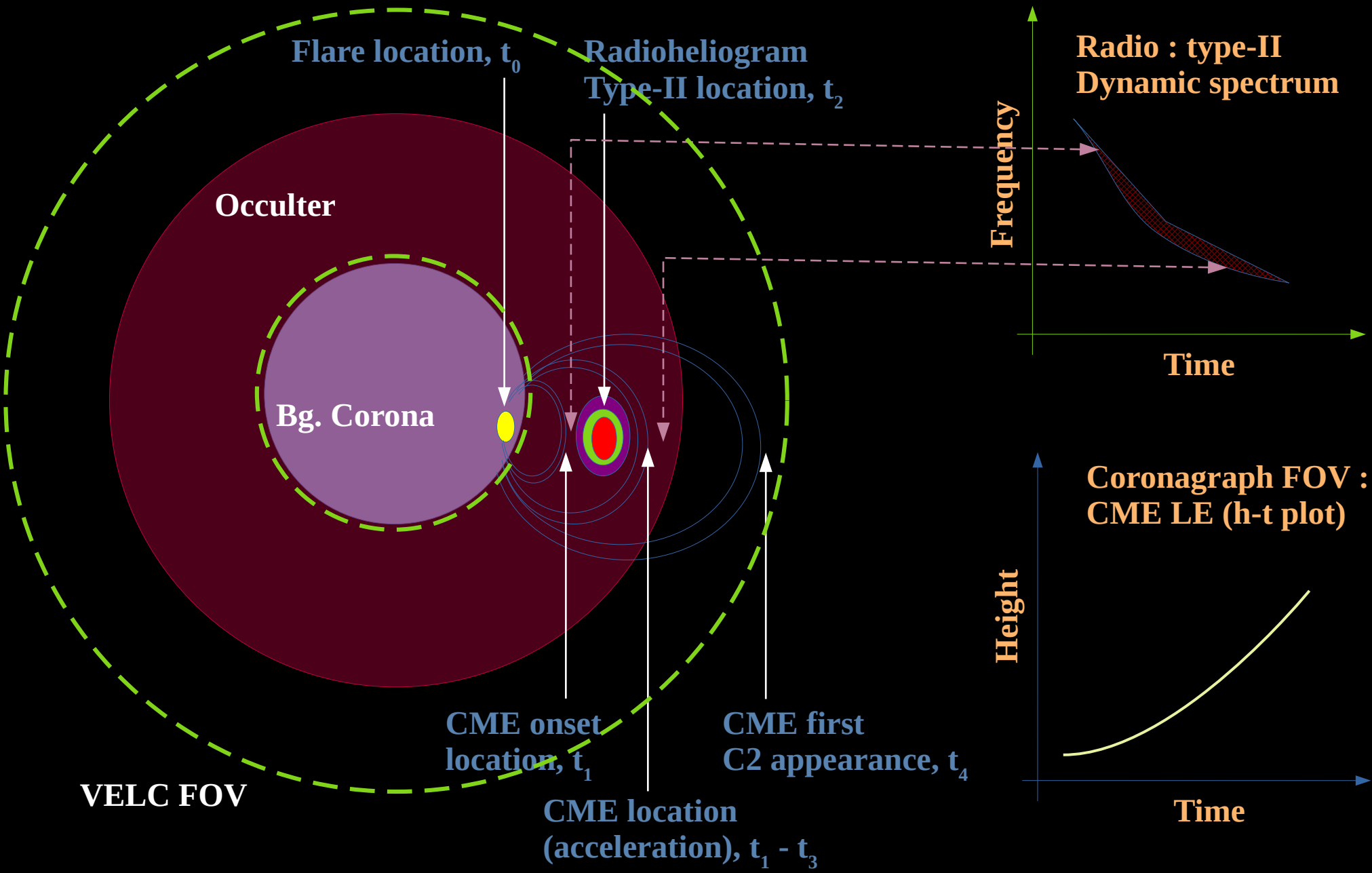
**CME → Non-thermal ✓**

---

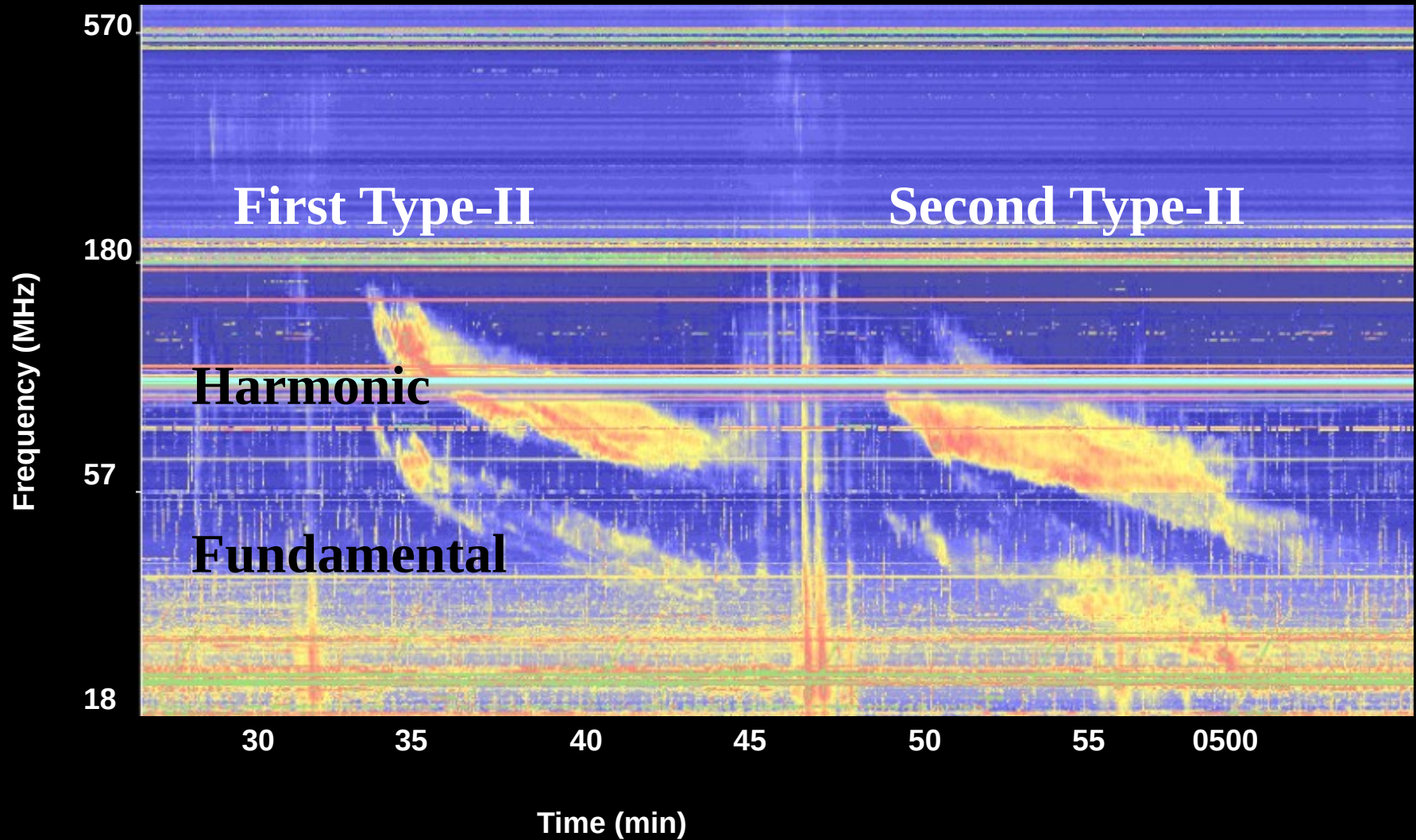
---

**CME → Non-thermal  
Type-II radio bursts**

---



# CME → Coronal type-II burst



# CME → Coronal type-II burst

## Type-II burst :

1. A slow drifting non-thermal continuum emission.
2.  $T_b \sim 10^7 - 10^9$  K.
3. The drift rate is lower ( $\sim$ MHz/s) than type-III.
4. They generally appear in pairs (Fundamental & Harmonic)
5. These are the signatures of coronal shock that are generated by the bulk motion of plasma material (associated with CMEs) from the inner to the outer coronal atmosphere.

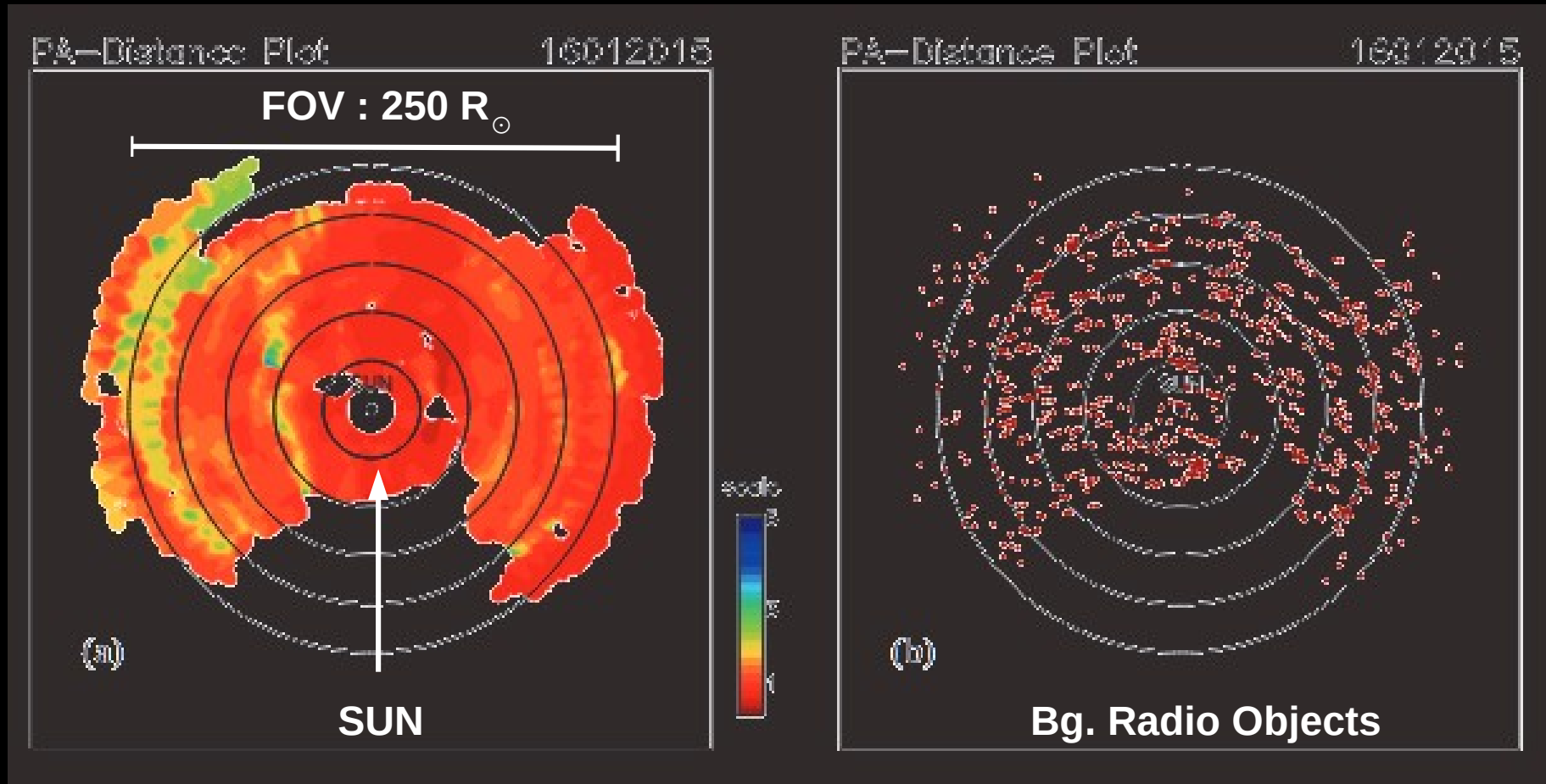
---

**Can't the CMEs be  
observed beyond  
15 MHz ??**

---

**Yet another Radio technique – IPS Obs.**

# CME / ICME IPS Observations



Ooty Wide Field Array (OWFA)

Manoharan, P. K. et al., JApA, 38, 16 (2017)

## Interplanetary Scintillation

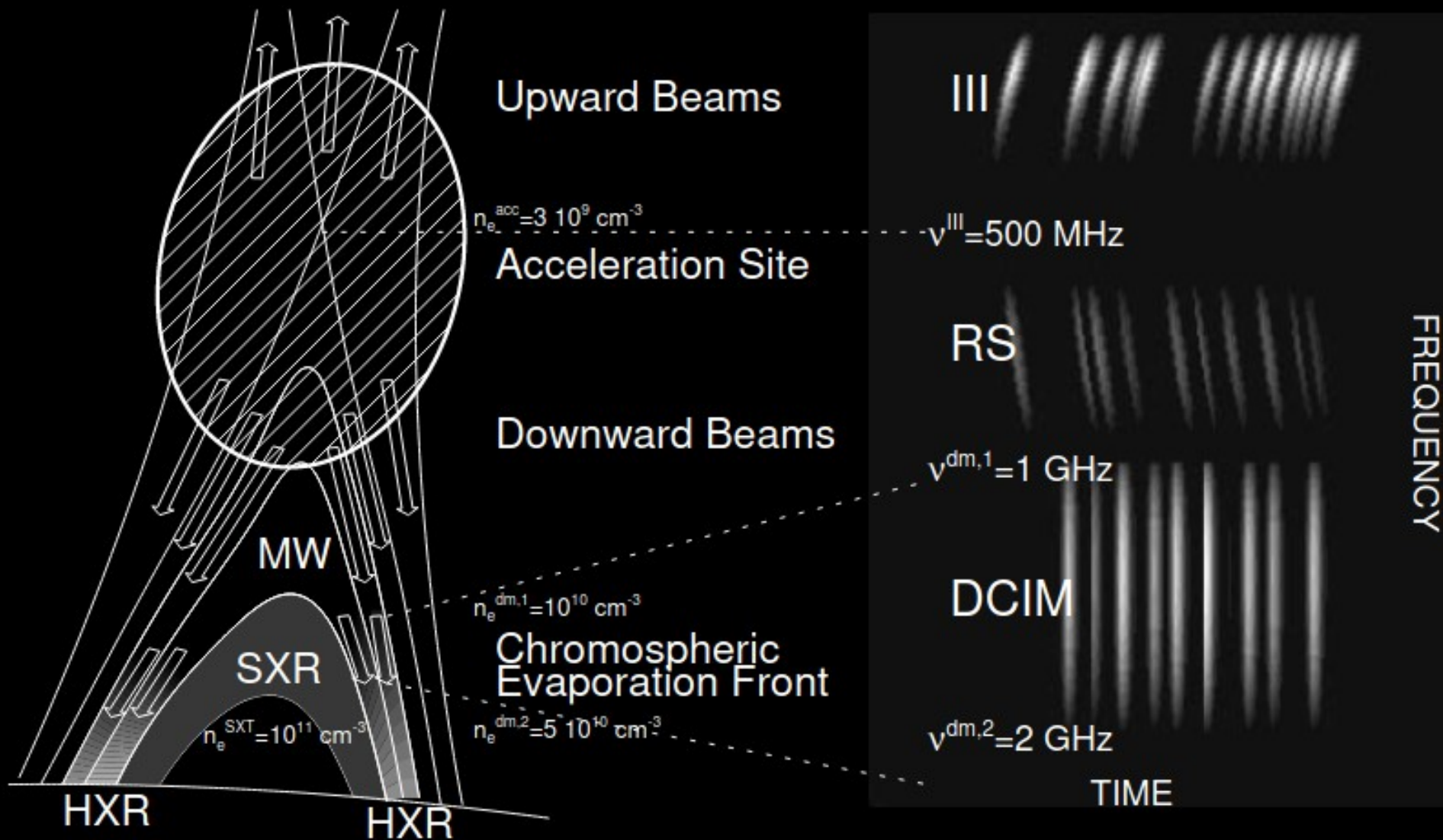
1

---

# Flare associated Radio signatures

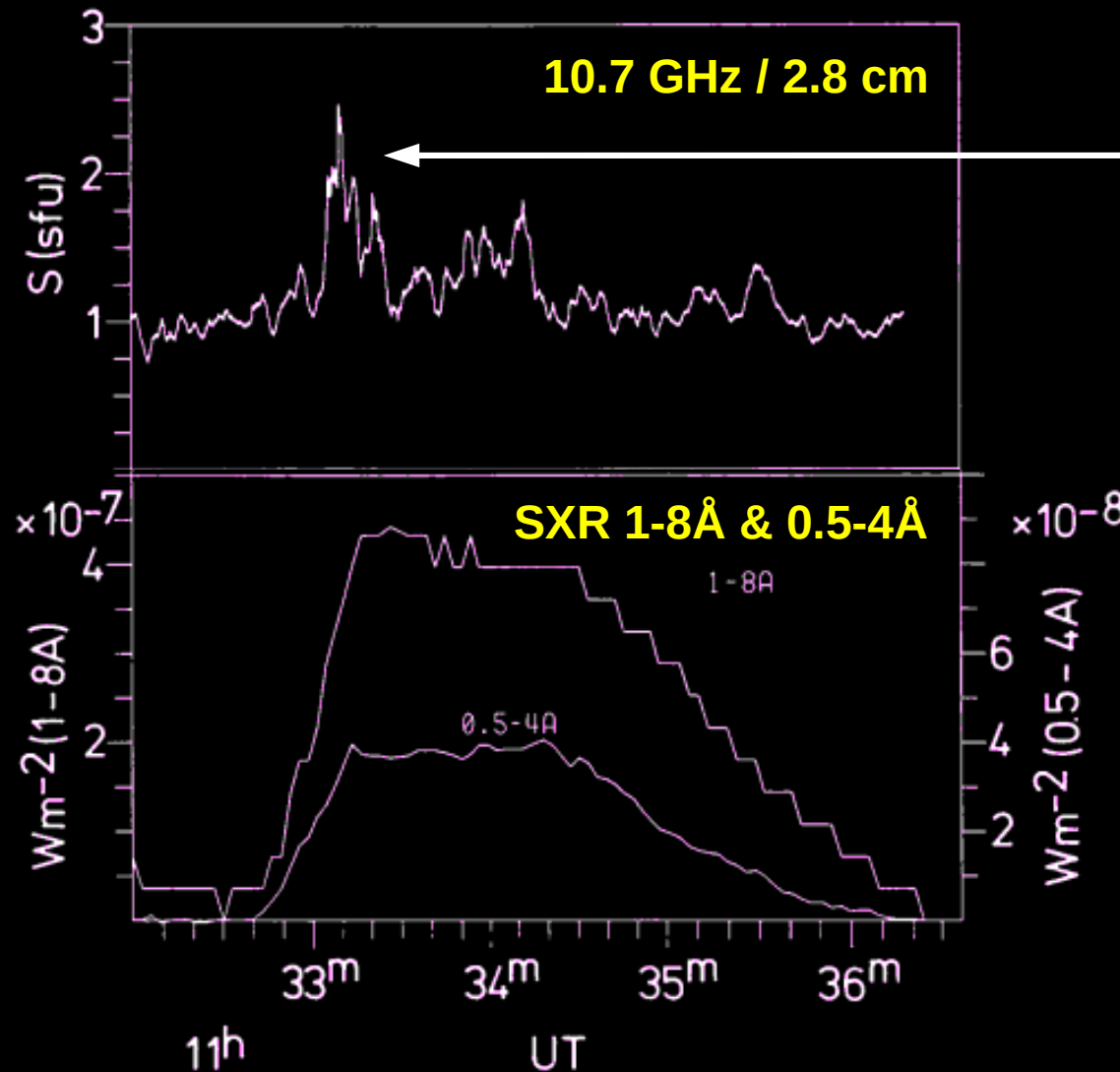
---

# Standard FLARE model



**Bastian, T. S. et al., ARAA, 36, 131 (1998)**

# Radio (cm- $\lambda$ ) & Soft X-ray emission

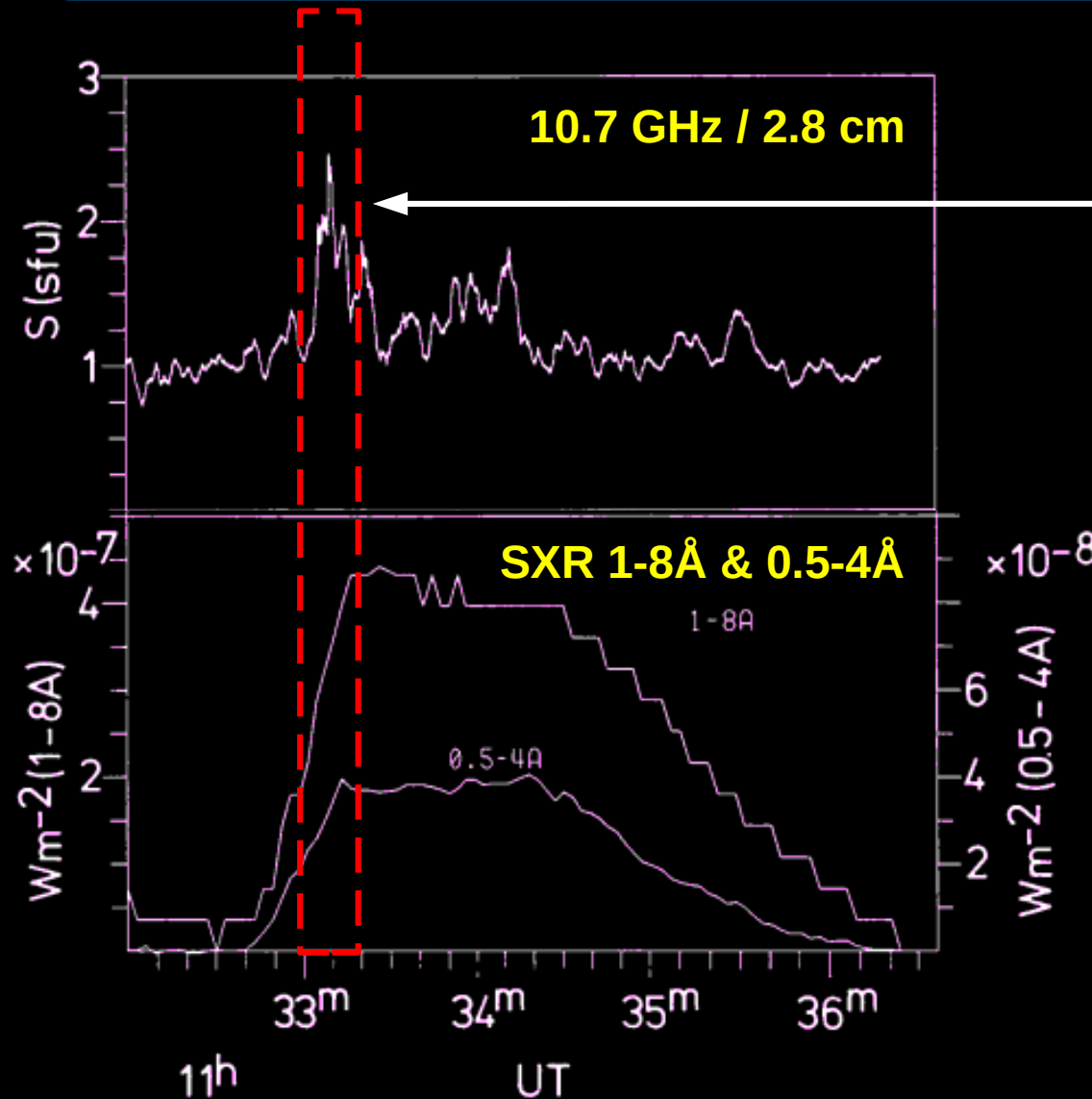


**Radio blips  
(microwave)**

**X-ray Continuum +  
Line emission  
(He-like Iron ions)  
1.8 Å  
~ tens of keV**

Fuerst et al., *A&A*, 107, 1, 178 (1982)

# Radio (cm- $\lambda$ ) & Soft X-ray emission



**Radio blips  
(microwave)**

**X-ray Continuum +  
Line emission  
(He-like Iron ions)  
1.8 Å  
~ tens of keV**

Fuerst et al., *A&A*, 107, 1, 178 (1982)

# Radio (cm- $\lambda$ ) & Soft X-ray emission

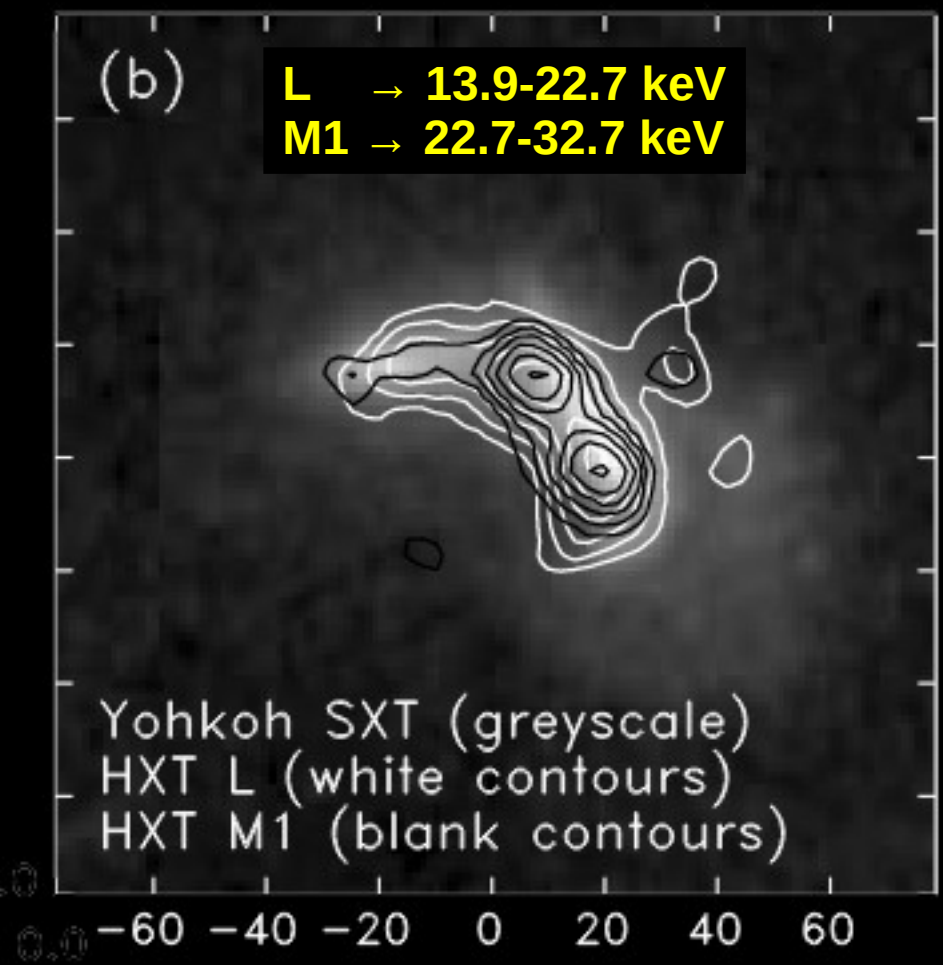
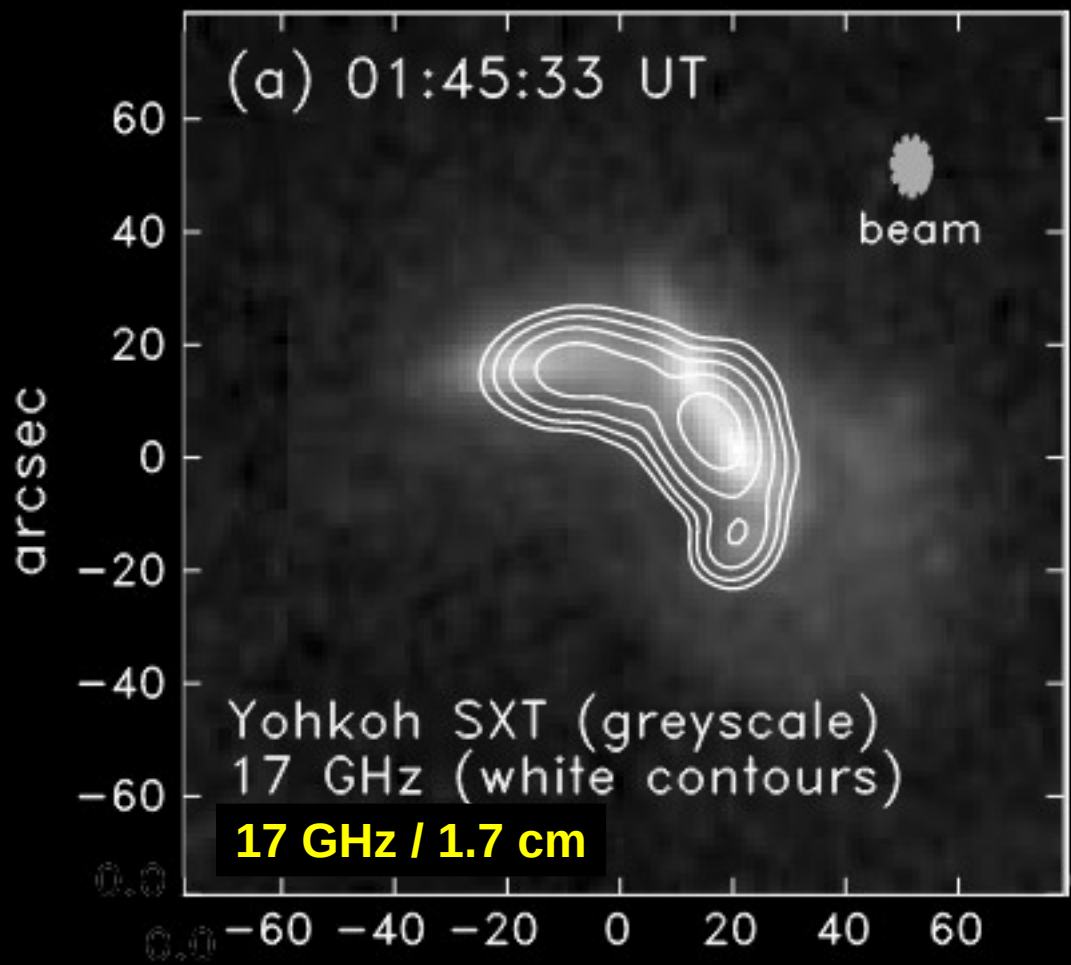
## Radio blips:

10.7 GHz / 2.8 cm

1. Predominantly occur in the rise phase of SXR flares.
2. Are due to non-thermal ( $10^7$  K) radiation from fast electrons. SXR emission is due to thermal flare plasma at a similar temperature.
3. Sources are located at flux emerging sites.  
Radio blips and SXR flares are indicators of energy dissipation by fast electrons.

Fuerst et al., A&A, 107, 1, 178 (1982)

# Radio (cm- $\lambda$ ) & X-ray (S&H) emission



Takakura et al., PASJ, 46, 653 (1994)

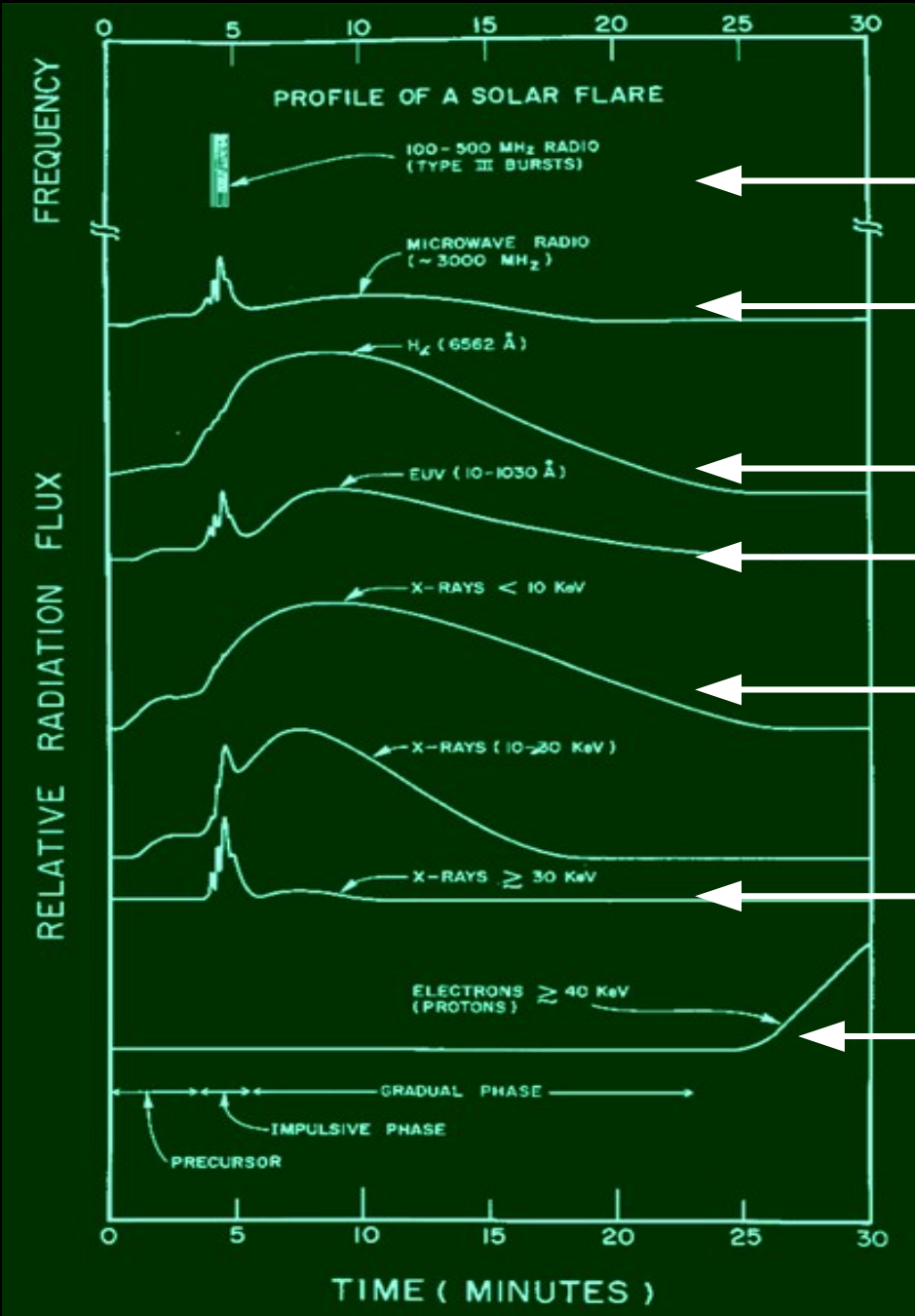
# Radio (cm- $\lambda$ ) & X-ray (S&H) emission

## HXR & Radio overlay:

1. The emissions are almost co-spatial.
2. The emissions involve the foot-points of a complex / system of magnetic loops that fan out across an AR.
3. HXR are due to  $e^-$  accelerated to very high energies ( $\sim$ MeV) at flare onset which then hit atoms at inner dense layers and produce bremsstrahlung continuum.
4. Same  $e^-$  are responsible for high freq. radio emission.

Takakura et al., PASJ, 46, 653 (1994)

**Radio obs. + Other  $\lambda$ s**



**Radio – m  $\lambda$ s**

**Radio – dcm  $\lambda$ s**

**H $\alpha$**

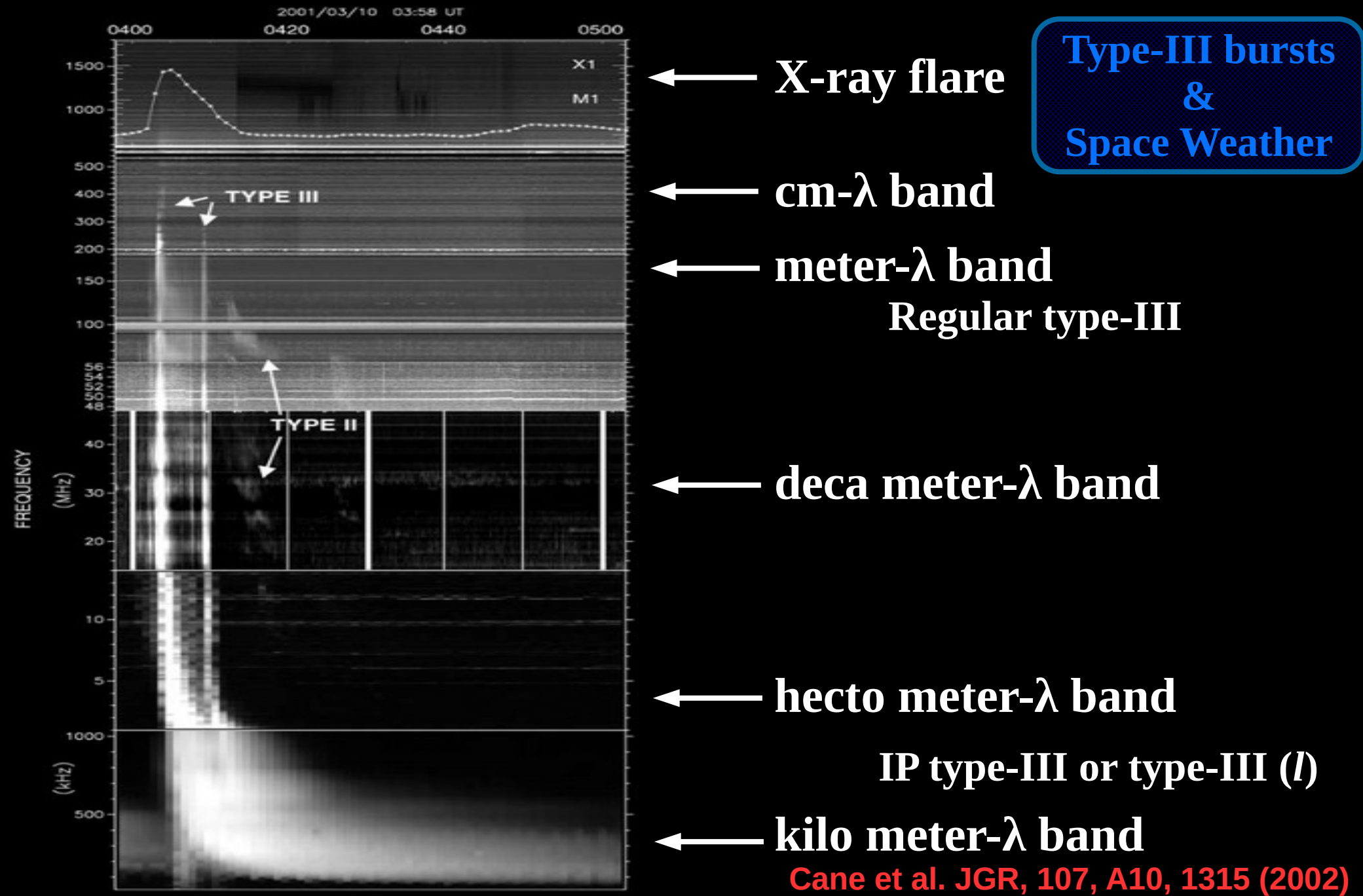
**EUV**

**SXR**

**HXR**

**Electrons & Protons**

**Shibata, K. et al, LRSP, 8, 6 (2011)**



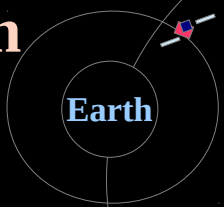
# Sun - Earth Connection

**Transient activities of outer solar atmosphere**

- i. Flares**
- ii. Mass expulsions (CMEs)**
- iii. Particles .....**

Systematic around the clock

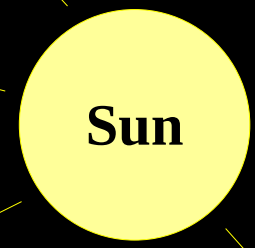
Solar  from the Earth



Earth

**Space climate**

**Harsh Sudden Unpredictable**

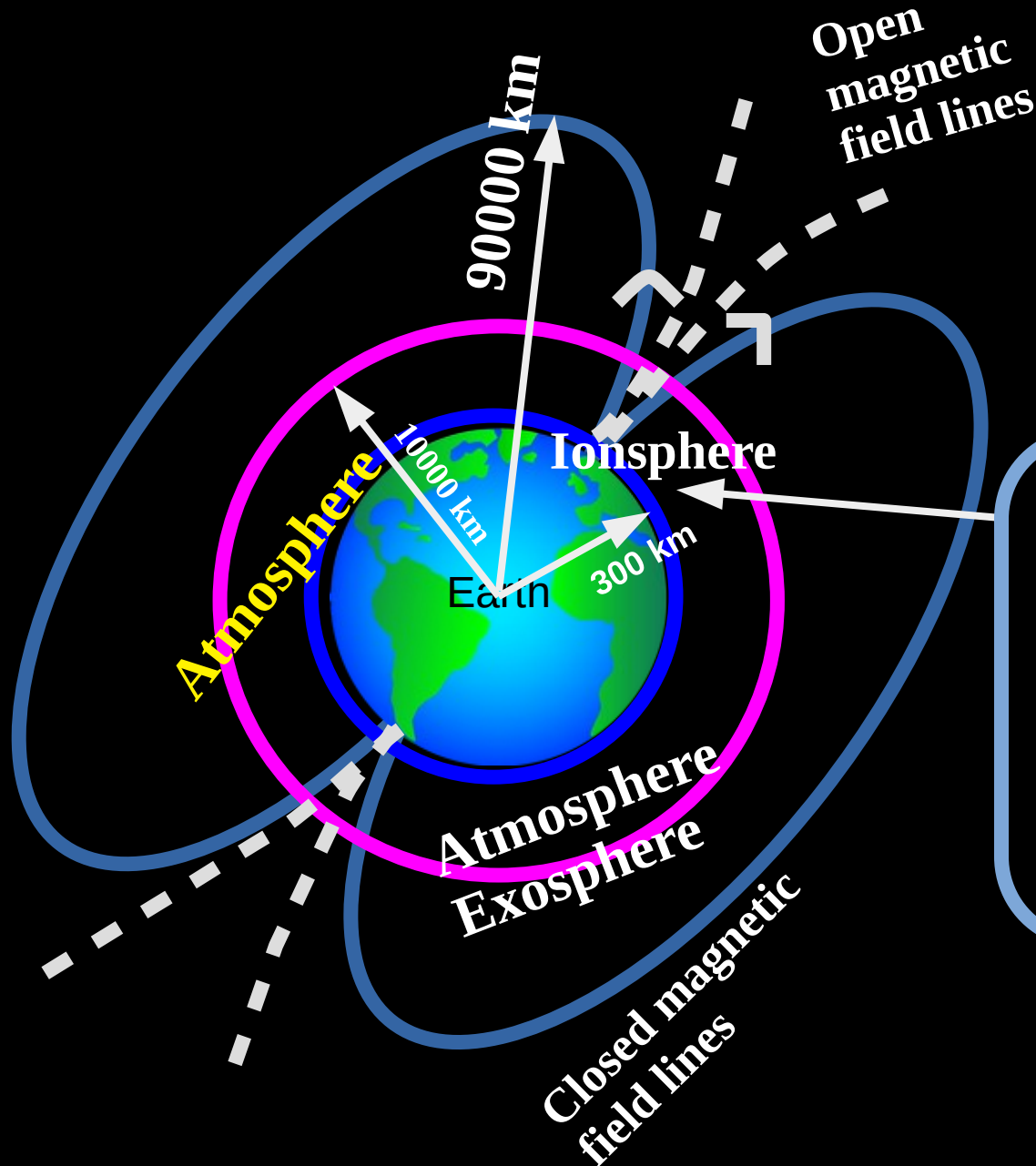


Sun

Space-borne instruments operation

**Interplanetary medium**

Solar Particle entry  
– onset of **Geo-magnetic Storms, Aurora,**  
..... formation of **Ring Current** above equator



**Earth – Geospace**

Place of  
**Communication satellites**  
Remote sensing satellites  
**Military surveillance satellites**  
International space station

**Thank you ALL**

**Organizers**

**(SU-UZB, COSPAR, ISWI, SCOSTEP, e-CALLISTO)**

**Participants**

**IIA & GBR observatory staff**